

Low Stage High Order Explicit Runge–Kutta Methods via Q- and D-Conditions: General Theory and Efficient Recursive Construction

Junyuan He and Jizu Huang

May 19, 2026

Abstract

Constructing explicit Runge–Kutta (ERK) methods with as few stages as possible for a given order is a classical problem in numerical analysis. In this work, we introduce a Q/D -space framework of sufficient order conditions for ERK methods. This framework generalizes Butcher’s classical simplifying assumptions by reformulating them in terms of simplified Q - and D -spaces defined through their residual vectors. It yields sufficient conditions which, together with $B(p)$, ensure order p . It also leads to a recursive construction procedure for ERK methods of arbitrary even order, in which the Butcher coefficients are obtained from two structured linear systems. For every even order $p \geq 4$, the construction produces ERK methods with stage number $s(p) = (p^2 - 2p + 8)/4$. This stage count has the same leading term as that of the classical Gragg families, while improving the linear term. The free parameters retained by the construction further provide a systematic framework for designing methods with enhanced stability and short-time accuracy.

1 Introduction

Explicit Runge–Kutta (ERK) methods form one of the central families of time-stepping schemes for nonstiff ordinary differential equations. Their popularity rests on several well-known advantages: easy to implement, require no nonlinear solves, and offer considerable flexibility in practice. At the same time, designing high-order ERK methods has long been recognized as a difficult task. The classical order theory, based on Butcher’s rooted trees [4], leads to a rapidly increasing collection of nonlinear algebraic conditions. The number of rooted trees of order p grows exponentially, so that even verifying order for moderate p becomes cumbersome. Constructing methods directly from these conditions is therefore feasible only at relatively low orders.

Several approaches have been developed to bypass this difficulty. Gragg’s extrapolation procedure [19] improves this to the currently asymptotically optimal value $\sim \frac{1}{4}p^2$, but the resulting

schemes are tied to the structure of Richardson extrapolation and do not yield general families of formulas for Runge–Kutta coefficients. Butcher’s constructive theory, based on quadrature formulas and generalized order condition, provides methods with on the order of $\sim \frac{3}{8}p^2$ stages [8]. Other families—for example, those developed by Verner and collaborators [38, 37]—achieve high accuracy or good embedded pairs, but typically rely on stage numbers $\sim \frac{1}{2}p^2$ or specialized procedures. Overall, while many high-order schemes exist, there is still no simple and general mechanism for constructing ERK methods of arbitrary order, and no upper bound estimates for general order p that is lower than the Gragg’s result.

The purpose of this work is to introduce such a mechanism, which yields better estimates than Gragg’s and provides concrete ways to construct families of ERK methods with much freedom. The central idea is to separate the order theory into two components that are usually intertwined: one governing the quadrature properties of the weights and nodes, and the other governing how stage values interact through the Runge–Kutta matrix. We formalize this through a pair of linear subspaces, the Q -spaces and D -spaces, which track the deviations from the classical simplifying assumptions. This leads to a set of linear Q - and D -conditions whose satisfaction guarantees order p . These conditions are less general than the full rooted-tree relations but have the advantage of being transparent and directly aligned with a recursive construction.

Based on this reformulation, we develop a constructive procedure that produces ERK methods of arbitrary order. The construction proceeds by enlarging the Q - and D -spaces in a controlled manner and enforcing orthogonality relations that ensure the satisfaction of our sufficient conditions for order. Coefficients are obtained from solving two structured linear systems: one associated with the Q -conditions and one with the D -conditions. The two systems are block diagonal and block lower-triangular respectively and can therefore be solved inexpensively with excellent numerical stability. As a result, the coefficients can be generated in essentially quadratic time in the number of nonzero coefficients, without enumerating trees or performing symbolic manipulations.

The methods produced in this way have several notable features. Their stage number satisfies

$$s(p) = \frac{1}{4}(p^2 - 2p + 8)$$

for even $p \geq 4$, improving Gragg’s $\frac{1}{4}p^2 + 1$ estimate. In addition, the stability regions generated by this method is generally larger than Gragg’s and Butcher’s method, and can potentially be further optimized by choosing the free parameters.

The remainder of the paper is organized as follows.

- Section 2 reviews the classical order conditions and the simplifying assumption that serves as the foundation for our reformulation.
- Section 3 introduces the Q - and D -spaces and states the associated sufficiency theorems.
- Section 4 presents the recursive formulation for constructing the coefficients of the RK method.

- Section 5 analyzes its structural and asymptotic properties.
- Section 6 contains numerical examples illustrating the method.
- Section 8 offers further discussion and open questions.
- Section 9 summarizes the main conclusions.

2 Preliminaries

We briefly recall the standard formulation of ERK methods, their classical order theory based on rooted trees, and the simplifying assumptions introduced by Butcher. The presentation is selective and focuses on the structures most relevant to the reformulation developed in Section 3. We begin this section by introducing the notation.

2.1 Notations

Viewing the order conditions and simplifying assumptions as expressions using tensor operations greatly simplifies the notation in the description of our framework. Although we use tensor contractions and Hadamard products, we are only dealing with scalars, vectors and matrices, viewed as results of tensor networks. Thus the standard notations in tensor numerical analysis are too complicated for our use. In this subsection, we give our notations for the operations we need in this article and connect them with standard notations both in tensor numerical algebra and in traditional linear algebra.

Notation 2.1 (Hadamard product [27]). The Hadamard product of two vectors $\mathbf{x} = (x_i)$ and $\mathbf{y} = (y_i)$ from \mathbb{R}^n is still a vector in \mathbb{R}^n , denoted as

$$\mathbf{x} \odot \mathbf{y},$$

whose elements are defined by $(\mathbf{x} \odot \mathbf{y})_i = x_i y_i$ for $1 \leq i \leq n$.

Notation 2.2 (Contracted product [27]). We denote the mode- $(M, 1)$ contracted product of tensors $\mathbf{A} \in \mathbb{R}^{I_1 \times \dots \times I_M}$ and $\mathbf{B} \in \mathbb{R}^{J_1 \times \dots \times J_N}$ with $I_M = J_1$ as

$$\mathbf{C} := \mathbf{A} \times^1 \mathbf{B} \in \mathbb{R}^{I_1 \times \dots \times I_{M-1} \times J_2 \times \dots \times J_N},$$

with elements

$$\mathbf{C}[i_1, \dots, i_{M-1}, j_2, \dots, j_N] = \sum_{i_M=1}^{I_M} \mathbf{A}[i_1, \dots, i_{M-1}, i_M] \mathbf{B}[i_M, j_2, \dots, j_N].$$

Here the $(i_1, \dots, i_N)^{\text{th}}$ element of a tensor \mathbf{A} with size $I_1 \times \dots \times I_N$ is denoted as $\mathbf{A}[i_1, \dots, i_N]$.

The mode- $(M, 1)$ contracted product is consistent with linear algebra notations for vectors and matrices. Specifically, for matrices $\mathbf{A} \in \mathbb{R}^{m \times n}$ and $\mathbf{B} \in \mathbb{R}^{n \times r}$, their contracted product

$\mathbf{A} \times^1 \mathbf{B}$ coincides with the usual matrix multiplication \mathbf{AB} . Moreover, for vector $\mathbf{b} \in \mathbb{R}^m$, $\mathbf{c} \in \mathbb{R}^n$, and a matrix $\mathbf{A} \in \mathbb{R}^{m \times n}$, the contracted products $\mathbf{b} \times^1 \mathbf{A}$ and $\mathbf{A} \times^1 \mathbf{c}$ correspond to the left and right multiplication of a matrix by vectors, respectively, namely $(\mathbf{b}^\top \mathbf{A})^\top$ and \mathbf{Ac} .

Proposition 2.1 (Associativity [27, Proposition 2.3]). *Suppose that $\mathbf{A} \in \mathbb{R}^{I_1 \times \dots \times I_M}$, $\mathbf{B} \in \mathbb{R}^{J_1 \times \dots \times J_N}$, and $\mathbf{C} \in \mathbb{R}^{K_1 \times \dots \times K_R}$, with $I_M = J_1$, $J_N = K_1$, and $N \geq 2$, then $\mathbf{A} \times^1 (\mathbf{B} \times^1 \mathbf{C}) = (\mathbf{A} \times^1 \mathbf{B}) \times^1 \mathbf{C}$.*

Definition 2.1 (Restriction). Suppose $\mathbf{x} = (x_1, x_2, \dots, x_n)^\top \in \mathbb{R}^n$. $S \subseteq \{1, 2, \dots, n\}$ is an index set and $s = |S|$. Define the restriction of \mathbf{x} on the indices S to be $\mathbf{x}|_S \in \mathbb{R}^s$. If $S = \{i_1, i_2, \dots, i_s\}$, $1 \leq i_1 < i_2 < \dots < i_s \leq n$, then $\mathbf{x}|_S = (x_{i_1}, x_{i_2}, \dots, x_{i_s})^\top$.

Definition 2.2 (Projection). Suppose $\mathbf{x} = (x_1, x_2, \dots, x_n)^\top \in \mathbb{R}^n$. $S \subseteq \{1, 2, \dots, n\}$ is an index set and $s = |S|$. Define the projection onto the subspace activated by indices belong to S to be $P_S \mathbf{x} \in \mathbb{R}^n$, defined by

$$(P_S \mathbf{x})_i := \begin{cases} x_i, & i \in S, \\ 0, & i \notin S. \end{cases}$$

Notation 2.3 (Inner product). The standard inner product of two vectors $\mathbf{x} = (x_i)$ and $\mathbf{y} = (y_i)$ from \mathbb{R}^n is a scalar denoted by

$$\mathbf{x} \cdot \mathbf{y} := \sum_{i=1}^n x_i y_i.$$

If an index set $S \subset \{1, 2, \dots, n\}$ is given, we denote the inner product restricted to S by the restriction notation

$$\mathbf{x}|_S \cdot \mathbf{y}|_S := \sum_{i \in S} x_i y_i.$$

Notation 2.4 (Powers). We would encounter two types of powers in this paper.

- One is the power of a square matrix $\mathbf{A} \in \mathbb{R}^{n \times n}$, denoted by $\mathbf{A}^k \in \mathbb{R}^{n \times n}$, which is the result of sequentially performing mode-(2,1) contracted product, or matrix multiplication, of the k matrices \mathbf{A} .
- Another is the element-wise power of a vector $\mathbf{c} \in \mathbb{R}^n$, which should be denoted $\mathbf{c}^{\odot k} \in \mathbb{R}^n$ formally. However, since there should be no confusion with contracted products, we sometime simplify the notation and only write \mathbf{c}^k for the element-wise k^{th} power of \mathbf{c} .

Notation 2.5 (Set notations). The set operations are understood in the Minkowski sense (see [29] for example). Take the binary operation Hadamard product “ \odot ” as an example, if $\mathbf{x} \in \mathbb{R}^n$ is a fixed vector, and Q and D are two sets of vectors in \mathbb{R}^n , then

$$\begin{aligned} Q \odot \mathbf{x} &= \{\mathbf{q} \odot \mathbf{x} : \mathbf{q} \in Q\}, \\ Q \odot D &= \{\mathbf{q} \odot \mathbf{d} : \mathbf{q} \in Q, \mathbf{d} \in D\}. \end{aligned}$$

Unary operations are similar. Take the restriction operation as an example, if S is the index set, then

$$Q|_S = \{\mathbf{q}|_S : \mathbf{q} \in Q\} \subseteq \mathbb{R}^{|S|}.$$

2.2 Runge–Kutta method and order conditions based on rooted trees

An s -stage ERK method applied to $\dot{\mathbf{y}} = \mathbf{f}(t, \mathbf{y})$ has the form

$$\begin{aligned} \mathbf{Y}_i &= \mathbf{y}_n + h \sum_{j=1}^s a_{ij} \mathbf{f}(\tau_j, \mathbf{Y}_j), & i = 1, \dots, s, \\ \mathbf{y}_{n+1} &= \mathbf{y}_n + h \sum_{i=1}^s b_i \mathbf{f}(\tau_j, \mathbf{Y}_i), \end{aligned}$$

where $\tau_j = t_n + hc_j$, and the tableau $(\mathbf{A}, \mathbf{b}, \mathbf{c}) = ((a_{ij}), (b_i), (c_i)) \in (\mathbb{R}^{s \times s}, \mathbb{R}^s, \mathbb{R}^s)$ satisfies $c_i = \sum_{j=1}^s a_{ij}$ and $a_{ij} = 0$ for $i \leq j$. Throughout the paper we use vector notation

$$\mathbf{1} = (1, \dots, 1)^\top, \quad \mathbf{c} = (c_1, \dots, c_s)^\top, \quad \mathbf{b} = (b_1, \dots, b_s)^\top.$$

Let \mathcal{T} denote the set of rooted trees. For a tree $t \in \mathcal{T}$, let $|t|$ be its order (number of nodes) and let

$$\phi(t) \equiv \text{elementary weight of } t \quad \text{and} \quad \gamma(t) \equiv t! \equiv \text{density of } t,$$

as in Butcher's theory [4, 8]. An RK method has order p if and only if

$$\phi(t) = \frac{1}{\gamma(t)} \quad \text{for every tree } t \text{ with } |t| \leq p. \quad (1)$$

The number of rooted-tree conditions grows exponentially. In fact, if T_p is the number of non-isomorphic rooted trees of size p , then

$$T_p \sim C\alpha^p p^{-3/2},$$

where $\alpha \approx 2.956$ and $C \approx 0.4399$. These constants were first studied by Otter [31], and later rigorously derived in analytic combinatorics [2, 17, 24]. The exponential growth rate makes direct symbolic enforcement impractical for moderate p .

To reduce the combinatorial complexity of (1) with respect to order p , Butcher introduced the *simplifying assumptions* [5, 8], written $B(q)$, $C(q)$, and $D(q)$. For a given integer $q \geq 1$:

$B(q)$ (Quadrature condition)

$$\mathbf{b}^\top \mathbf{c}^{\odot k} = \frac{1}{k+1}, \quad 0 \leq k \leq q-1. \quad (2)$$

$C(q)$ (Stage order condition)

$$\mathbf{A}\mathbf{c}^{\odot k} = \frac{\mathbf{c}^{\odot(k+1)}}{k+1}, \quad 0 \leq k \leq q-1. \quad (3)$$

$D(q)$ (Internal consistency condition)

$$(\mathbf{b} \odot \mathbf{c}^{\odot k}) \times^1 \mathbf{A} = \frac{1}{k+1} \mathbf{b} \odot (\mathbf{1} - \mathbf{c}^{\odot(k+1)}), \quad 0 \leq k \leq q-1. \quad (4)$$

It is known that $B(p)$, $C(q)$, $D(r)$ with $p \leq q+r+1$ and $p \leq 2q+2$ imply order p [5]. For implicit RK methods, these conditions are often attainable. However, explicit methods impose structural constraints that these simplifying assumptions cannot hold beyond small q and r .

2.3 Limitations of the simplifying assumptions for ERK methods

Explicit methods require \mathbf{A} to be strictly lower triangular. Substituting this structure into $C(q)$ yields: For $k=0$, this is the stage condition we typically require

$$\mathbf{A}\mathbf{1} = \mathbf{c}. \quad (5)$$

For any $k \geq 1$, the conditions

$$\mathbf{A}\mathbf{c}^{\odot k} = \frac{\mathbf{c}^{\odot(k+1)}}{k+1} \quad (6)$$

would imply that $c_2 = 0$ and in turn $c_3 = 0, c_4 = 0, \dots$, and eventually all components of \mathbf{c} are zero, which cannot be consistent with the quadrature conditions $\mathbf{b}^\top \mathbf{c} = \frac{1}{2}$. Thus, only $C(1)$ is possible in explicit methods, while $C(q)$, $q \geq 2$ is not possible.

Likewise, the conditions $D(q)$ can be written as

$$\frac{1}{k+1} \mathbf{b} \odot (\mathbf{1} - \mathbf{c}^{\odot(k+1)}) = (\mathbf{b} \odot \mathbf{c}^{\odot k}) \times^1 \mathbf{A}, \quad 0 \leq k \leq q-1.$$

For the s^{th} component, due to the strictly lower-diagonal structure of \mathbf{A} , we have $b_s c_s^{k+1} = b_s$ for $0 \leq k \leq q-1$. For the $(s-1)^{\text{th}}$ component, a similar argument yields

$$\frac{1}{k+1} b_{s-1} (1 - c_{s-1}^{k+1}) = b_s c_s^k a_{s,s-1} = b_s a_{s,s-1}, \quad 0 \leq k \leq q-1,$$

which implies

$$b_{s-1} (1 - c_{s-1}) = \frac{1}{n} b_{s-1} (1 - c_{s-1}^n), \quad \forall n = 2, 3, \dots, q.$$

Equivalently, this can be written in the simplified form

$$b_{s-1} (c_{s-1}^n - n c_{s-1} + n - 1) = 0, \quad \forall n = 2, 3, \dots, q.$$

Taking $n = 2$, we obtain $b_{s-1}(1 - c_{s-1}) = 0$. If $q \geq 2$, repeating this argument inductively yields

$$\mathbf{b} \odot (\mathbf{1} - \mathbf{c}) = \mathbf{0},$$

or, equivalently, in component-wise form $b_j(1 - c_j) = 0$ for all $j = 1, \dots, s$. However, $\mathbf{b}^\top(\mathbf{1} - \mathbf{c}) = 0$ results in $\mathbf{b}^\top \mathbf{1} = \mathbf{b}^\top \mathbf{c}$, which is contradictory with the quadrature conditions $B(2)$.

Thus the classical simplifying assumptions do not provide a practical route for constructing high-order ERK schemes. A different approach is required, one that replaces the unattainable $C(q)$ and $D(q)$ constraints with a reformulation that preserves sufficiency for order p , while respecting the structural constraints of explicit tableaux. This reformulation is developed in Section 3.

3 Reformulation: Q- and D-conditions

In this section, we propose a framework to construct simplifying conditions for RK methods, which can be viewed as a more general version of simplifying conditions $B(q)$, $C(q)$ and $D(q)$. This idea of this framework is inspired by [37], which categorized and reduced the order conditions into 4 types of trees, and also by [36], which first formalized the Q- and D-type order conditions in a recursive way. We follow the idea of this recursive definition, but slightly alter the definitions to increase consistency and simplicity.

3.1 Motivation and reformulation

Classical order analysis of RK methods relies on Butcher's order conditions given by rooted trees. While these conditions provide a consistent way to verify order, they are often inconvenient for the construction of RK schemes because of the strong nonlinearity in these conditions and the exponential growth in the number of order conditions with respect to order. For implicit methods, Butcher's simplifying assumptions $B(p)$, $C(q)$ and $D(r)$ can be used to overcome this problem. By careful selection of stage quadrature points as Gaussian nodes, one can construct RK methods satisfying certain B , C , and D -conditions, resulting in high-order implicit RK methods, such as the Gauss-Legendre family, Gauss-Radau family and Gauss-Lobatto family [8]. However, the simplifying conditions $B(q)$, $C(q)$, and $D(q)$ are inconvenient for ERK scheme because

1. Stage to stage dependency of ERK schemes ($a_{ij} = 0$ for $j \geq i$) imposes a strictly lower-triangular structure on the coefficient matrix A . This structural constraint severely limits the applicability of the simplifying assumptions $C(q)$ and $D(r)$. In fact, one can verify that ERK methods only satisfy $C(q)$ and $D(r)$ with $q, r \leq 1$ as discussed in Section 2;
2. They do not directly support recursive or algorithmic construction of coefficients.

As a result, deriving high-order explicit schemes still requires handling a rapidly growing number

of coupled nonlinear algebraic equations, posing a fundamental difficulty since nonlinear systems do not, in general, admit guaranteed solutions. In practice, these systems are typically addressed either by reducing them to simpler subsystems and deriving closed-form expressions by hand, or by resorting to iterative solution procedures; however, both approaches suffer from significant limitations and do not scale to the construction of methods of arbitrary order. To overcome these issues, we propose a framework tailored to the explicit case for constructing a generalized version of simplifying assumptions, called the Q - and D -conditions, which allows for the matrix A to be obtained by solving a linear algebraic system. In this section we will introduce our framework for reformulating the simplifying assumptions, and in Section 4 we will give a concrete construction of RK methods utilizing this framework.

The key idea behind this reformulation is to analyze how ERK methods deviate from the classical simplifying assumptions $C(q)$ and $D(r)$, which they generally cannot satisfy due to the strict lower-triangular structure of their Butcher table. So, instead of enforcing these conditions directly, we consider the differences between the two sides of the C - and D -conditions and denote the resulting residual vectors by q_n and d_n . By studying the algebraic relations that these residual vectors must satisfy for a method to achieve order p , we arrive at two structured sets of sufficient conditions — the Q -conditions and D -conditions. These conditions retain the spirit of Butcher’s simplifying assumptions but are expressed in a way compatible with explicit methods. In particular, the construction of the conditions has a recursive structure, allowing stage coefficients to be determined successively in a decoupled way.

3.2 Tree tensor networks and graphical representations

As discussed in [26], for a given rooted tree t , the elementary weight $\phi(t)$ can be computed through the contraction of an associated tree tensor network. The Q - and D -conditions considered in this paper are built from recursively generated multilinear expressions involving RK coefficients, matrix actions, inner products, and Hadamard products. When expressed purely in algebraic form, these expressions quickly become cumbersome, and their contraction structure is often obscured. To make this structure explicit, we introduce a tree-based graphical notation. In this paper, the notation serves solely as a representational tool for organizing the Q - and D -conditions and streamlining their proofs. We refer the reader to [1, 9, 26] for further details.

3.2.1 Graphical representation

In the graphical representation of standard tensor network [1, 9], each vector, matrix, or higher-order tensor is represented by a vertex. Internal edges represent contraction indices, while open edges correspond to free indices. Leaves represent input objects, and the root records the output of the multilinear expression. Since all constructions considered below are recursive and acyclic, we restrict our attention to tree-shaped contraction graphs. A tree tensor network is defined as follows.

Definition 3.1 (Tree tensor network). A *tree tensor network* (TTN) is a tensor-network representation whose contraction graph is a tree. If \mathbb{E} denotes the set of internal edges and \mathbb{E}° the set of open edges, then a TTN can be written in the compact form

$$\mathbf{U}[\mathbb{E}^\circ] = \sum_{\mathbb{E}} \prod_{\alpha=1}^V \mathbf{U}_\alpha[\mathbb{E}_\alpha^\circ, \mathbb{E}_\alpha]. \quad (7)$$

Figure 1 illustrates several TTN contraction graphs corresponding to basic multilinear operations.

$$\begin{aligned} x &= \text{---} \uparrow x & x \cdot x &= \text{---} \uparrow \begin{array}{c} x \\ x \end{array} & \mathbf{A}x &= \text{---} \uparrow \begin{array}{c} x \\ \mathbf{A} \end{array} & y^\top \mathbf{A}x &= \begin{array}{c} x \\ \mathbf{A} \\ y \end{array} & \mathbf{B} &= \text{---} \vee \mathbf{B} & \mathbf{B}x &= \begin{array}{c} x \\ \vee \mathbf{B} \end{array} \in \mathbb{R}^{n_2 \times n_3} \\ (\mathbf{B}x)(\mathbf{A}x) &= \begin{array}{c} x \\ \vee \mathbf{A} \\ \vee \mathbf{B} \end{array} \in \mathbb{R}^{n_3} & z^\top (\mathbf{B}x)(\mathbf{A}x) &= \begin{array}{c} x \\ \vee \mathbf{A} \\ \vee \mathbf{B} \\ z \end{array} \end{aligned}$$

Figure 1: Graphical conventions for basic multilinear operations. Vertices represent tensors or linear operators, internal edges represent contraction indices, and open edges correspond to free indices.

3.2.2 TTN interpretation of the Q- and D-expressions

The quantities entering the recursive constructions of Q_m and D_n admit a natural interpretation in this notation. The point is not to introduce a new algebraic formalism, but to record the nesting pattern of the multilinear operations.

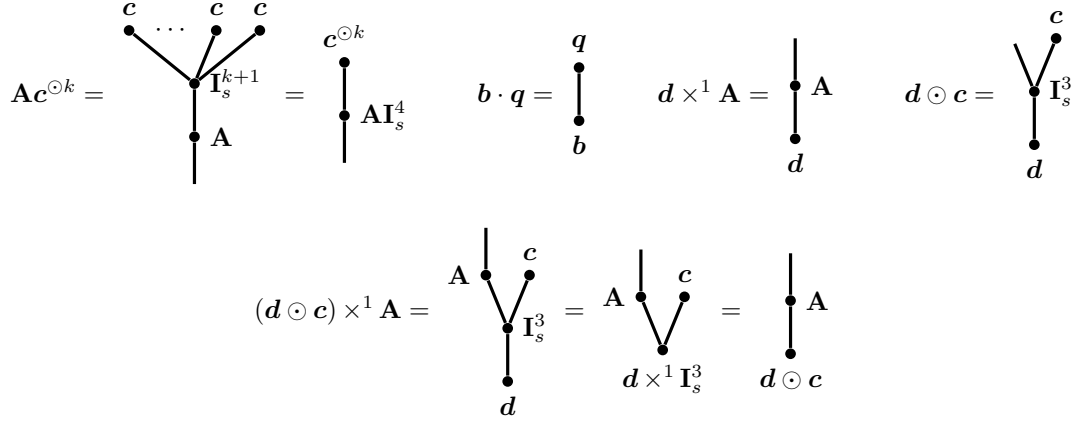
Typical examples used throughout the paper are:

- $\mathbf{A}c^{\odot k}$, represented by a tree whose root is the matrix \mathbf{A} and whose leaf is the vector $c^{\odot k}$;
- $\mathbf{b} \cdot \mathbf{q}$, represented by a binary tree with leaves \mathbf{b} and \mathbf{q} and scalar output at the root;
- $\mathbf{d} \times^1 \mathbf{A}$, represented by a contraction tree in which the vector \mathbf{d} is contracted with one mode of \mathbf{A} ;
- $\mathbf{d} \odot \mathbf{c}$, represented by a tree with two vector leaves and vector output.

More generally, every vector generated in the recursive definitions of Q_m and D_n can be represented by a rooted tree whose leaves belong to the basic set

$$\{\mathbf{b}, \mathbf{c}, \mathbf{A}, \mathbf{d}_k, \mathbf{q}_k, \mathbf{e}_j, \varepsilon_{ij}\},$$

and whose internal vertices encode matrix action, inner product, contraction, or Hadamard multiplication. Fortunately, all of the above operations can be represented as contractions. We illustrate this representation with a few examples.

Figure 2: TTN representations of typical expressions appearing in the Q - and D -conditions.

This representation makes it possible to write all the expressions in Q_m and D_n and in the reduction process in a uniform way as TTNs, which is crucial for the subsequent analysis.

The TTN notation will be used in the subsequent sections for three purposes. First, it provides a uniform way to organize the families of expressions appearing in the Q - and D -conditions. Second, it makes the recursive generation of the spaces Q_m and D_n easier to track, since each recursion step corresponds to a simple extension of an existing tree. Third, it clarifies the later proofs by separating the combinatorial shape of an expression from its coefficient values. For this reason, TTN diagrams will be used below as an auxiliary notation in the formulation and verification of the QD conditions.

3.3 Stepanov's formulation of the Q - and D - conditions

We begin by introducing Stepanov's formulation of the Q - and D -conditions, in which the q -vectors and d -vectors are defined as the residuals of the corresponding C - and D - conditions.

Definition 3.2 ($\Phi(t)$ -vectors). For a rooted tree $t = [t_1 t_2 \dots t_k]$, consider a vector function $\Phi : \mathcal{T} \rightarrow \mathbb{R}^s$ on the set of all rooted trees, defined recursively by

$$\begin{aligned} \Phi([1]) &= \mathbf{1}, \\ \Phi([t_1 t_2 \dots t_k]) &= \bigodot_{i=1}^k (\mathbf{A} \Phi(t_i)), \end{aligned}$$

where $[1] = \bullet$ is a tree with a single vertex.

Definition 3.3 ($Q(t)$ - and $D(t)$ -vectors). For any rooted tree t , define

$$\begin{aligned} Q(t) &= \mathbf{A} \Phi(t) - \mathbf{c}^{|t|}/t!, \\ D(t) &= (\mathbf{b} \odot \Phi(t)) \times^1 \mathbf{A} - (\mathbf{b} \odot (\mathbf{1} - \mathbf{c}^{|t|})/t!). \end{aligned}$$

By the definition, $\mathbf{Q}(t)$ is the difference of $\mathbf{A}\Phi(t)$ and $\frac{1}{t!}\Phi([\bullet^{|t|}])$. These two trees are equivalent if $\mathbf{Q}(t) = \mathbf{0}$. $\mathbf{D}(t)$ is similar but more complicated.

The definition of $\mathbf{Q}(t)$ and $\mathbf{D}(t)$ mimics the C and D simplifying conditions (3) and (4). In fact, $\mathbf{Q}([\bullet^q]) = \mathbf{0}$, $0 \leq q \leq n-1$ is equivalent to $C(n)$, and $\mathbf{D}([\bullet^r]) = \mathbf{0}$, $0 \leq r \leq m-1$ is equivalent to $D(m)$. These vectors measure the deviation of the method from satisfying the C and D conditions, and they play a crucial role in defining the Q - and D -spaces, so we give them a special name as \mathbf{q} - and \mathbf{d} -vectors.

Definition 3.4 (\mathbf{q} - and \mathbf{d} -vectors). For each nonnegative integer n , define

$$\mathbf{q}_n := \mathbf{Q}([\bullet^n]) = \mathbf{A}\mathbf{c}^{\odot n} - \frac{1}{n+1}\mathbf{c}^{\odot(n+1)}, \quad (8)$$

$$\mathbf{d}_n := \mathbf{D}([\bullet^n]) = (\mathbf{b} \odot \mathbf{c}^{\odot n}) \times^1 \mathbf{A} - \frac{1}{n+1}\mathbf{b} \odot (\mathbf{1} - \mathbf{c}^{\odot(n+1)}). \quad (9)$$

The vectors \mathbf{q}_j and \mathbf{d}_j ($j = 0, \dots, n$) measure the deviation of the explicit method from satisfying $C(n+1)$ and $D(n+1)$ conditions. In the implicit case, these residuals would typically vanish, since high order are achieved by satisfying $C(q)$ and $D(r)$ exactly; for explicit schemes, they play a constructive role in defining the $Q^{(\text{St})}$ - and $D^{(\text{St})}$ -*type spaces* introduced below. We add a superscript (St) indicating that this is the type of space defined in Stepanov's article [36].

Before defining the Q - and D -spaces, we introduce auxiliary spaces Φ_p that contain all stage-type vectors up to order p . They correspond to the spans generated by rooted trees of order $\leq p$ in Butcher's theory.

Definition 3.5 (Φ -spaces).

$$\begin{aligned} \Phi_0 &= \text{span}\{\mathbf{1}\}, \\ \Phi_1 &= \text{span}\{\mathbf{1}, \mathbf{c}\}, \\ \Phi_2 &= \text{span}\{\mathbf{1}, \mathbf{c}, \mathbf{A}\mathbf{c}, \mathbf{c}^{\odot 2}\}. \end{aligned} \quad (10)$$

Generally, for $p \geq 3$

$$\Phi_p = \text{span}\{\Phi_{p-1}, \mathbf{A}\Phi_{p-1}, \Phi_q \odot \Phi_{p-q}, 1 \leq q \leq p-1\}. \quad (11)$$

The Φ_p spaces provide the building blocks for defining Q_p and D_p .

The $Q^{(\text{St})}$ -type and $D^{(\text{St})}$ -type spaces are defined in [36] as follows:

Definition 3.6 ($Q^{(\text{St})}$ -spaces).

$$\begin{aligned} Q_0^{(\text{St})} &= \text{span}\{\mathbf{0}\}, \\ Q_1^{(\text{St})} &= \text{span}\{\mathbf{q}_0\}, \\ Q_2^{(\text{St})} &= \text{span}\{\mathbf{q}_1, \mathbf{A}\mathbf{q}_0, \mathbf{q}_0 \odot \mathbf{c}, \mathbf{q}_0\}. \end{aligned}$$

and recursively for $p \geq 3$,

$$Q_p^{(\text{St})} = \text{span}\{\mathbf{q}_{p-1}, \mathbf{A}Q_{p-1}^{(\text{St})}, Q_q^{(\text{St})} \odot \Phi_{p-q}, 1 \leq q \leq p-1\}. \quad (12)$$

Definition 3.7 ($D^{(\text{St})}$ -spaces).

$$\begin{aligned} D_0^{(\text{St})} &= \text{span}\{\mathbf{0}\}, \\ D_1^{(\text{St})} &= \text{span}\{\mathbf{d}_0\}, \\ D_2^{(\text{St})} &= \text{span}\{\mathbf{d}_1, \mathbf{d}_0 \times^1 \mathbf{A}, \mathbf{d}_0 \odot \mathbf{c}, \mathbf{d}_0\}, \end{aligned}$$

and generally for $p \geq 3$,

$$D_p^{(\text{St})} = \text{span}\{\mathbf{d}_{p-1}, D_{p-1}^{(\text{St})} \times^1 \mathbf{A}, D_{p-1}^{(\text{St})} \odot \Phi_1, D(t)(\forall |t| = p)\}. \quad (13)$$

The recursive definitions (12) and (13) imply that the $Q_p^{(\text{St})}$ and $D_p^{(\text{St})}$ spaces depend only on lower-order terms, so they are well-defined. This hierarchical structure is complicated, and leads to quick growth in the number of generators of these spaces. However, it is possible to reduce the number of generators by enforcing linear dependency, which is done in [36] by enforcing the newly added generators to be in the span of the previous ones, so that the dimension of these spaces can be controlled. This strategy can be applied to relatively low orders, but it becomes increasingly difficult to implement for higher orders. This becomes our main motivation to design simpler spaces and give sufficient conditions to guarantee order. In Section 3.4, we will introduce a simplified version of the Q - and D -spaces, which has a much cleaner hierarchical structure and is more suitable for recursive construction of high-order ERK methods.

Q - and D -orthogonality conditions. With the above definitions, the order of the method can be characterized by orthogonality relations between the vectors \mathbf{b} , \mathbf{c} and the subspaces $Q_m^{(\text{St})}$, $D_n^{(\text{St})}$.

Definition 3.8 (Q - and D -orthogonality conditions).

1. Q -orthogonality:

$$\mathbf{b} \cdot Q_m^{(\text{St})} = \{0\}.$$

2. D -orthogonality:

$$D_n^{(\text{St})} \cdot \mathbf{c}^{k-1} = \{0\}, \quad k = 1, \dots, p-n.$$

These conditions can be viewed as generalizations of Butcher's $C(q)$ and $D(r)$ simplifying assumptions. Specifically, the $C(q)$ assumptions can be rewritten compactly as

$$Q_q^{(\text{St})} = \{\mathbf{0}\}, \quad D_r^{(\text{St})} = \{\mathbf{0}\}$$

in the notations of the above orthogonality conditions.

3.4 Simplified Q- and D-spaces for constructive purposes

To enable an efficient recursive construction of ERK methods for arbitrary order p , we introduce simplified definitions of the Q - and D -spaces. These spaces form a subset of those defined by Stepanov, but they preserve all conditions necessary for our constructive framework.

The Q -type spaces. We define the Q -type and D -type spaces as follows:

Definition 3.9 (Q -spaces).

$$\begin{aligned} Q_0 &= \text{span}\{\mathbf{0}\}, \\ Q_1 &= \text{span}\{\mathbf{q}_0\}, \\ Q_2 &= \text{span}\{\mathbf{q}_1, \mathbf{A}\mathbf{q}_0, \mathbf{q}_0 \odot \mathbf{c}, \mathbf{q}_0\}, \end{aligned}$$

and recursively for $p \geq 1$,

$$Q_p = \text{span}\{\mathbf{q}_{p-1}, \mathbf{A}Q_{p-1}, Q_{p-1} \odot \Phi_1\}. \quad (14)$$

The D -type spaces.

Definition 3.10 (D -spaces).

$$\begin{aligned} D_0 &= \text{span}\{\mathbf{0}\}, \\ D_1 &= \text{span}\{\mathbf{d}_0\}, \\ D_2 &= \text{span}\{\mathbf{d}_1, \mathbf{d}_0 \times^1 \mathbf{A}, \mathbf{d}_0 \odot \mathbf{c}, \mathbf{d}_0\}, \end{aligned}$$

and generally for $p \geq 1$,

$$D_p = \text{span}\{\mathbf{d}_{p-1}, D_{p-1} \times^1 \mathbf{A}, D_{p-1} \odot \Phi_1\}. \quad (15)$$

The recursive definitions (14) and (15) imply that the Q_p and D_p spaces depend only on the previous spaces Q_{p-1} and D_{p-1} . This property makes the recursive behavior simpler, so that the elements in these simplified Q - and D -spaces are easy to enumerate. The number of elements in $Q^{(\text{St})}$ - and $D^{(\text{St})}$ -spaces may grow factorially, and we will see it is possible to cut it down to quadratic by carefully enforcing linear dependency. This clean hierarchical structure makes it possible to construct high-order ERK methods recursively.

The Φ -spaces, $Q^{(\text{St})}/D^{(\text{St})}$ -spaces and Q/D -spaces have the following inclusion relations:

$$\begin{array}{ccccccccccc}
\Phi_0 & \subseteq & \Phi_1 & \subseteq & \Phi_2 & \subseteq & \Phi_3 & \subseteq & \cdots & \subseteq & \mathbb{R}^s \\
\cup & & \cup & & \cup & & \cup & & & & \\
Q_0^{(\text{St})} & = & Q_1^{(\text{St})} & \subseteq & Q_2^{(\text{St})} & \subseteq & Q_3^{(\text{St})} & \subseteq & \cdots & \subseteq & \mathbb{R}^s \\
\parallel & & \parallel & & \cup & & \cup & & & & \\
Q_0 & = & Q_1 & \subseteq & Q_2 & \subseteq & Q_3 & \subseteq & \cdots & \subseteq & \mathbb{R}^s
\end{array} \tag{16}$$

and

$$\begin{array}{ccccccccccc}
D_0^{(\text{St})} & \subseteq & D_1^{(\text{St})} & \subseteq & D_2^{(\text{St})} & \subseteq & D_3^{(\text{St})} & \subseteq & \cdots & \subseteq & \mathbb{R}^s \\
\parallel & & \parallel & & \cup & & \cup & & & & \\
D_0 & = & D_1 & \subseteq & D_2 & \subseteq & D_3 & \subseteq & \cdots & \subseteq & \mathbb{R}^s.
\end{array} \tag{17}$$

Our definition of Q - and D -spaces is a subset of Stepanov's definition. The simplification is obtained by removing the $Q_q^{(\text{St})} \odot \Phi_{p-q}$ terms in the definition of $Q_p^{(\text{St})}$ and the $D(t)$ terms in the definition of $D_p^{(\text{St})}$, replacing them with $Q_{p-1} \odot \Phi_1$ and $D_{p-1} \odot \Phi_1$ respectively. The removed Q -terms will be dealt with by simultaneous reduction of the trees using the \mathbf{q} -vectors and the application of Q -ring conditions; the removed D -terms are redundant, which are dealt with by the Q -and- D mutual orthogonality conditions, with no additional conditions needed. The simplified definitions of Q - and D -spaces are sufficient for our construction of high-order ERK methods, and they have a much simpler recursive structure, which makes it easier to enumerate the elements in these spaces and to perform reduction of trees.

3.5 Sufficiency theorem

We now turn the simplified Q - and D -space construction into sufficient order conditions for ERK methods. The purpose of this subsection is to show that, together with the quadrature condition $B(p)$, a finite set of orthogonality and closure conditions on these spaces implies the rooted-tree order conditions up to order p . The proof is organized as a reduction of tree contributions into quadrature terms and residual terms controlled by the Q - and D -spaces.

We now outline the proof strategy for Theorem 3.2. The argument is a reduction of rooted-tree contributions into terms handled by the five stated conditions:

1. **Quadrature terms.** The parts that reduce to pure powers of the stage vector \mathbf{c} are exactly the classical quadrature contributions and are handled by $B(p)$.
2. **Q -residuals.** Local residuals generated inside subtrees are placed in the Q -space hierarchy. The closure condition $QR(m)$ keeps these residuals inside the admissible Q -spaces, and $QO(m)$ eliminates them after weighting at the root.
3. **D -residuals.** If a subtree is too large to be reduced only by the Q -mechanism, the reduction is transferred to the root and represented by a D -space residual. These root-level residuals are eliminated by $DO(n)$.
4. **Mixed residuals.** Terms involving both a Q -residual and a D -residual are eliminated by

the mutual orthogonality condition $QD(m, n)$.

Thus every nonclassical term produced by the tree expansion is assigned to one of the mechanisms above, and a finite induction over the tree structure leaves only the quadrature terms covered by $B(p)$.

To perform the \mathbf{q} -reduction, we establish the following lemma.

Lemma 3.1 (\mathbf{q} -reduction). *For any subtree term $\mathbf{A}\Phi(t)$ with $|t| \leq m$, if the $QR(m)$ condition*

$$Q_{m_1} \odot Q_{m_2} = Q_{m_1}, \quad \forall m_2 \leq m_1 \leq m$$

holds, then it can be decomposed into

$$\mathbf{A}\Phi(t) = \mathbf{q} + \frac{1}{t!} \mathbf{c}^{\odot |t|}$$

for some $\mathbf{q} \in Q_m$.

Proof. Consider any part of the tree t where leaves are attached to a common parent node. This part corresponds to the term

$$\mathbf{A}\mathbf{c}^{\odot k} = \mathbf{q}_k + \frac{1}{k+1} \mathbf{c}^{\odot (k+1)}.$$

for some $k \leq m-1$. Apply this to all leaves attached to the common parent node, we get a new tree with leaves being the form $\mathbf{q}_k + \frac{1}{k+1} \mathbf{c}^{\odot (k+1)}$. To perform the reduction, we focus on any part of the new tree where leaves are attached to a common parent node, and expand by multilinearity of the contraction operation. The result is a sum of terms in one of the following three forms:

1. $\mathbf{A}\mathbf{c}^{\odot k}$ for some $k \leq m-1$;
2. $\mathbf{A} \odot_{i=1}^r \tilde{\mathbf{q}}_i$ for some $\tilde{\mathbf{q}}_i \in Q_{m_i}$, $i = 1, \dots, r$;
3. $\mathbf{A} \left(\odot_{i=1}^r \tilde{\mathbf{q}}_i \odot \mathbf{c}^{\odot k} \right)$ for some $\tilde{\mathbf{q}}_i \in Q_{m_i}$, $i = 1, \dots, r$ and $k \leq m-1 - \sum_{i=1}^r m_i$.

The three types of terms are illustrated in Figure 3. We can perform the reduction for each type of terms as follows.

For the first type of terms, we can perform the reduction again, and the height of the tree is reduced by one. For the second type of terms, we can apply the $QR(m)$ condition to know that $\odot_{i=1}^r \tilde{\mathbf{q}}_i \in Q_{\max_i m_i}$. By the definition of Q_m , we can reduce it to a term of the form

$$\mathbf{q} := \mathbf{A} \odot_{i=1}^r \tilde{\mathbf{q}}_i \in Q_{1+\max_i m_i} \subseteq Q_m.$$

so that the height of the tree is reduced by one. For the third type of terms, we can apply the $QR(m)$ condition to know that $\odot_{i=1}^r \tilde{\mathbf{q}}_i \in Q_{\max_i m_i}$, and then apply the definition of Q_m to

reduce it to a term of the form

$$\bar{q} := \mathbf{A} \left(\bigodot_{i=1}^r \tilde{q}_i \odot \mathbf{c}^{\odot k} \right) \in Q_{1+k+\max_i m_i} \subseteq Q_m.$$

so that the height of the tree is reduced by one. By iterating this reduction procedure, we can eventually reduce the original term $\mathbf{A}\Phi(t)$ into a sum of a term in Q_m and a term in $\text{span}\{\mathbf{c}^{\odot |t|}\}$. The coefficient of the $\mathbf{c}^{\odot |t|}$ term comes from all reductions of the first type, which gives the reciprocal of the size of the reduced subtree. So the final coefficient is $\frac{1}{t!}$ because it is the product of the reciprocal of the size of all reduced subtrees. \square

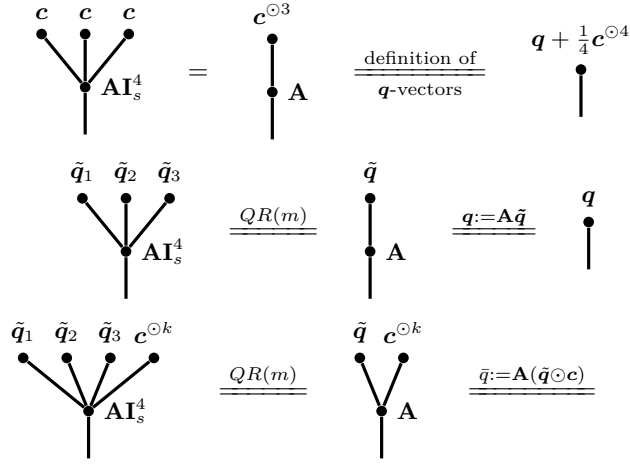


Figure 3: Illustration of the Q -reduction procedure.

The following theorem summarizes the sufficient conditions for an explicit RK method to achieve order p within our framework.

Theorem 3.2. *An explicit Runge–Kutta method has order at least p if the following conditions hold for some m, n with $m \geq n - 1$ and $m + n + 1 \geq p$:*

1. *Quadrature conditions for $[\cdot^{k-1}]$, denoted $B(p)$:*

$$\mathbf{b} \cdot \mathbf{c}^{\odot(k-1)} = \frac{1}{k}, \quad k = 1, \dots, p.$$

2. *Q -orthogonality conditions, denoted $QO(m)$:*

$$\mathbf{b} \odot Q_m = \{\mathbf{0}\}.$$

3. *D -orthogonality conditions, denoted $DO(n)$:*

$$D_n \cdot \mathbf{c}^{\odot(k-1)} = \{0\}, \quad k = 1, \dots, p - n.$$

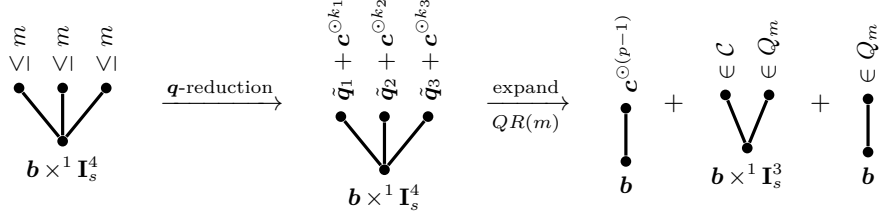
4. *Q-and-D mutual orthogonality conditions, denoted $QD(m, n)$:*

$$Q_m \odot D_n = \{\mathbf{0}\}.$$

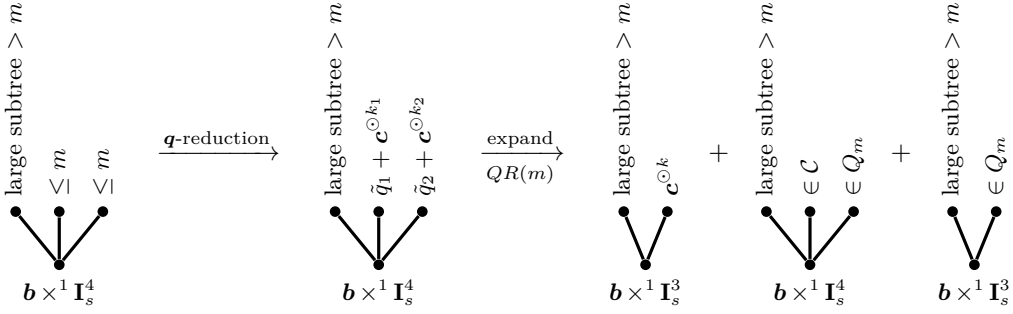
5. *Q-ring condition (the space Q_m form a ring under Hadamard product), denoted $QR(m)$:*

If $m_2 \leq m_1 \leq m$,

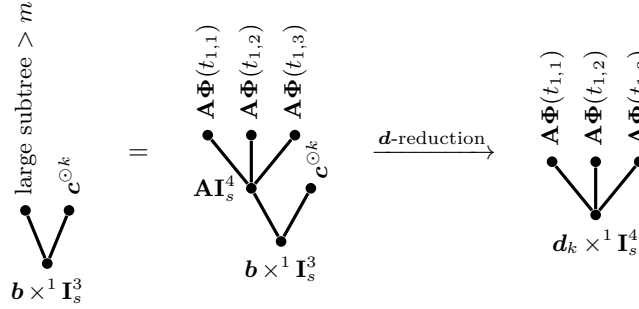
$$Q_{m_1} \odot Q_{m_2} = Q_{m_1}.$$



(a) Case 1: reduction into a pure \mathbf{c} principal term and Q_m remainder terms eliminated by $QO(m)$



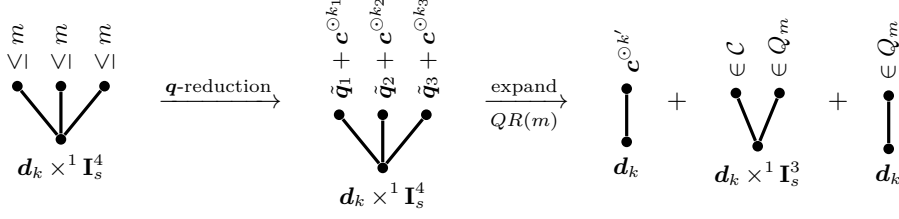
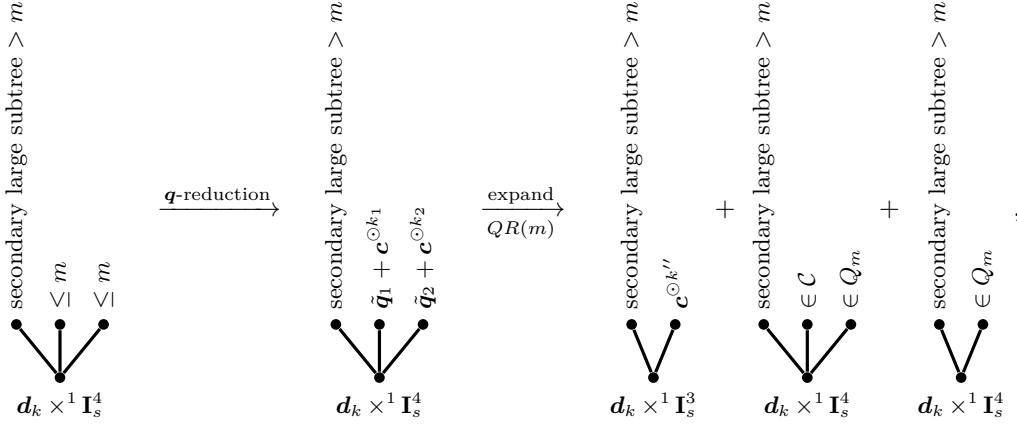
where



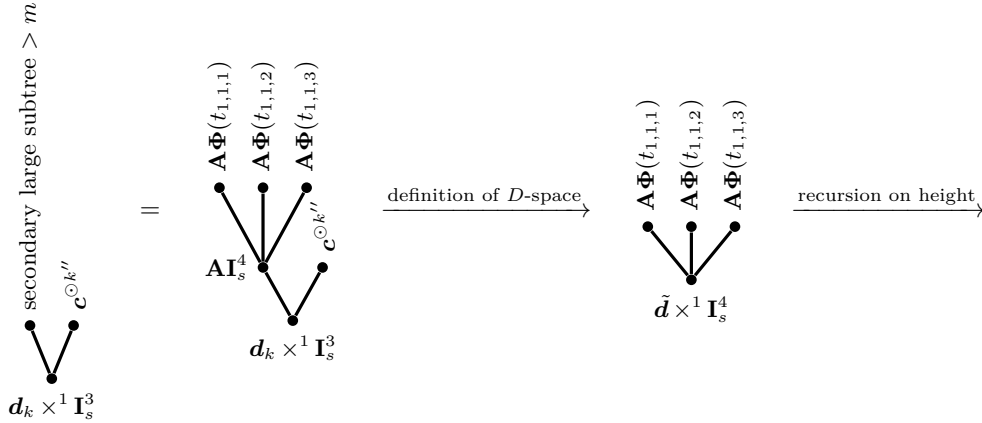
(b) Case 2: reduction into \mathbf{b} -principal terms and a remainder term involving the new root \mathbf{d}_k

Figure 4: Schematic tree decomposition and cancellation mechanism in the sufficiency proof for the Q/D order conditions. The set $\mathcal{C} = \{\mathbf{c}^{\odot k} : k \in \mathbb{Z}_{\geq 0}\}$.

Proof. Consider an arbitrary tree term t of order at most p . The overall idea is to reduce the


 (a) Case 2.1: the remainder is closed by $QR(m)$ and then shown to vanish by $QD(m, n)$.


where



... reduced recursively to Case 2.1 ...

(b) Case 2.2: when a higher-order large subtree remains, induction on the tree height reduces the argument to Case 2.1.

 Figure 5: Schematic tree decomposition and cancellation mechanism for the two subcases of case 2 in the sufficiency proof for the Q/D order conditions. The set $\mathcal{C} = \{c^{\odot k} : k \in \mathbb{Z}_{\geq 0}\}$.

expression by means of the definitions of the \mathbf{q} - and \mathbf{d} -vectors. Compared with the proof based on the original simplifying assumptions, this reduction generates additional remainder terms, and it therefore suffices to show that all such remainder terms vanish.

Let $t = [t_1, \dots, t_r]$. Exactly one of the following two cases must occur:

1. all subtrees have order at most m , that is, $|t_1|, \dots, |t_r| \leq m$;
2. at least one subtree has order greater than m , that is, $\max\{|t_1|, \dots, |t_r|\} > m$.

In case 1, we have

$$\phi(t) = \mathbf{b}^\top \Phi(t) = \mathbf{b}^\top \bigcirc_{i=1}^r \mathbf{A} \Phi(t_i).$$

We reduce each subtree by repeatedly using \mathbf{q} -reduction in Lemma 3.1. This produces two types of terms: a pure \mathbf{c} -term and terms involving \mathbf{q} -vectors. There is only one pure \mathbf{c} -term, which we call the principal term. It already corresponds to a bushy tree and is therefore covered by the $B(p)$ condition, so no further argument is needed. The terms involving \mathbf{q} -vectors are remainder terms. For every such remainder term, the TTN corresponding to each subtree with a \mathbf{q} -vector lies in the space Q_m . Hence all remainder terms vanish by the $QO(m)$ condition.

In case 2, we first show that there exists exactly one subtree whose order is greater than m . Suppose, to the contrary, that there are two subtrees t_i and t_j with orders greater than m . Then

$$|t| \geq |t_i| + |t_j| + 1 \geq 2m + 3.$$

However, by condition $m \geq n - 1$ and $m + n + 1 \geq p$, we have

$$|t| \geq 2m + 3 \geq m + n + 2 \geq p + 1,$$

which contradicts $|t| \leq p$. Therefore, exactly one subtree has order greater than m . Without loss of generality, assume that $|t_1| > m$, so that $|t_2|, \dots, |t_r| \leq m$. For t_2, \dots, t_r , we again reduce by the definition of the \mathbf{q} -vector and the $QR(m)$ condition. By the $QO(m)$ condition, all resulting remainder terms vanish. Thus it remains to consider only the principal term.

In this principal term, t_2, \dots, t_r have all been reduced to pure \mathbf{c} -terms, so the principal term takes the form

$$\mathbf{b}^\top (\mathbf{A} \Phi(t_1) \odot \mathbf{c}^{\odot k}), \quad k = \sum_{i=2}^r |t_i| = p - 1 - |t_1|.$$

We now reduce this term by the definition of the \mathbf{d} -vector.

$$\begin{aligned} \mathbf{b}^\top (\mathbf{A} \Phi(t_1) \odot \mathbf{c}^{\odot k}) &= ((\mathbf{b} \odot \mathbf{c}^{\odot k}) \times^1 \mathbf{A})^\top \Phi(t_1) \\ &= \frac{1}{k+1} (\mathbf{b} \odot (\mathbf{1} - \mathbf{c}^{\odot(k+1)}))^\top \Phi(t_1) + \mathbf{d}_k^\top \Phi(t_1) \end{aligned}$$

Then the principal terms produced by the \mathbf{d} -reduction are $\mathbf{b}^\top \Phi(t_1)$ and $\mathbf{b}^\top (\Phi(t_1) \odot \mathbf{c}^{\odot(k+1)})$, the height of the highest subtree is 1 level lower than $|t_1|$. These are exactly the same terms as those

arising in the reduction under the simplifying order conditions, and reduction proceeds inductively on height hence require no further treatment. Write $t_1 = [t_{1,1}, \dots, t_{1,r_1}]$. The remainder term is

$$R_2 = \mathbf{d}_k^\top \Phi(t_1) = \mathbf{d}_k^\top \left(\bigodot_{i=1}^{r_1} \mathbf{A} \Phi(t_{1,i}) \right).$$

It remains to prove that this term is zero. We distinguish two subcases:

1. If $|t_{1,1}|, \dots, |t_{1,r_1}| \leq m$, then we reduce by the definition of the \mathbf{q} -vector. The tensor associated with each subtree then lies in the space Q_m . By the $QR(m)$ condition, their Hadamard product still belongs to Q_m . Applying the $QD(m, n)$ condition, we conclude that this remainder term is zero. The corresponding principal term, in which all subtrees are replaced by \mathbf{c} , also vanishes by the $DO(n)$ condition.
2. If one of the subtrees, say $t_{1,1}$, has order greater than m , then the remaining subtrees $t_{1,2}, \dots, t_{1,r_1}$ all have order at most m . Performing the \mathbf{q} -reduction and using the $QR(m)$ condition on these subtrees, by $QD(m, n)$, the remainder terms involving \mathbf{q} -vectors vanish. In the principal term, $t_{1,2}, \dots, t_{1,r_1}$ are replaced by \mathbf{c} -terms, so the resulting term is

$$\mathbf{d}_k^\top \left(\mathbf{A} \Phi(t_{1,1}) \odot \mathbf{c}^{\odot \sum_{j=2}^{r_1} |t_{1,j}|} \right) = \left((\mathbf{d}_k \odot \mathbf{c}^{\odot \sum_{j=2}^{r_1} |t_{1,j}|}) \times^1 \mathbf{A} \right)^\top \Phi(t_{1,1}).$$

Since $\sum_{j=2}^{r_1} |t_{1,j}| = |t_1| - 1 - |t_{1,1}| = (p-1-k) - 1 - |t_{1,1}| \leq p-2-k-(m+1) \leq n-2-k$, we have

$$\tilde{\mathbf{d}} := (\mathbf{d}_k \odot \mathbf{c}^{\odot \sum_{j=2}^{r_1} |t_{1,j}|}) \times^1 \mathbf{A} \in D_n.$$

If we write $t_{1,1} = [t_{1,1,1}, \dots, t_{1,1,r_{1,1}}]$, then this term can be written as

$$R_3 = \tilde{\mathbf{d}}^\top \left(\bigodot_{j=1}^{r_{1,1}} \mathbf{A} \Phi(t_{1,1,j}) \right).$$

R_3 has the same form as R_2 , but the height of $t_{1,1}$ is smaller than that of t_1 . We can then apply the same argument to R_3 . By a finite induction on the height of the tree, we eventually reach a tree with all subtrees with sizes at most m , which reduces to subcase 1.

We have thus shown that every remainder term generated in the reduction vanishes. This completes the proof. \square

Next, we give a more general version of the sufficiency theorem.

Theorem 3.3. *An ERK method has order at least p if the following conditions hold for some m, n with $m \geq n-1$ and $m+n+1 \geq p$:*

1. *Quadrature conditions for $[\bullet^{k-1}]$, denoted $B(p)$:*

$$\mathbf{b} \cdot \mathbf{c}^{\odot(k-1)} = \frac{1}{k}, \quad k = 1, \dots, p.$$

2. *Q-orthogonality conditions, denoted $QO(m)$:*

$$\mathbf{b} \odot Q_m = \{\mathbf{0}\}.$$

3. *D-orthogonality conditions, denoted $DO(n)$:*

$$D_n \cdot \mathbf{c}^{\odot(k-1)} = \{0\}, \quad k = 1, \dots, p-n.$$

4. *Weak Q-and-D mutual orthogonality conditions, denoted $QD_{\text{weak}}(m, n)$:*

$$Q_m \cdot D_n = \{0\}.$$

5. *Pivot residual condition, denoted $PR(n)$: Define the space of pivot residual vectors:*

$$W_n = \{(\mathbf{q} \odot \mathbf{d}) \times^1 \mathbf{A} - \mathbf{q} \odot (\mathbf{d} \times^1 \mathbf{A}) \mid \mathbf{q} \in Q_{l_1}, \mathbf{d} \in D_{l_2}, l_1 + l_2 \leq n-1\}.$$

The $PR(n)$ condition is that

$$W_n \cdot \{\Phi(t) \mid m+1 \leq |t| \leq p-3\} = \{0\}. \quad (18)$$

6. *Q-ring condition (the space Q_m form a ring under Hadamard product), denoted $QR(m)$:*

If $m_2 \leq m_1 \leq m$,

$$Q_{m_1} \odot Q_{m_2} = Q_{m_1}.$$

Proof. The proof is essentially the same as that of Theorem 3.2 except case 2.1 and case 2.2, in which the weak Q-and-D mutual orthogonality conditions prevents direct reduction, and the pivot residual condition $PR(n)$ is used to proceed with the reduction and show that the remainder term vanishes. We give a sketch of the argument for these two cases.

In case 2.1, we have two kinds of remainder terms:

$$R_{11} = \mathbf{d}_k^\top \mathbf{q}, \quad R_{12} = \mathbf{d}_k^\top (\mathbf{q} \odot \mathbf{c}^{\odot k'})$$

for some $\mathbf{q} \in Q_m$. By the $QD_{\text{weak}}(m, n)$ condition, R_{11} vanishes. For R_{12} , we write it as

$$R_{12} = (\mathbf{d}_k \odot \mathbf{c}^{\odot k'_1}) \cdot (\mathbf{q} \odot \mathbf{c}^{\odot k'_2}) = 0,$$

where $k'_1 + k'_2 = k'$. Choose $k'_1 = n - k - 1$ and $k'_2 = k' - k'_1$. We have $(\mathbf{d}_k \odot \mathbf{c}^{\odot k'_1}) \in D_n$, and since $m + n + 1 \geq p$, we also have $(\mathbf{q} \odot \mathbf{c}^{\odot k'_2}) \in Q_m$, so R_{12} also vanishes by the $QD_{\text{weak}}(m, n)$ condition (illustrated in Section 3.5).

In case 2.2, we have a remainder term of the form

$$R_2 = \mathbf{d}_k^\top \bigcirc_{j=1}^{r_1} \mathbf{A} \Phi(t_{1,i}).$$

We still perform the \mathbf{q} -reduction using Lemma 3.1 on the subtrees $t_{1,1}, \dots, t_{1,r_1}$, where $|t_{1,1}| > m$ and $|t_{1,j}| \leq m$ for $j = 2, \dots, r_1$. We arrive at 3 types of terms.

$$\begin{aligned} \text{Principal term: } & \mathbf{d}_k^\top (\mathbf{A}\Phi(t_{1,1}) \odot \mathbf{c}^{\odot k''}), \\ \text{Remainder term (type 1): } & R_{21} = \mathbf{d}_k^\top (\mathbf{A}\Phi(t_{1,1}) \odot \mathbf{q}), \\ \text{Remainder term (type 2): } & R_{22} = \mathbf{d}_k^\top (\mathbf{A}\Phi(t_{1,1}) \odot (\tilde{\mathbf{q}} \odot \mathbf{c}^{\odot k''})) \end{aligned}$$

for some $\mathbf{q}, \tilde{\mathbf{q}} \in Q_m$. The principal term of this reduction is dealt with the same way as before, but the remainder terms are not immediately zero because the $QD(m, n)$ condition is not applicable. To deal with the remainder terms, we first claim that the type 2 terms can be transformed to type 1 terms. Define $\tilde{\mathbf{q}}' := \tilde{\mathbf{q}} \odot \mathbf{c}^{\odot k''}$. Since $|t_{1,1}| \geq m + 1$, by some simple calculation we get $\tilde{\mathbf{q}}' \in Q_m$. This becomes exactly the type 1 term. Now we only need to consider the type 1 terms, which can be written as the form

$$\begin{aligned} R_{21} &= ((\mathbf{q} \odot \mathbf{d}_k) \times^1 \mathbf{A}) \cdot \Phi(t_{1,1}) \\ &= ((\mathbf{q} \odot \mathbf{d}_k) \times^1 \mathbf{A}) \cdot \left(\bigodot_{j=1}^{r_{1,1}} \mathbf{A}\Phi(t_{1,1,j}) \right), \end{aligned}$$

for some $\mathbf{q} \in Q_{l_1}$ and $l_1 \leq p - k - 2 - |t_{1,1}| \leq p - k - m - 3 \leq n - k - 2$. By definition, $\mathbf{d}_k \in D_{l_2}$ with $l_2 = k + 1$, so $l_1 + l_2 \leq n - 1$. Hence the pivot residual condition $PR(n)$ applies: there exists some $\mathbf{w} \in W_n$ such that

$$\mathbf{w} = (\mathbf{q} \odot \mathbf{d}_k) \times^1 \mathbf{A} - \mathbf{q} \odot (\mathbf{d}_k \times^1 \mathbf{A}).$$

So, R_2 splits into two terms:

$$R_2 = \mathbf{w} \cdot \left(\bigodot_{j=1}^{r_{1,1}} \mathbf{A}\Phi(t_{1,1,j}) \right) + (\mathbf{q} \odot (\mathbf{d}_k \times^1 \mathbf{A})) \cdot \left(\bigodot_{j=1}^{r_{1,1}} \mathbf{A}\Phi(t_{1,1,j}) \right).$$

The first term vanishes by the $PR(n)$ condition. Denote $\tilde{\mathbf{d}}_{k+1} = \mathbf{d}_k \times^1 \mathbf{A}$, then the second term is actually

$$R_3 := (\mathbf{q} \odot \tilde{\mathbf{d}}_{k+1}) \cdot \left(\bigodot_{j=1}^{r_{1,1}} \mathbf{A}\Phi(t_{1,1,j}) \right)$$

Suppose the largest subtree of $t_{1,1}$ is $t_{1,1,1}$. If $|t_{1,1,1}| \geq m$, then we can perform the \mathbf{q} -reduction on the other subtrees $t_{1,1,2}, \dots, t_{1,1,r_{1,1}}$, and proceed with the same argument as before to reduce to a lower height tree with the same structure as R_3 . By a finite induction on the tree height, we eventually reach a tree of with all subtrees of sizes at most m , which reduces to subcase 2.1 and hence vanishes. \square

$$\begin{array}{c}
 q \quad c^{\odot k} \\
 \diagdown \quad \diagup \\
 \bullet \\
 \mathbf{d}_k \times^1 \mathbf{I}_s^3
 \end{array}
 =
 \begin{array}{c}
 q \odot c^{k_2} \\
 \bullet \\
 \mathbf{d}_k \odot c^{k_1}
 \end{array}$$

Figure 6: Case 2.1: reduction to a weak QD orthogonality term.

$$\begin{array}{c}
 \mathbf{A}\Phi(t_{1,1}) \\
 \bullet \\
 \mathbf{q} \in Q_m \\
 \bullet \\
 \mathbf{d}_k \times^1 \mathbf{I}_s^3
 \end{array}
 =
 \begin{array}{c}
 \mathbf{A}\Phi(t_{1,1,1}) \\
 \bullet \\
 \mathbf{A}\Phi(t_{1,1,2}) \\
 \bullet \\
 \mathbf{A}\Phi(t_{1,1,3}) \\
 \bullet \\
 \mathbf{AI}_s^4 \\
 \bullet \\
 \mathbf{q} \\
 \bullet \\
 \mathbf{d}_k \times^1 \mathbf{I}_s^3
 \end{array}
 \xrightarrow{\text{definition of } W_n}
 \begin{array}{c}
 \mathbf{A}\Phi(t_{1,1,1}) \\
 \bullet \\
 \mathbf{A}\Phi(t_{1,1,2}) \\
 \bullet \\
 \mathbf{A}\Phi(t_{1,1,3}) \\
 \bullet \\
 \mathbf{w} \times^1 \mathbf{I}_s^4
 \end{array}
 +
 \begin{array}{c}
 \mathbf{A}\Phi(t_{1,1,1}) \\
 \bullet \\
 \mathbf{A}\Phi(t_{1,1,2}) \\
 \bullet \\
 \mathbf{A}\Phi(t_{1,1,3}) \\
 \bullet \\
 \mathbf{AI}_s^5 \\
 \bullet \\
 \mathbf{q} \\
 \bullet \\
 \mathbf{d}_k
 \end{array}$$

where

$$\begin{array}{c}
 \mathbf{A}\Phi(t_{1,1,1}) \\
 \bullet \\
 \mathbf{A}\Phi(t_{1,1,2}) \\
 \bullet \\
 \mathbf{A}\Phi(t_{1,1,3}) \\
 \bullet \\
 \mathbf{AI}_s^5 \\
 \bullet \\
 \mathbf{q} \\
 \bullet \\
 \mathbf{d}_k
 \end{array}
 \xrightarrow{\underline{\underline{\mathbf{d}_{k+1} = \mathbf{d}_k \times^1 \mathbf{A}}}}
 \begin{array}{c}
 \mathbf{A}\Phi(t_{1,1,1}) \\
 \bullet \\
 \mathbf{A}\Phi(t_{1,1,2}) \\
 \bullet \\
 \mathbf{A}\Phi(t_{1,1,3}) \\
 \bullet \\
 \mathbf{d}_{k+1} \times^1 \mathbf{I}_s^5
 \end{array}$$

Figure 7: The pivot residual condition $PR(n)$ is used to show that the remainder term in case 2.2 vanishes. The term is split into two terms by the definition of W_n , where the first term vanishes by the $PR(n)$ condition and the second term is reduced to a similar tree with a new root and smaller height.

Remark 3.1. The PR condition is a technical condition that is only needed for the proof, and it is not clear whether it is necessary for the order conditions. It would be interesting to investigate whether this condition can be removed or replaced by a more natural one.

By our observation in the analysis of various high order ERK schemes, the PR condition is often satisfied in a specific way by letting W_n be the zero space, for example in Example 3.3. Even more specifically, the $QD(m, n)$ condition already guarantees $PR(n)$ when m and n satisfy the requirement in the theorem, which makes Theorem 3.2 a special case of Theorem 3.3.

3.6 Examples

To illustrate the previous definition and theorems, we consider several well-known explicit schemes. We show that these schemes all satisfy the conditions of the sufficiency theorem we gave above.

Example 3.1 (classical RK4 method). The classical RK4 method is one of the most famous examples of the RK family, whose Butcher tableau is given below.

$$\begin{array}{c|ccc} 0 & & & \\ \frac{1}{2} & \frac{1}{2} & & \\ \frac{1}{2} & 0 & \frac{1}{2} & \\ 1 & 0 & 0 & 1 \\ \hline & \frac{1}{6} & \frac{1}{3} & \frac{1}{3} & \frac{1}{6} \end{array} .$$

This method satisfies the conditions of Theorem 3.2 till Q_1 and D_2 , and is a special case of our construction presented in this article when $m = 1$, $n = 2$, $p = 4$. The theorem guarantees that it has order 4.

Example 3.2 (Nyström's method of order 5). Nyström's method is a correction of the one originally proposed by Kutta [7]. The method has the following tableau

$$\begin{array}{c|cccccc} 0 & 0 & 0 & 0 & 0 & 0 & 0 \\ \frac{1}{3} & \frac{1}{3} & 0 & 0 & 0 & 0 & 0 \\ \frac{2}{5} & \frac{4}{25} & \frac{6}{25} & 0 & 0 & 0 & 0 \\ 1 & \frac{1}{4} & -3 & \frac{15}{4} & 0 & 0 & 0 \\ \frac{2}{3} & \frac{2}{27} & \frac{10}{9} & -\frac{50}{81} & \frac{8}{81} & 0 & 0 \\ \frac{4}{5} & \frac{2}{25} & \frac{12}{25} & \frac{2}{15} & \frac{8}{75} & 0 & 0 \\ \hline & \frac{23}{192} & 0 & \frac{125}{192} & 0 & -\frac{27}{64} & \frac{125}{192} \end{array} .$$

We can compute the \mathbf{d} and \mathbf{q} -vectors of this tableau.

$$\begin{aligned} \mathbf{d}_0 &= \left[\frac{1}{192} \quad 0 \quad -\frac{25}{576} \quad \frac{1}{36} \quad \frac{9}{64} \quad -\frac{25}{192} \right]^\top, \\ \mathbf{d}_1 &= \left[\frac{1}{384} \quad 0 \quad -\frac{35}{1152} \quad \frac{1}{36} \quad \frac{15}{128} \quad -\frac{15}{128} \right]^\top, \\ \mathbf{q}_0 &= \left[0 \quad 0 \quad 0 \quad 0 \quad 0 \quad 0 \right]^\top, \\ \mathbf{q}_1 &= \left[0 \quad -\frac{1}{18} \quad 0 \quad 0 \quad 0 \quad 0 \right]^\top. \end{aligned}$$

We know that $D_1 = \text{span}\{\mathbf{d}_0\}$, $D_2 = \text{span}\{\mathbf{d}_0, \mathbf{d}_1, \mathbf{d}_0 \times^1 \mathbf{A}, \mathbf{d}_0 \odot \mathbf{c}\}$ and $Q_1 = \text{span}\{\mathbf{q}_0\} = \{\mathbf{0}\}$,

$Q_2 = \text{span}\{\mathbf{q}_1\}$, where $\mathbf{d}_0\mathbf{A}$ and $\mathbf{d}_0 \odot \mathbf{c}$ are computed to be

$$\mathbf{d}_0 \times^1 \mathbf{A} = \begin{bmatrix} 0 & 0 & 0 & 0 & 0 & 0 & 0 \\ 0 & 0 & -\frac{5}{288} & \frac{1}{36} & \frac{3}{32} & -\frac{5}{48} \end{bmatrix}^\top,$$

One can check that they satisfy all conditions 1-5 of Theorem 3.2 till Q_2 and D_2 , the theorem guarantees that it has order 5.

Example 3.3 (Cooper and Verner's 8th order method). Cooper and Verner constructed the 11-stage, 8-th order method in 1972 [10]. Its Butcher tableau is as follows:

0	0	0	0	0	0	0	0	0	0	0	0	
$\frac{1}{2}$	$\frac{1}{2}$	0	0	0	0	0	0	0	0	0	0	
$\frac{1}{2}$	$\frac{1}{4}$	$\frac{1}{4}$	0	0	0	0	0	0	0	0	0	
$\frac{7+\sqrt{21}}{14}$	$\frac{1}{7}$	$-\frac{7-3\sqrt{21}}{98}$	$\frac{21+5\sqrt{21}}{49}$	0	0	0	0	0	0	0	0	
$\frac{7+\sqrt{21}}{14}$	$\frac{11+\sqrt{21}}{84}$	0	$\frac{18+4\sqrt{21}}{63}$	$\frac{21-\sqrt{21}}{252}$	0	0	0	0	0	0	0	
$\frac{1}{2}$	$\frac{5+\sqrt{21}}{48}$	0	$\frac{9+\sqrt{21}}{36}$	$-\frac{231+14\sqrt{21}}{360}$	$\frac{63-7\sqrt{21}}{80}$	0	0	0	0	0	0	
$\frac{7-\sqrt{21}}{14}$	$\frac{10-\sqrt{21}}{42}$	0	$-\frac{432+92\sqrt{21}}{315}$	$\frac{633-145\sqrt{21}}{90}$	$-\frac{504+115\sqrt{21}}{70}$	$\frac{63-13\sqrt{21}}{35}$	0	0	0	0	0	
$\frac{7+\sqrt{21}}{14}$	$\frac{1}{14}$	0	0	0	$\frac{14-3\sqrt{21}}{126}$	$\frac{13-3\sqrt{21}}{63}$	$\frac{1}{9}$	0	0	0	0	
$\frac{1}{2}$	$\frac{1}{32}$	0	0	0	$\frac{91-21\sqrt{21}}{576}$	$\frac{11}{72}$	$-\frac{385-75\sqrt{21}}{1152}$	$\frac{63+13\sqrt{21}}{128}$	0	0	0	
$\frac{7+\sqrt{21}}{14}$	$\frac{1}{14}$	0	0	0	$\frac{1}{9}$	$-\frac{733-147\sqrt{21}}{2205}$	$\frac{515+111\sqrt{21}}{504}$	$-\frac{51-11\sqrt{21}}{56}$	$\frac{132+28\sqrt{21}}{245}$	0	0	
1	0	0	0	0	$-\frac{42+7\sqrt{21}}{18}$	$-\frac{18+28\sqrt{21}}{45}$	$-\frac{273-53\sqrt{21}}{72}$	$\frac{301+53\sqrt{21}}{72}$	$\frac{28-28\sqrt{21}}{45}$	$\frac{49-7\sqrt{21}}{18}$	0	
	$\frac{1}{20}$	0	0	0	0	0	0	0	$\frac{49}{180}$	$\frac{16}{45}$	$\frac{49}{180}$	$\frac{1}{20}$

Compute the \mathbf{d} and \mathbf{q} -vectors of this tableau according to the definitions:

$$\begin{aligned} \mathbf{d}_0 &= \begin{bmatrix} 0 & 0 & 0 & 0 & 0 & 0 & 0 & 0 & 0 & 0 & 0 & 0 \end{bmatrix}^\top, \\ \mathbf{d}_1 &= \begin{bmatrix} 0 & 0 & 0 & 0 & -\frac{7}{144} + \frac{7\sqrt{21}}{720} & -\frac{4}{225} + \frac{8\sqrt{21}}{1575} & -\frac{7}{1440} - \frac{\sqrt{21}}{1440} & \frac{\sqrt{21}}{1440} + \frac{7}{1440} & \frac{4}{225} - \frac{8\sqrt{21}}{1575} & \frac{7}{144} - \frac{7\sqrt{21}}{720} & 0 \end{bmatrix}^\top, \\ \mathbf{d}_2 &= \begin{bmatrix} 0 & 0 & 0 & 0 & -\frac{77}{1080} + \frac{\sqrt{21}}{72} & -\frac{5}{189} + \frac{\sqrt{21}}{105} & -\frac{83}{4320} - \frac{\sqrt{21}}{288} & \frac{\sqrt{21}}{288} + \frac{83}{4320} & \frac{5}{189} - \frac{\sqrt{21}}{105} & \frac{77}{1080} - \frac{\sqrt{21}}{72} & 0 \end{bmatrix}^\top, \\ \mathbf{d}_3 &= \begin{bmatrix} 0 & 0 & 0 & 0 & -\frac{121}{1440} + \frac{23\sqrt{21}}{1440} & -\frac{187}{6300} + \frac{146\sqrt{21}}{11025} & -\frac{113}{2880} - \frac{149\sqrt{21}}{20160} & \frac{149\sqrt{21}}{20160} + \frac{113}{2880} & \frac{187}{6300} - \frac{146\sqrt{21}}{11025} & \frac{121}{1440} - \frac{23\sqrt{21}}{1440} & 0 \end{bmatrix}^\top, \\ \mathbf{q}_0 &= \begin{bmatrix} 0 & 0 & 0 & 0 & 0 & 0 & 0 & 0 & 0 & 0 & 0 \end{bmatrix}^\top, \\ \mathbf{q}_1 &= \begin{bmatrix} 0 & -\frac{1}{8} & 0 & 0 & 0 & 0 & 0 & 0 & 0 & 0 & 0 \end{bmatrix}^\top, \\ \mathbf{q}_2 &= \begin{bmatrix} 0 & -\frac{1}{24} & \frac{1}{48} & -\frac{\sqrt{21}}{392} - \frac{1}{168} & 0 & 0 & 0 & 0 & 0 & 0 & 0 \end{bmatrix}^\top. \end{aligned}$$

Thus, the D -type spaces are $D_1 = \text{span}\{\mathbf{d}_0\} = \mathbf{0}$, $D_2 = \text{span}\{\mathbf{d}_1\}$, $D_3 = \text{span}\{\mathbf{d}_1, \mathbf{d}_2, \mathbf{d}_1 \times^1 \mathbf{A}, \mathbf{d}_1 \odot \mathbf{c}\}$, where

$$\begin{aligned}\mathbf{d}_1 \times^1 \mathbf{A} &= \begin{bmatrix} 0 & 0 & 0 & 0 & 0 & -\frac{1}{350} - \frac{\sqrt{21}}{3150} & \frac{1}{160} + \frac{\sqrt{21}}{720} & -\frac{1}{160} - \frac{\sqrt{21}}{720} & \frac{1}{350} + \frac{\sqrt{21}}{3150} & 0 & 0 \end{bmatrix}^\top, \\ \mathbf{d}_1 \odot \mathbf{c} &= \begin{bmatrix} 0 & 0 & 0 & 0 & -\frac{7}{720} + \frac{\sqrt{21}}{720} & -\frac{2}{225} + \frac{4\sqrt{21}}{1575} & -\frac{1}{720} & \frac{1}{720} & \frac{2}{225} - \frac{4\sqrt{21}}{1575} & \frac{7}{720} - \frac{\sqrt{21}}{720} & 0 \end{bmatrix}^\top.\end{aligned}$$

Since the four vectors in D_3 only span a 3-dimensional space, D_3 can be written as $D_3 = \text{span}\{\mathbf{d}_1, \mathbf{d}_2, \mathbf{d}_1 \odot \mathbf{c}\}$. Then, $D_4 = \text{span}\{D_3, \mathbf{d}_2 \odot \mathbf{c}, \mathbf{d}_1 \odot \mathbf{c}^2, \mathbf{d}_2 \times^1 \mathbf{A}, (\mathbf{d}_1 \odot \mathbf{c}) \times^1 \mathbf{A}\}$, where

$$\begin{aligned}\mathbf{d}_2 \times^1 \mathbf{A} &= \begin{bmatrix} 0 & 0 & \frac{3}{1400} + \frac{\sqrt{21}}{4200} & \frac{\sqrt{21}}{1200} & -\frac{\sqrt{21}}{1200} & -\frac{13}{1800} - \frac{239\sqrt{21}}{264600} & \frac{43}{2880} + \frac{29\sqrt{21}}{8640} & -\frac{43}{2880} - \frac{29\sqrt{21}}{8640} & \frac{8}{1575} + \frac{22\sqrt{21}}{33075} & 0 & 0 \end{bmatrix}^\top, \\ \mathbf{d}_2 \odot \mathbf{c} &= \begin{bmatrix} 0 & 0 & 0 & 0 & -\frac{2}{135} + \frac{\sqrt{21}}{540} & -\frac{5}{378} + \frac{\sqrt{21}}{210} & -\frac{19}{4320} - \frac{11\sqrt{21}}{30240} & \frac{19}{4320} + \frac{11\sqrt{21}}{30240} & \frac{5}{378} - \frac{\sqrt{21}}{210} & \frac{2}{135} - \frac{\sqrt{21}}{540} & 0 \end{bmatrix}^\top, \\ (\mathbf{d}_1 \odot \mathbf{c}) \times^1 \mathbf{A} &= \begin{bmatrix} 0 & 0 & \frac{1}{4200} - \frac{\sqrt{21}}{4200} & -\frac{7}{2400} + \frac{\sqrt{21}}{2400} & \frac{7}{2400} - \frac{\sqrt{21}}{2400} & -\frac{3}{1400} - \frac{11\sqrt{21}}{88200} & \frac{1}{240} + \frac{\sqrt{21}}{1008} & -\frac{1}{240} - \frac{\sqrt{21}}{1008} & \frac{1}{525} + \frac{4\sqrt{21}}{11025} & 0 & 0 \end{bmatrix}^\top, \\ \mathbf{d}_1 \odot \mathbf{c}^2 &= \begin{bmatrix} 0 & 0 & 0 & 0 & -\frac{1}{360} & -\frac{1}{225} + \frac{2\sqrt{21}}{1575} & -\frac{1}{1440} + \frac{\sqrt{21}}{10080} & \frac{1}{1440} - \frac{\sqrt{21}}{10080} & \frac{1}{225} - \frac{2\sqrt{21}}{1575} & \frac{1}{360} & 0 \end{bmatrix}^\top.\end{aligned}$$

The Q -type spaces are given by $Q_1 = \text{span}\{\mathbf{q}_0\} = \{\mathbf{0}\}$, $Q_2 = \text{span}\{\mathbf{q}_1\}$, $Q_3 = \text{span}\{\mathbf{q}_1, \mathbf{q}_2, \mathbf{A}\mathbf{q}_1\}$, where

$$\mathbf{A}\mathbf{q}_1 = \begin{bmatrix} 0 & 0 & -\frac{1}{32} & \frac{1}{112} + \frac{3\sqrt{21}}{784} & 0 & 0 & 0 & 0 & 0 & 0 \end{bmatrix}^\top.$$

One can check that they satisfy all conditions 1-5 of Theorem 3.2 till Q_3 and D_4 , and the theorem guarantees that it has order 8.

Discussion The above examples all satisfy conditions of both sufficiency theorem. It is untrivial to see whether it is possible to construct (explicit) RK schemes that does not satisfy all conditions of either sufficiency theorem, while still achieve the desired order. It looks like that these two sufficiency theorems are not equivalent by construction, but it is also untrivial (though looks easier) to construct an explicit RK scheme that can use one theorem to give the order while not the other.

We give the following conjecture on the necessity of the conditions in the sufficiency theorem:

Conjecture 3.1. The set of conditions in Theorem 3.2 is not only sufficient but also necessary for a vector-valued explicit/implicit RK method to achieve order p .

Proving or giving a counterexample of the conjecture will yield significant impact on the theoretical foundation of simplifying assumptions for explicit RK methods, and further innovate other ideas for construction of related schemes. Unfortunately, this goal is far from accomplished. We don't have a universal way to test all possible methods, and up to now all methods we have tested manually satisfy all conditions for the sufficiency theorem for some m, n , which successfully give the correct order.

4 Recursive construction of high-order ERK methods

4.1 Motivation and overview

The sufficient conditions established in Section 3 provide a structured way to express order requirements through the Q - and D -spaces. In this section, we show that these conditions naturally lead to a recursive procedure for constructing ERK methods of arbitrary order p .

Utilizing the simplified Q/D conditions, it is sufficient to only consider the \mathbf{q}_j or \mathbf{d}_j vectors, their matrix-vector multiplication with \mathbf{A} and their Hadamard product with \mathbf{c} , which significantly reduces the number of vectors in the Q - and D -spaces. The dimension of the Q_j - and D_j -spaces is controlled by choosing the newly added vectors as the subscript j grows. Some of these newly added vectors is uniquely determined by corresponding elements in matrix \mathbf{A} in a linear way, and others, though nonlinear with respect to elements of \mathbf{A} , can be transformed into linear dependency by a carefully designed recursive construction.

Conceptually, the recursion is built from two mutually orthogonal sequences of subspaces — the Q -type and D -type spaces — that expand stage by stage. By controlling the dimension growth of these spaces, we can design methods of arbitrarily high order while maintaining a compact stage structure.

4.2 Strategy of the construction

The recursive construction aims to enforce the Q - and D -orthogonality relations while keeping the dimensions of the Q - and D -spaces small and tractable. The construction follows a sequential linear approach: first, we solve a system derived from the D -space requirements to determine a subset of the RK coefficients; then, these results are used to form and solve a second system derived from the Q -space requirements.

The three guiding principles are:

1. **Enforce orthogonality through subspace design:** place \mathbf{b} , Q_m and D_n into carefully chosen coordinate subspaces V_l, V_l^*, V_l^0 so that the required orthogonality relations hold automatically;
2. **Use cluster conditions to localize constraints:** exploit stage clusters (groups of equal or related c_i) to simplify and localize the D -conditions; and
3. **Suppress dimension growth:** control $\dim Q_m$ and $\dim D_n$ at each recursion step so that only a small number of new unknowns appear when a new column of \mathbf{A} is determined.

The rest of this section makes these principles precise and explains the step-by-step construction of the matrix \mathbf{A} .

4.2.1 Principle 1: Enforce orthogonality through subspace design

The essence of the construction lies in pre-positioning \mathbf{b} , Q_m , and D_n into carefully designed complementary coordinate subspaces, such that most abstract orthogonality requirements are

automatically satisfied. We define the following coordinate subspaces:

$$\begin{aligned} V_l &= \{v \in \mathbb{R}^s : v = (*, \underbrace{0, \dots, 0}_l, \underbrace{*, \dots, *}_{s-1-l})^\top\}, \\ V_l^* &= \{u \in \mathbb{R}^s : u = (0, \underbrace{*, \dots, *}_l, \underbrace{0, \dots, 0}_{s-1-l})^\top\}, \\ V_l^0 &= \{v \in \mathbb{R}^s : v = (0, \underbrace{0, \dots, 0}_l, \underbrace{*, \dots, *}_{s-1-l})^\top\}, \end{aligned}$$

where $*$ means that the corresponding coordinate can be any real number. In words:

- V_l contains vectors that are **possibly nonzero** in the first coordinate and in the last $s-1-l$ coordinates, but are **zero** in the middle block of length l ;
- V_l^* contains vectors supported exactly on that middle block of length l (and zero elsewhere); and
- V_l^0 contains vectors supported on the last $s-1-l$ coordinates (and zero in the first coordinate and the middle block).

In the construction, we require

$$\mathbf{b} \in V_l, \quad Q_m \subseteq V_l^*, \quad D_n \subseteq V_l^0. \quad (19)$$

These strategies bring several benefits:

1. **Automatic satisfaction of Q -orthogonality:** Since $Q_m \subseteq V_l^*$ and $\mathbf{b} \in V_l$, we have $\mathbf{b} \odot \mathbf{q} = \mathbf{0}$ for all $\mathbf{q} \in Q_m$; thus the $QO(m)$ condition is enforced by construction.
2. **Q -and- D -mutual orthogonality:** Since $Q_m \subseteq V_l^*$ and $D_n \subseteq V_l^0$ have disjoint supports (middle block vs. last block), this ensures $\mathbf{d} \odot \mathbf{q} = \mathbf{0}$ for any a vector $\mathbf{q} \in Q_m$ and $\mathbf{d} \in D_n$.
3. **Separation from the subsequent construction:** placing D_n in V_l^0 means that the coefficients adjusted to satisfy the D -constraints act only on the coordinate block corresponding to the lower-right part of the Butcher tableau. As a result, the prescribed support-separation structure is preserved, and the D -part remains algebraically separated from the middle coordinate block used later for the Q -part. This separation is guaranteed by Propositions 4.3 and 4.4.

Thus the subspaces V_l, V_l^*, V_l^0 are designed exactly to convert the abstract orthogonality relations into simple block-support conditions on vectors. In the recursion we choose l (and hence these subspaces) according to the dimension of the Q -space.

4.2.2 Principle 2: Use cluster conditions to localize constraints

To further simplify and localize the constraints on the D -type spaces, we introduce node clusters and the corresponding cluster conditions.

Definition 4.1 (Node cluster). Let $\mathbf{c} = (c_1, \dots, c_s)^\top$ be the stage vector, and fix a node value ξ . The node cluster associated with ξ is defined as the set of stage indices lying in the support range of V_l^0 and carrying the same node value:

$$S(\xi) := \{i \in \{l+2, \dots, s\} : c_i = \xi\}.$$

If S is a node cluster, we denote by $\mathbf{1}_S \in \mathbb{R}^s$ its indicator vector, namely

$$(\mathbf{1}_S)_i = \begin{cases} 1, & i \in S, \\ 0, & i \notin S. \end{cases}$$

Definition 4.2 (Cluster condition). Let \mathcal{S} be the collection of all node clusters contained in $\{l+2, \dots, s\}$. We say that a vector $\mathbf{d} = (d_1, \dots, d_s)^\top \in \mathbb{R}^s$ satisfies the cluster condition if

$$\mathbf{d} \cdot \mathbf{1}_S = 0$$

for every node cluster $S \in \mathcal{S}$, or equivalently,

$$\sum_{i \in S} d_i = 0.$$

If this relation holds for every $\mathbf{d} \in D_n$, then we say that the space D_n satisfies the cluster condition.

We impose the following cluster condition on D_n : For all node clusters S ,

$$D_n \cdot \mathbf{1}_S = \{0\}. \tag{20}$$

This condition requires the D -type residuals to sum to zero within each prescribed node cluster. It has two important advantages:

- it substantially reduces the number of D -constraints that would otherwise have to be enforced independently across different rows; and
- it allows us to satisfy complicated inter-stage couplings by modifying only a few coefficients within each cluster, thereby producing a localized decoupling of the system.

Although this cluster condition is weaker than the cluster co-order conditions used in some other formulations, for example in [36], it is sufficient for our recursive construction. Indeed, it reduces the effective degrees of freedom of D_n to a range that remains controllable through the subspace design described above.

4.2.3 Principle 3: Suppress dimension growth

The number of stages s is now determined by the dimensions of the Q - and D -spaces. In order to construct methods with fewer stages, we have to limit the growth of the Q - and D -spaces. In practice, we enforce the following conditions:

$$D_i \odot \mathbf{c} \subseteq D_i, \quad i = 1, 2, \dots, n-1, \quad (21)$$

$$Q_j \odot \mathbf{c} \subseteq Q_j, \quad j = 1, 2, \dots, m-1. \quad (22)$$

These conditions ensure that the Hadamard products with \mathbf{c} do not increase the dimension of the Q - and D -spaces. This is a crucial step to control the growth of these spaces and thus the number of stages. These conditions can be enforced by carefully designing the basis vectors that span the Q - and D -spaces, details of which will be given in Sections 4.4 and 4.5.

As a result, a *dimensional suppression* effect occurs, where the dimension of the Q - and D -spaces grows much more slowly than the number of rooted trees. In particular, we can ensure that

$$\dim Q_m - \dim Q_{m-1} \leq m-1, \quad \text{and} \quad \dim D_n - \dim D_{n-1} \leq n-1.$$

Concretely, when we design the m -th level in the recursion way:

1. Choose the new column(s) of \mathbf{A} so that the newly produced \mathbf{q}_{m-1} , $Q_{m-1}\mathbf{A}$ (and the generated span) lie inside the prescribed support set V_l^* and thus $\dim Q_m$ increases by only a controlled amount; and
2. Use the bottom right triangular part (starting from column $l+2$) of \mathbf{A} to enforce the cluster conditions and to ensure $D_n \subseteq V_l^0$.

This strategy yields several practical benefits: it reduces the number of stages needed and produces a highly structured tableau. In particular:

- **Computational efficiency and locality:** the recursion is decomposed into a sequential solution of small linear systems. The right-hand side of each system depends only on previously determined quantities, which avoids globally ill-conditioned couplings.
- **Parametrization and analyticity:** because of the imposed subspace design and cluster conditions, most entries of \mathbf{A} become analytic functions of only a few free parameters. This greatly simplifies symbolic derivations, automated scheme generation, and coefficient verification.
- **Reuse of structural features:** the resulting Butcher tableau naturally exhibits block structure and repeated nodes. In practical time stepping, this can be exploited to reuse stage-function evaluations; in theoretical developments, it also helps in deriving accurate embedded pairs.
- **Numerical robustness:** the small-scale and well-conditioned coefficient systems substan-

tially improve the accuracy of coefficient computation for high-order methods, especially for $p \geq 10$, and reduce the risk that rounding errors invalidate the construction conditions.

Summary. In summary, the core idea of the construction is to convert the abstract orthogonality requirements into simple **support constraints** and **component-sum constraints**. Using these mechanisms, we may choose, in the main construction for even order $p \geq 4$,

$$m = \frac{p}{2} - 1, \quad n = \frac{p}{2}, \quad (23)$$

and define

$$l := \dim(Q_m) = \frac{m(m-1)}{2}. \quad (24)$$

This choice satisfies the parameter relations from Section 3 and matches the block structure used in the subsequent construction.

4.3 Stage arrangement and quadrature initialization

To initialize the recursion, we fix the quadrature nodes and weights. These define the basic skeleton of the method and determine the natural partition of stages into clusters.

For the construction of ERK methods of order p , we select the N -point Lobatto quadrature on $[0, 1]$ such that $2N - 2 \geq p$. The number N should be chosen as small as possible, e.g., $N = \lceil (p+2)/2 \rceil$. In the even-order construction below, this gives $N = n+1$. The Lobatto points are denoted as $\{x_i\}_{i=1}^N$, and the corresponding weights are denoted as $\{w_i\}_{i=1}^N$.

Remark 4.1. The Gauss-Lobatto quadrature is chosen to satisfy the quadrature conditions. Since $\mathbf{b} \in V_l$, it takes zeros in the middle block of length l . So, in order to achieve high order, a Gauss-type quadrature is preferred to lower stage number and form clusters. We choose the Gauss-Lobatto quadrature mainly because it includes endpoints and the number of internal nodes fits our construction of D -type spaces well. Gauss-Legendre quadrature is not a valid choice, since for explicit methods, the left endpoint must be zero. But the Gauss-Radau quadrature of type I, which includes the left endpoint, is also a valid choice.

The arrangement of the stage vector $\{c_i\}_{i=1}^s$ and the weight vector $\{b_i\}_{i=1}^s$ is designed to match exactly the coordinate subspaces V_l , V_l^* , and V_l^0 defined in Section 4.2:

1. Endpoint initialization: First, use c_1 and c_s for the first and the last quadrature points, i.e. stages $c_1 = x_1$ and $c_s = x_N$, and weights $b_1 = w_1$ and $b_s = w_N$.

2. Q-type group nodes c_2, \dots, c_{l+1} (corresponding to V_l^*): For the nodes within the V_l^* subspace, the b_i are set to zero, and the c_i nodes remain undetermined. We call these the

Q -groups:

$$\begin{array}{l|llll} Q\text{-group 1} & c_2 & & & \\ Q\text{-group 2} & c_3 & c_4 & & \\ \vdots & \vdots & \vdots & \ddots & \\ Q\text{-group } (m-1) & c_{l-m+2} & c_{l-m+3} & \cdots & c_{l+1} \end{array}$$

where $l = \frac{m(m-1)}{2}$ is the number of stages in the Q -group.

3. D -type group nodes c_{l+2}, \dots, c_{s-1} (corresponding to V_l^0): For the internal nodes, we form clusters in the V_l^0 subspace, which are arranged in the following way. Positions $l+2$ to $l+N-1$ are ghost nodes:

$$\text{ghost group : } c_{l+2} = x_{N-1}, \quad c_{l+3} = x_{N-2}, \quad \cdots, \quad c_{l+N-1} = x_2.$$

Positions $l+N$ to $l+s-1$ are $N-2$ groups of nodes:

$$\begin{array}{l|llllll} D\text{-group } (N-2) & c_{l+N} = x_{N-1} & c_{l+N+1} = x_{N-2} & c_{l+N+2} = x_{N-3} & \cdots & c_{l+2N-4} = x_3 & c_{l+2N-3} = x_2 \\ D\text{-group } (N-3) & c_{l+2N-2} = x_{N-1} & c_{l+2N-1} = x_{N-2} & c_{l+2N} = x_{N-3} & \cdots & c_{l+3N-6} = x_3 & \\ \vdots & \vdots & \vdots & \vdots & \ddots & & \\ D\text{-group 3} & c_{s-7} = x_{N-1} & c_{s-6} = x_{N-2} & c_{s-5} = x_{N-3} & & & \\ D\text{-group 2} & c_{s-4} = x_{N-1} & c_{s-3} = x_{N-2} & & & & \\ D\text{-group 1} & c_{s-2} = x_{N-1} & & & & & \end{array}$$

In the above arrangement, each row is viewed as a group. The j^{th} group has j elements. The general arrangement in the j^{th} group is as follows:

$$\begin{aligned} c_{s-2-(j+1)j/2+1} &= x_{N-1}, \\ c_{s-2-(j+1)j/2+2} &= x_{N-2}, \\ c_{s-2-(j+1)j/2+3} &= x_{N-3}, \\ &\vdots \\ c_{s-2-(j+1)j/2+j} &= x_{N-j}. \end{aligned}$$

As notational convenience, we now define a set of "basis" vectors with respect to the groups.

In Table 1, the basis vectors $\varepsilon_{j,i} \in \mathbb{R}^s$ corresponding to stage $k_j = s - 2 - (j+1)j/2 + i$ (we write it on the same line with c_k) is defined as

$$\varepsilon_{j,i}(r) = \begin{cases} 1, & r = k_j, \\ -1 & r = l + 1 + i, \\ 0, & \text{otherwise,} \end{cases}$$

for $r = 1, \dots, s$.

Table 1: The basis vectors with respect to the groups, where $j = 1, 2, \dots, N - 2$ is the D -group index.

stage values	basis vectors
$c_{s-2-(j+1)j/2+1} = x_{N-1}$	$\boldsymbol{\varepsilon}_{j,1}$
$c_{s-2-(j+1)j/2+2} = x_{N-2}$	$\boldsymbol{\varepsilon}_{j,2}$
$c_{s-2-(j+1)j/2+3} = x_{N-3}$	$\boldsymbol{\varepsilon}_{j,3}$
\vdots	\vdots
$c_{s-2-(j+1)j/2+j} = x_{N-j}$	$\boldsymbol{\varepsilon}_{j,j}$

It is straightforward to verify that, for fixed $i \leq N - 2$, the stages at positions

$$k_j = s - 2 - \frac{(j+1)j}{2} + i, \quad i \leq j \leq N - 2,$$

and the ghost stage at position $l + 1 + i$ all have the same node value x_{N-i} . Therefore, by Definition 4.1, the node cluster associated with x_{N-i} in the present construction is precisely formed by these stages. For later use in the construction of the D -type spaces, we define the vector $\boldsymbol{\mu}_i$ associated with this node cluster by

$$\boldsymbol{\mu}_i(r) = \mathbf{1}_{S(x_{N-i})}, \quad (25)$$

where $\mathbf{1}_{S(x_{N-i})}$ is the characteristic vector of the node cluster set $S(x_{N-i})$.

After the stage values are determined, we construct the weights b_i . The first weight b_1 is set to w_1 , and the last weight b_s is set to w_N . Since we require $\mathbf{b} \in V_l$, positions 2 to $l + 1$ of \mathbf{b} are zero. For the remaining entries, the weights assigned to stages carrying the same node value must sum to the corresponding quadrature weight, namely

$$\sum_{i \in S(x_j)} b_i = w_j, \quad j = 1, \dots, N. \quad (26)$$

Equation (26) guarantees that the node-cluster arrangement is consistent with the quadrature condition $B(p)$.

Remark 4.2. The way of arranging the stage vector \mathbf{c} is not unique. The idea is that it is arranged in a similar recursive way as the D -type spaces, so that solvability of the conditions arising from the construction of D -type spaces can be ensured.

Under the same structure, other valid arrangements can be given by shuffling the bases in the same group. Of course, other types of arrangements are also valid as long as they do not result in internally contradictory systems when we construct spaces to fulfill the sufficient conditions for order.

Example 4.1. We illustrate the stage arrangement for $p = 10$ in Figure 8, where $n = 5$, $N = 6$, $l = 6$, $s = 22$. A 6-point Lobatto quadrature rule with nodes $\{x_i\}_{i=1}^6$ and weights $\{w_i\}_{i=1}^6$ is

used to construct the stage vector \mathbf{c} and weights \mathbf{b} . The stage vector \mathbf{c} is shown vertically on the left of the tableau, and the weight vector \mathbf{b} is shown horizontally at the bottom of the tableau. $c_i, i = 1, \dots, 6$ are free parameters, and the weights satisfy

$$\begin{aligned} w_{44} + w_{54} &= w_2, \\ w_{33} + w_{43} + w_{53} &= w_3, \\ w_{22} + w_{32} + w_{42} + w_{52} &= w_4, \\ w_{11} + w_{21} + w_{31} + w_{41} + w_{51} &= w_5. \end{aligned}$$

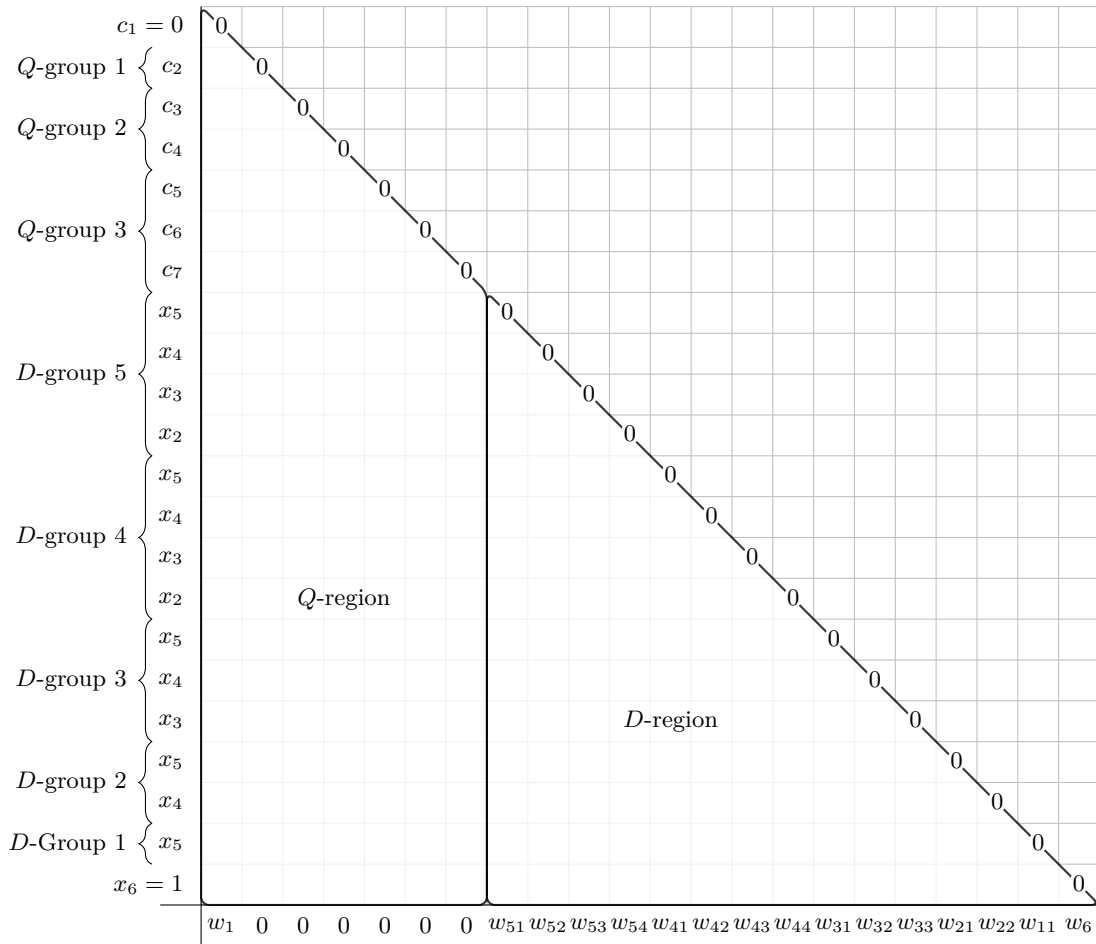


Figure 8: Stage arrangement for $p = 10$.

The two regions, D -region and Q -region in the figure, correspond to the parameters in matrix \mathbf{A} that will be utilized to construct D -type spaces and Q -type spaces, respectively.

4.4 Construction of the D -type spaces

We now formulate the recursive constraints defining the D -type spaces. These constraints are imposed in the D -region of the tableau, from the bottom rows upward, so as to enforce the cluster conditions and ultimately obtain $D_n \subset V_l^0$. The first few levels make the general pattern explicit and show how the dimensions of the D -spaces are controlled.

4.4.1 Systematic imposition of D -space constraints

D_1 .

By definition,

$$D_1 = \text{span}\{\mathbf{d}_0\}.$$

We require that $\mathbf{d}_0 = \mathbf{0}$, this is equivalent to the condition $\mathbf{b} \times^1 \mathbf{A} = \mathbf{b} \odot (\mathbf{1} - \mathbf{c})$. We use the last row of \mathbf{A} to enforce this condition.

Now, under this condition, we have $D_1 = \{\mathbf{0}\}$, and the dimension of D_1 is 0.

D_2 .

By definition,

$$D_2 = \text{span}\{\mathbf{d}_1\}.$$

For \mathbf{d}_1 , we require that $\mathbf{d}_1 \in \text{span}\{\boldsymbol{\varepsilon}_{11}\}$. We assign the $(s-1)$ th row of \mathbf{A} to satisfy this condition. Note that since $\boldsymbol{\varepsilon}_{11}$ satisfies the cluster conditions, so \mathbf{d}_1 will also satisfy the cluster conditions by construction. This requirement can also be written as

$$D_2 \subseteq \text{span}\{\boldsymbol{\varepsilon}_{11}\}.$$

D_3 .

Since $\mathbf{d}_1 \in \text{span}\{\boldsymbol{\varepsilon}_{11}\}$, $c_{s-2} = x_{N-1} = c_{l+2}$, we have $\mathbf{d}_1 \odot \mathbf{c}^{\odot k} \in \text{span}\{\boldsymbol{\varepsilon}_{11}\}$ and $D_2 \odot \mathbf{c}^{\odot k} \subseteq D_2$ for any $k \in \mathbb{Z}_+$.

Using D_2 ,

$$D_3 = \text{span}\{\mathbf{d}_2, \mathbf{d}_1 \times^1 \mathbf{A}, \mathbf{d}_1 \odot \mathbf{c}, \mathbf{d}_1\} \subseteq \text{span}\{\boldsymbol{\varepsilon}_{11}, \boldsymbol{\varepsilon}_{11} \times^1 \mathbf{A}, \mathbf{d}_2\}.$$

We require that

$$\boldsymbol{\varepsilon}_{11} \times^1 \mathbf{A}, \mathbf{d}_2 \in \text{span}\{\boldsymbol{\varepsilon}_{11}, \boldsymbol{\varepsilon}_{21}, \boldsymbol{\varepsilon}_{22}\},$$

so that

$$D_3 \subseteq \text{span}\{\boldsymbol{\varepsilon}_{11}, \boldsymbol{\varepsilon}_{21}, \boldsymbol{\varepsilon}_{22}\}.$$

This will occupy another part of 2 rows (row $s-2$ and $s-3$) in the table of \mathbf{A} . Similar to D_2 , we have $D_3 \odot \mathbf{c} \subseteq D_3$.

D_4 .

Using D_3 ,

$$D_4 = \text{span}\{\mathbf{d}_3, D_3 \times^1 \mathbf{A}, D_3 \odot \mathbf{c}, D_3\} \subseteq \text{span}\{\boldsymbol{\varepsilon}_{11}, \boldsymbol{\varepsilon}_{21}, \boldsymbol{\varepsilon}_{22}, \boldsymbol{\varepsilon}_{21} \times^1 \mathbf{A}, \boldsymbol{\varepsilon}_{22} \times^1 \mathbf{A}, \mathbf{d}_3\}$$

We require that

$$\boldsymbol{\varepsilon}_{21} \times^1 \mathbf{A}, \boldsymbol{\varepsilon}_{22} \times^1 \mathbf{A}, \mathbf{d}_3 \in D_3 + \text{span}\{\boldsymbol{\varepsilon}_{31}, \boldsymbol{\varepsilon}_{32}, \boldsymbol{\varepsilon}_{33}\},$$

which implies

$$D_4 \subseteq \text{span}\{\boldsymbol{\varepsilon}_{11}, \boldsymbol{\varepsilon}_{21}, \boldsymbol{\varepsilon}_{22}, \boldsymbol{\varepsilon}_{31}, \boldsymbol{\varepsilon}_{32}, \boldsymbol{\varepsilon}_{33}\}.$$

This will occupy row $s-4$, $s-5$ and $s-6$ in the table of \mathbf{A} . Similar to D_3 , we have $D_4 \odot \mathbf{c} \subseteq D_4$.

General D_n .

For general D_n , using the same construction pattern as above, we can show that

$$D_n \subseteq \text{span}\{\boldsymbol{\varepsilon}_{11}, \boldsymbol{\varepsilon}_{21}, \boldsymbol{\varepsilon}_{22}, \dots, \boldsymbol{\varepsilon}_{n-1,1}, \boldsymbol{\varepsilon}_{n-1,2}, \dots, \boldsymbol{\varepsilon}_{n-1,n-2}, \boldsymbol{\varepsilon}_{n-1,n-1}\}. \quad (27)$$

For $n \leq 4$ we have already shown that our construction of D_n satisfies (27). The general construction follows a recursive process: Suppose that D_{n-1} space satisfies (27). By definition of the D_n space,

$$D_n = \text{span}\{\mathbf{d}_{n-1}, D_{n-1} \times^1 \mathbf{A}, D_{n-1} \odot \mathbf{c}, D_{n-1}\}.$$

Since

$$D_{n-1} \subseteq \text{span}\{\boldsymbol{\varepsilon}_{11}, \boldsymbol{\varepsilon}_{21}, \boldsymbol{\varepsilon}_{22}, \dots, \boldsymbol{\varepsilon}_{n-2,1}, \boldsymbol{\varepsilon}_{n-2,2}, \dots, \boldsymbol{\varepsilon}_{n-2,n-3}, \boldsymbol{\varepsilon}_{n-2,n-2}\},$$

we know that $D_{n-1} \odot \mathbf{c} \subseteq D_{n-1}$. Since $D_{n-2} \times^1 \mathbf{A} \subseteq D_{n-1}$, by requiring

$$\boldsymbol{\varepsilon}_{n-2,1} \times^1 \mathbf{A}, \dots, \boldsymbol{\varepsilon}_{n-2,n-2} \times^1 \mathbf{A}, \mathbf{d}_{n-1} \in D_{n-1} + \text{span}\{\boldsymbol{\varepsilon}_{n-1,1}, \boldsymbol{\varepsilon}_{n-1,2}, \dots, \boldsymbol{\varepsilon}_{n-1,n-1}\}, \quad (28)$$

we have

$$\begin{aligned} D_n &= \text{span}\{\mathbf{d}_{n-1}, D_{n-1} \times^1 \mathbf{A}, D_{n-1} \odot \mathbf{c}, D_{n-1}\} \\ &= D_{n-1} + \text{span}\{\boldsymbol{\varepsilon}_{n-2,1} \times^1 \mathbf{A}, \dots, \boldsymbol{\varepsilon}_{n-2,n-2} \times^1 \mathbf{A}, \mathbf{d}_{n-1}\} \\ &\subseteq \text{span}\{\boldsymbol{\varepsilon}_{11}, \boldsymbol{\varepsilon}_{21}, \boldsymbol{\varepsilon}_{22}, \dots, \boldsymbol{\varepsilon}_{n-1,1}, \boldsymbol{\varepsilon}_{n-1,2}, \dots, \boldsymbol{\varepsilon}_{n-1,n-2}, \boldsymbol{\varepsilon}_{n-1,n-1}\}. \end{aligned}$$

The requirement (28) will occupy row $s - \frac{(n-1)(n-2)}{2} - 1, \dots, s - \frac{(n-1)(n-2)}{2} - (n-1)$ in the table of \mathbf{A} .

We prove this by induction using the above construction, and the general pattern can be deduced from the proof. Suppose that the above hold for D_k for $k = 1, \dots, n-1$. By definition of D -type spaces,

$$D_n = \text{span}\{D_{n-1}, D_{n-1} \times^1 \mathbf{A}, D_{n-1} \odot \mathbf{c}, \mathbf{d}_{n-1}\}.$$

Since

$$D_{n-1} = \text{span}\{\boldsymbol{\varepsilon}_{11}, \boldsymbol{\varepsilon}_{21}, \boldsymbol{\varepsilon}_{22}, \dots, \boldsymbol{\varepsilon}_{n-2,1}, \boldsymbol{\varepsilon}_{n-2,2}, \dots, \boldsymbol{\varepsilon}_{n-2,n-3}, \boldsymbol{\varepsilon}_{n-2,n-2}\},$$

we know that $D_{n-1} \odot \mathbf{c} \subseteq D_{n-1}$. We require that

$$\begin{aligned} D_{n-1} \times^1 \mathbf{A} + \text{span}\{\mathbf{d}_{n-1}\} &\subseteq \text{span}\{\boldsymbol{\varepsilon}_{11}, \boldsymbol{\varepsilon}_{21}, \boldsymbol{\varepsilon}_{22}, \dots \\ &\quad \boldsymbol{\varepsilon}_{n-3,1}, \boldsymbol{\varepsilon}_{n-3,2}, \dots, \boldsymbol{\varepsilon}_{n-3,n-4}, \boldsymbol{\varepsilon}_{n-3,n-3}, \\ &\quad \boldsymbol{\varepsilon}_{n-2,1}, \boldsymbol{\varepsilon}_{n-2,2}, \dots, \boldsymbol{\varepsilon}_{n-2,n-3}, \boldsymbol{\varepsilon}_{n-2,n-2}\}. \end{aligned}$$

The right hand side is exactly D_n .

4.4.2 Formulation of the D -system

Similar to the Q -type spaces, we convert the subspace inclusion requirements for D_n into a structured linear system. This system determines the rows of \mathbf{A} corresponding to the cluster indices.

Variables The variables for the D -system are the entries a_{ij} in the bottom right part (D -region) of \mathbf{A} . More precisely, for each D_k , $1 \leq k \leq n$, define an associated index set I_k^D by

$$\begin{aligned} I_1^D &= \{(i, j) \in \mathbb{Z}^2 : i = s, l + 2 \leq j \leq s - 1\} \\ I_k^D &= \left\{ (i, j) \in \mathbb{Z}^2 : s - 1 - \frac{k(k-1)}{2} < i \leq s - 1 - \frac{(k-1)(k-2)}{2}, \right. \\ &\quad \left. l + 2 \leq j \leq s - 1 - \frac{k(k-1)}{2} \right\}, \quad \text{for } 2 \leq k \leq n. \end{aligned}$$

where l is the same number as in V_l , and $n = N - 1$ is the level of the target D_n -space. I_1^D correspond to the last row of \mathbf{A} and I_k^D correspond to a $(k - 1)$ -row block in the table of \mathbf{A} in the D -system region. The index set $I^D = \cup_{k=1}^n I_k^D$ gives the position of elements of matrix \mathbf{A} to be variables in the D -system.

Equations Define W_k^D as the linear space spanned by the cluster basis vectors $\{\boldsymbol{\varepsilon}_{i,j} : i, j \in \mathbb{Z}_+, 1 \leq i \leq k - 1, 1 \leq j \leq i\}$ for $1 \leq k \leq n$, specifically, we set $W_1^D = \text{span}\{\mathbf{0}\}$. According to the definition of W_k^D , we have $W_k^D \subseteq W_{k+1}^D$ for all $1 \leq k \leq n$ and the dimension of W_k^D is $\frac{k(k-1)}{2}$. The condition $D_k \subseteq W_k^D$ is equivalent to requiring that the D -residuals \mathbf{d}_{k-1} and the products $D_{k-1} \times^1 \mathbf{A}$ lie within the span of the cluster basis vectors. Replace D_{k-1} by $W_{k-1}^D \supseteq D_{k-1}$. This leads to a set of linear equations:

$$\mathbf{d}_{k-1} \cdot \mathbf{v} = 0, \quad \forall \mathbf{v} \in (W_k^D)^\perp, \quad 1 \leq k \leq n, \quad (29)$$

$$(\mathbf{u} \times^1 \mathbf{A}) \cdot \mathbf{v} = 0, \quad \forall \mathbf{u} \in W_{k-1}^D, \forall \mathbf{v} \in (W_k^D)^\perp, \quad 2 \leq k \leq n. \quad (30)$$

Since we have required in (19) that $D_n \subseteq V_l^0$, it is not necessary to test outside the support of V_l^0 . The satisfaction of this requirement in our construction will be shown in Lemma 4.3 and

Lemma 4.4. We restrict the test space to be inside V_l^0 to remove redundant equations:

$$\mathbf{d}_{k-1} \cdot \mathbf{v} = 0, \quad \forall \mathbf{v} \in (W_k^D)^\perp \cap V_l^0, \quad 1 \leq k \leq n, \quad (31)$$

$$(\mathbf{u} \times^1 \mathbf{A}) \cdot \mathbf{v} = 0, \quad \forall \mathbf{u} \in W_{k-1}^D, \forall \mathbf{v} \in (W_k^D)^\perp \cap V_l^0, \quad 2 \leq k \leq n. \quad (32)$$

Since \mathbf{A} is strictly lower triangular, and by definition of \mathbf{d}_j and D -spaces, the last element of any vector $\mathbf{d} \in D_k$ is always zero. Similarly, by definition of W_k^D , the last element of any vector $\mathbf{u} \in W_k^D$ is always zero. So, the testing on $\text{span}\{\mathbf{e}_s\}$ is also redundant. Thus (31) and (32) can be rewritten as

$$\mathbf{d}_{k-1} \cdot \mathbf{v} = 0, \quad \forall \mathbf{v} \in (\tilde{W}_k^D)^\perp \cap V_l^0, \quad \text{for } 1 \leq k \leq n, \quad (33)$$

$$(\mathbf{u} \times^1 \mathbf{A}) \cdot \mathbf{v} = 0, \quad \forall \mathbf{u} \in W_{k-1}^D, \forall \mathbf{v} \in (\tilde{W}_k^D)^\perp \cap V_l^0, \quad \text{for } 2 \leq k \leq n. \quad (34)$$

where $\tilde{W}_k^D = W_k^D \oplus \text{span}\{\mathbf{e}_s\}$, and \mathbf{e}_s is the s -th standard basis vector.

Moreover, since $W_{k-2}^D \subseteq W_{k-1}^D \subseteq W_k^D$, we have $(\tilde{W}_{k-2}^D)^\perp \supseteq (\tilde{W}_{k-1}^D)^\perp \supseteq (\tilde{W}_k^D)^\perp$. Thus, if (34) holds for $k-1$, then (34) can be written as

$$(\mathbf{u} \times^1 \mathbf{A}) \cdot \mathbf{v} = 0, \quad \forall \mathbf{u} \in W_{k-1}^D \cap (W_{k-2}^D)^\perp, \forall \mathbf{v} \in (\tilde{W}_k^D)^\perp \cap V_l^0, \quad \text{for } 3 \leq k \leq n. \quad (35)$$

to avoid duplications of the equations.

To summarize, the equations to be assembled for the D -system are

$$\mathbf{d}_{k-1} \cdot \mathbf{v} = 0, \quad \forall \mathbf{v} \in (\tilde{W}_k^D)^\perp \cap V_l^0, \quad D_k \text{ equation, } 1 \leq k \leq n, \quad (36)$$

$$(\mathbf{u} \times^1 \mathbf{A}) \cdot \mathbf{v} = 0, \quad \forall \mathbf{u} \in W_1^D, \forall \mathbf{v} \in (\tilde{W}_2^D)^\perp \cap V_l^0, \quad D_2 \text{ equation, } k = 2, \quad (37)$$

$$(\mathbf{u} \times^1 \mathbf{A}) \cdot \mathbf{v} = 0, \quad \forall \mathbf{u} \in W_{k-1}^D \cap (W_{k-2}^D)^\perp, \forall \mathbf{v} \in (\tilde{W}_k^D)^\perp \cap V_l^0, \quad D_k \text{ equation, } 3 \leq k \leq n. \quad (38)$$

Since the system is purely linear, it can be formed using basis vectors of the former space $\tilde{W}_{k-1}^D \cap (\tilde{W}_{k-2}^D)^\perp$ and the test space $(\tilde{W}_k^D)^\perp \cap V_l^0$. Since $\dim((\tilde{W}_k^D)^\perp \cap V_l^0) = (s - \frac{k(k-1)}{2}) - (l+2)$, the total number of equations in (33) and (35) on the k^{th} level is $(k-1)[(s - \frac{k(k-1)}{2}) - (l+2)]$ for $k \geq 2$.

Example 4.2. Consider the construction of ERK methods of order $p = 10$. According to the theoretical framework established in this section, achieving order p requires constructing the D -type spaces up to level $D_{p/2}$. For $p = 10$, this corresponds to D_5 . We now illustrate the complete formulation of the D -system for this case, demonstrating how the abstract theory translates into concrete computational procedures.

For a tenth-order ERK method, we have $n = p/2 = 5$ and employ the Lobatto quadrature with $N = n + 1 = 6$ nodes. The D -space construction will occupy $s_2 = \frac{n(n+1)}{2} = \frac{(N-1)N}{2} = 15$ stages. The total number of stages is $s = 1 + l + s_2 = 22$, and the parameter $l = 6$ is the number of stages occupied by the Q -space construction, which will be discussed later in the next subsection. These values determine the structure of the Butcher tableau $\mathbf{A} \in \mathbb{R}^{22 \times 22}$ and the

index sets for the D -system variables.

Applying the general formulation from (31) and (35), the variable index sets for $p = 10$ are:

$$\begin{aligned} I_1^D &= \{(22, j) : 8 \leq j \leq 21\}, \\ I_2^D &= \{(21, j) : 8 \leq j \leq 20\}, \\ I_3^D &= \{(i, j) : i \in \{19, 20\}, 8 \leq j \leq 18\}, \\ I_4^D &= \{(i, j) : i \in \{16, 17, 18\}, 8 \leq j \leq 15\}, \\ I_5^D &= \{(i, j) : i \in \{12, 13, 14, 15\}, 8 \leq j \leq 11\}. \end{aligned}$$

The total number of variables in the D -system is $\sum_{k=1}^5 |I_k^D| = 14 + 13 + 2 \times 11 + 3 \times 8 + 4 \times 4 = 89$.

For each level $k = 1, \dots, 5$, the cluster space W_k has dimension $k(k-1)/2$. The orthogonal complement $(\tilde{W}_k)^\perp \cap V_l^0$ has dimension $(s - \frac{k(k-1)}{2}) - (l+2) = (22 - \frac{k(k-1)}{2}) - 8 = 14 - \frac{k(k-1)}{2}$. Consequently, the number of equations at level k is:

$$N_k^{\text{eq}} = \begin{cases} 14, & \text{for } k = 1, \\ (k-1) \left(14 - \frac{k(k-1)}{2}\right), & \text{for } k \geq 2. \end{cases}$$

yielding $N_1^{\text{eq}} = 14$, $N_2^{\text{eq}} = 13$, $N_3^{\text{eq}} = 22$, $N_4^{\text{eq}} = 24$, and $N_5^{\text{eq}} = 16$. The total number of equations is 89, which is exactly the same as the number of variables.

Table 2: Subspaces involved in the recursive D -type construction for tenth-order ERK methods: filtration levels W_k^D , increment spaces $W_k^D \cap (W_{k-1}^D)^\perp$, and test spaces $(\tilde{W}_k^D)^\perp \cap V_l^0$.

k	filtration level W_k^D	increment space	test space $(\tilde{W}_k^D)^\perp$
1	$W_1^D = \text{span}\{\mathbf{0}\}$	$W_1^D = \text{span}\{\mathbf{0}\}$	$(\tilde{W}_1^D)^\perp \cap V_l^0 = \text{span}\{\boldsymbol{\mu}_1, \boldsymbol{\mu}_2, \boldsymbol{\mu}_3, \boldsymbol{\mu}_4, e_{12}, e_{13}, \dots, e_{s-1}\}$
2	$W_2^D = \text{span}\{\boldsymbol{\varepsilon}_{11}\}$	$W_2^D \cap (W_1^D)^\perp = \text{span}\{\boldsymbol{\varepsilon}_{11}\}$	$(\tilde{W}_2^D)^\perp \cap V_l^0 = \text{span}\{\boldsymbol{\mu}_1, \boldsymbol{\mu}_2, \boldsymbol{\mu}_3, \boldsymbol{\mu}_4, e_{12}, e_{13}, \dots, e_{s-2}\}$
3	$W_3^D = \text{span}\{\boldsymbol{\varepsilon}_{11}, \boldsymbol{\varepsilon}_{21}, \boldsymbol{\varepsilon}_{22}\}$	$W_3^D \cap (W_2^D)^\perp = \text{span}\{\boldsymbol{\varepsilon}_{21}, \boldsymbol{\varepsilon}_{22}\}$	$(\tilde{W}_3^D)^\perp \cap V_l^0 = \text{span}\{\boldsymbol{\mu}_1, \boldsymbol{\mu}_2, \boldsymbol{\mu}_3, \boldsymbol{\mu}_4, e_{12}, e_{13}, \dots, e_{s-4}\}$
4	$W_4^D = \text{span}\{\boldsymbol{\varepsilon}_{11}, \boldsymbol{\varepsilon}_{21}, \boldsymbol{\varepsilon}_{22}, \boldsymbol{\varepsilon}_{31}, \boldsymbol{\varepsilon}_{32}, \boldsymbol{\varepsilon}_{33}\}$	$W_4^D \cap (W_3^D)^\perp = \text{span}\{\boldsymbol{\varepsilon}_{31}, \boldsymbol{\varepsilon}_{32}, \boldsymbol{\varepsilon}_{33}\}$	$(\tilde{W}_4^D)^\perp \cap V_l^0 = \text{span}\{\boldsymbol{\mu}_1, \boldsymbol{\mu}_2, \boldsymbol{\mu}_3, \boldsymbol{\mu}_4, e_{12}, e_{13}, \dots, e_{s-7}\}$

Table 3 provides a comprehensive listing of all constraints imposed by the construction of D_5 . Each entry in the table corresponds to a specific linear equation of the form $\mathbf{d}_{k-1} \cdot \mathbf{v} = 0$ or $(\mathbf{u} \times^1 \mathbf{A}) \cdot \mathbf{v} = 0$, where \mathbf{u} is a basis vector of $W_{k-1}^D \cap (W_{k-2}^D)^\perp$ and \mathbf{v} is a basis vector of $(\tilde{W}_k^D)^\perp \cap V_l^0$.

Figure 9 visualizes the spatial distribution of equations on the Butcher tableau \mathbf{A} . The figure illustrates how different types of constraints (\mathbf{d}_k residuals and $\boldsymbol{\varepsilon}_{i,j} \mathbf{A}$ products) occupy distinct regions of the matrix when the linear system is assembled (we refer our readers to appendix if you are interested). The shaded regions indicate entries that are zero by construction, while the labeled rectangles show the blocks affected by each type of equation.

This concrete example for $p = 10$ demonstrates the scalability and generality of the recursive construction framework. The same principles apply to arbitrary even orders p , with the number of levels $p/2$ and the dimensions of the index sets scaling accordingly. The efficient sequential

Table 3: The complete set of linear constraints imposed by the construction of D_5 for tenth-order ERK methods. Each row represents an equation of the form $\mathbf{d}_{k-1} \cdot \mathbf{v} = 0$ or $(\mathbf{u} \times^1 \mathbf{A}) \cdot \mathbf{v} = 0$, where $\mathbf{u} \in W_{k-1}^D \cap (W_{k-2}^D)^\perp$ and $\mathbf{v} \in (\tilde{W}_k^D)^\perp \cap V_l^0$.

k	equations
1	$\mathbf{d}_0 \cdot \mathbf{v} = 0, \quad \forall \mathbf{v} \in (\tilde{W}_1^D)^\perp \cap V_l^0$
2	$\mathbf{d}_1 \cdot \mathbf{v} = 0, \quad \forall \mathbf{v} \in (\tilde{W}_2^D)^\perp \cap V_l^0$ $(\mathbf{u} \times^1 \mathbf{A}) \cdot \mathbf{v} = 0, \quad \forall \mathbf{u} \in W_1^D, \forall \mathbf{v} \in (\tilde{W}_2^D)^\perp \cap V_l^0$
3	$\mathbf{d}_2 \cdot \mathbf{v} = 0, \quad \forall \mathbf{v} \in (\tilde{W}_3^D)^\perp \cap V_l^0$ $(\mathbf{u} \times^1 \mathbf{A}) \cdot \mathbf{v} = 0, \quad \forall \mathbf{u} \in W_2^D \cap (W_1^D)^\perp, \forall \mathbf{v} \in (\tilde{W}_3^D)^\perp \cap V_l^0$
4	$\mathbf{d}_3 \cdot \mathbf{v} = 0, \quad \forall \mathbf{v} \in (\tilde{W}_4^D)^\perp \cap V_l^0$ $(\mathbf{u} \times^1 \mathbf{A}) \cdot \mathbf{v} = 0, \quad \forall \mathbf{u} \in W_3^D \cap (W_2^D)^\perp, \forall \mathbf{v} \in (\tilde{W}_4^D)^\perp \cap V_l^0$

solution procedure enabled by the block lower-triangular structure is crucial for practical implementation at high orders, where the number of variables and equations only grows quadratically with p .

4.5 Construction of the Q -type spaces

Once the D -type conditions are solved and the corresponding entries of \mathbf{A} are fixed, we proceed to construct the Q -type spaces. This step determines the remaining coefficients by solving a second linear system.

Recall that the spaces Q_m are defined recursively and encode the order conditions by Q -orthogonality conditions, Q -and- D mutual orthogonality conditions and Q -ring conditions. The Q -orthogonality conditions and Q -and- D mutual orthogonality conditions are enforced through (19) by requiring them to lie in pre-chosen orthogonal subspaces. This requirement, along with the Q -ring condition, are fulfilled by carefully adding conditions to the generators of the Q -type spaces. Since the generators are linear in the elements of A , we can exploit this structure and assemble a linear system to construct part of the RK coefficients for a prescribed order.

4.5.1 Systematic imposition of Q -space constraints

Fix an even integer $p \geq 4$ and let $\mathbf{A} \in \mathbb{R}^{s \times s}$ denote the strictly lower triangular RK coefficient matrix. The goal is to determine \mathbf{A} such that the associated methods satisfy $Q_m \subset V_l^*$ and the Q -ring conditions.

We determine the structure of the Q -type spaces recursively, starting from the first few levels to illustrate the pattern, and a general construction is given afterwards. The construction proceeds by specifying columns of \mathbf{A} so that each Q_m remains within a low-dimensional subspace.

By viewing \mathbf{b} and \mathbf{c} as given vectors, we determine elements of the matrix \mathbf{A} in hope of

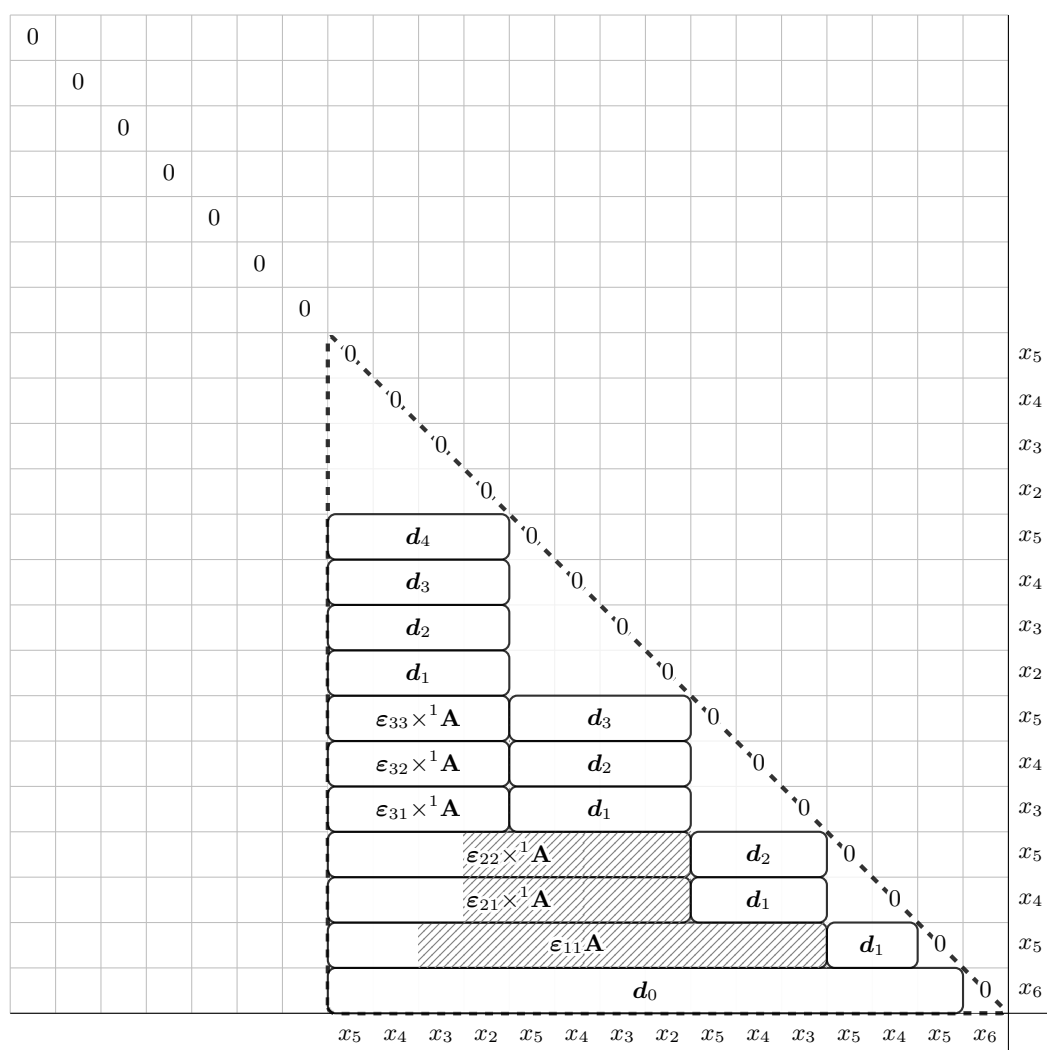


Figure 9: Spatial configuration of the D -system equations on the Butcher tableau \mathbf{A} for $p = 10$. The matrix shows the distribution of different equation types: \mathbf{d}_k regions and $\varepsilon_{i,j} \times^1 \mathbf{A}$ regions. Blank areas represent the entries that are initialized to zero, and shaded areas indicate entries that become zero as a direct consequence of solving the constructed D -system equations. Dashed lines represent the boundary of the D -region.

controlling the dimension of Q_m .

Q_1 .

By definition,

$$Q_1 = \text{span}\{\mathbf{q}_0\}.$$

We require that $\mathbf{q}_0 = \mathbf{0}$, this is equivalent to the condition $\mathbf{A}\mathbf{1} = \mathbf{c}$. We use the first column of

\mathbf{A} to enforce this condition, i.e., we set

$$a_{i1} = c_i - \sum_{j=2}^{i-1} a_{ij}, \quad i = 1, \dots, s.$$

Now, under this condition, we have $Q_1 = \{\mathbf{0}\}$, and the dimension of Q_1 is 0.

Q_2 .

By the definition of Q_2 and $\mathbf{q}_0 = 0$, it follows that

$$Q_2 = \text{span}\{\mathbf{q}_1, \mathbf{A}\mathbf{q}_0, \mathbf{q}_0 \odot \mathbf{c}, \mathbf{q}_0\} = \text{span}\{\mathbf{q}_1\}.$$

We require that $\mathbf{q}_1 = -\frac{1}{2}c_2^2\mathbf{e}_2$, where \mathbf{e}_2 is the second standard basis vector. This determines the second column of \mathbf{A} .

Now, we have

$$Q_2 = \text{span}\{\mathbf{e}_2\}.$$

The dimension of Q_2 is 1.

Q_3 .

By the definition of Q_3 and $Q_2 = \text{span}\{\mathbf{e}_2\}$, we have

$$Q_3 = \text{span}\{\mathbf{q}_2, \mathbf{A}Q_2, Q_2 \odot \mathbf{c}, \mathbf{q}_1\} = \text{span}\{\mathbf{q}_2, \mathbf{A}\mathbf{e}_2, \mathbf{e}_2\}.$$

We require that $Q_3 \subseteq \text{span}\{\mathbf{e}_2, \mathbf{e}_3, \mathbf{e}_4\}$.

Q_4 .

By the definition of Q_4 , $Q_3 \subseteq \text{span}\{\mathbf{e}_2, \mathbf{e}_3, \mathbf{e}_4\}$, $\mathbf{A}\mathbf{e}_2 \in Q_3$ and $Q_3 \cdot \mathbf{c} \subseteq Q_3$, we have

$$Q_4 = \text{span}\{\mathbf{q}_3, \mathbf{A}Q_3, Q_3 \odot \Phi_1\} \subseteq \text{span}\{\mathbf{q}_3, \mathbf{A}\mathbf{e}_3, \mathbf{A}\mathbf{e}_4, Q_3\}.$$

We require that $Q_4 \subseteq \text{span}\{\mathbf{e}_2, \mathbf{e}_3, \mathbf{e}_4, \mathbf{e}_5, \mathbf{e}_6, \mathbf{e}_7\}$.

Q_5

By the definition of Q_5 , $Q_4 \subseteq \text{span}\{\mathbf{e}_2, \mathbf{e}_3, \dots, \mathbf{e}_7\}$, $\mathbf{A}\mathbf{e}_2, \mathbf{A}\mathbf{e}_3, \mathbf{A}\mathbf{e}_4 \in Q_4$ and $Q_4 \cdot \mathbf{c} \subseteq Q_4$, we have

$$Q_5 = \text{span}\{\mathbf{q}_4, \mathbf{A}Q_4, Q_4 \odot \Phi_1\} \subseteq \text{span}\{\mathbf{q}_4, \mathbf{A}\mathbf{e}_5, \mathbf{A}\mathbf{e}_6, \mathbf{A}\mathbf{e}_7, Q_4\}.$$

We require that $Q_5 \subseteq \text{span}\{\mathbf{e}_2, \mathbf{e}_3, \mathbf{e}_4, \mathbf{e}_5, \mathbf{e}_6, \mathbf{e}_7, \mathbf{e}_8, \mathbf{e}_9, \mathbf{e}_{10}, \mathbf{e}_{11}\}$.

General Q_m .

$$Q_m \subseteq \text{span}\{\mathbf{e}_2, \mathbf{e}_3, \dots, \mathbf{e}_{m(m-1)/2+1}\}.$$

We prove this by induction. Suppose that

$$Q_k \subseteq \text{span}\{\mathbf{e}_2, \mathbf{e}_3, \dots, \mathbf{e}_{k(k-1)/2+1}\} \quad \text{for } k = 1, 2, \dots, m-1.$$

By definition, since $Q_{m-1}, Q_{m-1} \odot \mathbf{c} \subseteq \text{span}\{\mathbf{e}_2, \mathbf{e}_3, \dots, \mathbf{e}_{(m-1)(m-2)/2+1}\}$ and $\mathbf{A}\mathbf{e}_2, \mathbf{A}\mathbf{e}_3, \dots, \mathbf{A}\mathbf{e}_{(m-2)(m-3)/2+1} \in Q_{m-1}$, we have

$$\begin{aligned} Q_m &= \text{span}\{\mathbf{q}_{m-1}, \mathbf{A}Q_{m-1}, Q_{m-1} \odot \Phi_1\} \\ &\subseteq \text{span}\{\mathbf{q}_{m-1}, \mathbf{A}\mathbf{e}_{(m-2)(m-3)/2+2}, \dots, \mathbf{A}\mathbf{e}_{(m-1)(m-2)/2+1}, Q_{m-1}\}. \end{aligned}$$

We then add additional $m-1$ vectors to the span and require that

$$\mathbf{q}_{m-1}, \mathbf{A}\mathbf{e}_{(m-2)(m-3)/2+2}, \dots, \mathbf{A}\mathbf{e}_{(m-1)(m-2)/2+1} \in \text{span}\{\mathbf{e}_2, \mathbf{e}_3, \dots, \mathbf{e}_{m(m-1)/2+1}\}, \quad (39)$$

which implies

$$Q_m \subseteq \text{span}\{\mathbf{e}_2, \mathbf{e}_3, \dots, \mathbf{e}_{m(m-1)/2+1}\}.$$

Hence, the sequence $\{Q_m \cap Q_{m-1}^\perp\}$ grows linearly in dimension with respect to m , ensuring that each step of the recursion involves solving only a small linear system for the new column of \mathbf{A} .

4.5.2 Formulation of the Q-system

We have previously described the conditions using subspace inclusion, which is clean for the design of algorithm, but not precise enough for implementation. In this subsection, we convert the conditions to equations, and give a configuration for assembling the equations which yields well-structured linear systems.

Variables For each Q_k , $1 \leq k \leq m$, we define an associated index set I_k^Q by

$$\begin{aligned} I_1^Q &= \{(i, 1) \in \mathbb{Z}^2 : 2 \leq i \leq s\} \\ I_k^Q &= \{(i, j) \in \mathbb{Z}^2 : \frac{k(k-1)}{2} + 2 \leq i \leq s, \frac{(k-1)(k-2)}{2} + 2 \leq j \leq \frac{k(k-1)}{2} + 1\}, \quad 2 \leq k \leq m. \end{aligned}$$

Then, the index set $I^Q = \cup_{k=1}^m I_k^Q$ gives the position of elements of matrix \mathbf{A} to be variables in the linear system.

Equations Define W_k^Q as the linear space spanned by the basis vectors $\{\mathbf{e}_i : i \in \mathbb{Z}_+, 2 \leq i \leq \frac{k(k-1)}{2} + 1\}$ for $1 \leq k \leq m$. Specifically, we define $W_1^Q = \{\mathbf{0}\}$ with zero dimension, which is consistent with the result yield by the definition. By definition, we have $W_k^Q \subseteq W_{k+1}^Q$ for all

$1 \leq k \leq m-1$ and the dimension of W_k^Q is $\frac{k(k-1)}{2}$.

The condition (39) is equivalent to requiring that the Q -residuals \mathbf{q}_{k-1} and the products $\mathbf{A}\mathbf{e}_j$ lie within the span of the basis vectors in W_k^Q , where $\mathbf{e}_j \in W_{k-1}^Q$. This leads to a set of linear equations:

$$\mathbf{q}_{k-1} \cdot \mathbf{v} = 0, \quad \forall \mathbf{v} \in (W_k^Q)^\perp, \quad 1 \leq k \leq m, \quad (40)$$

$$(\mathbf{A}\mathbf{u}) \cdot \mathbf{v} = 0, \quad \forall \mathbf{v} \in (W_k^Q)^\perp, \forall \mathbf{u} \in W_{k-1}^Q, \quad 1 \leq k \leq m. \quad (41)$$

Since the matrix \mathbf{A} is strictly lower triangular, and by the definitions of \mathbf{q}_j and Q -space, the first element of any vector $\mathbf{q} \in Q_k$ is always zero. Similarly, by the definition of W_k^Q , the first element of any vector $\mathbf{v} \in W_k^Q$ is always zero. Thus, there is no need to test for the first element of any vector in (40) and (41). Equations (40) and (41) can be rewritten as

$$\mathbf{q}_{k-1} \cdot \mathbf{v} = 0, \quad \forall \mathbf{v} \in (\tilde{W}_k^Q)^\perp, \quad 1 \leq k \leq m, \quad (42)$$

$$(\mathbf{A}\mathbf{u}) \cdot \mathbf{v} = 0, \quad \forall \mathbf{v} \in (\tilde{W}_k^Q)^\perp, \forall \mathbf{u} \in W_{k-1}^Q, \quad 2 \leq k \leq m, \quad (43)$$

where $\tilde{W}_k^Q = W_k^Q \oplus \text{span}\{\mathbf{e}_1\} = \text{span}\{\mathbf{e}_j : j \in \mathbb{Z}_+, 1 \leq j \leq \frac{k(k-1)}{2} + 1\}$ is the test space for the k^{th} level, \mathbf{e}_1 is the first basis vector of \mathbb{R}^s .

Moreover, since $\tilde{W}_{k-2}^Q \subset \tilde{W}_{k-1}^Q \subset \tilde{W}_k^Q$, similar to the case of D -equations, some equations in (43) are already satisfied because of equations for the previous k , thus for $k \geq 3$, (43) can be rewritten as

$$(\mathbf{A}\mathbf{u}) \cdot \mathbf{v} = 0, \quad \forall \mathbf{v} \in (\tilde{W}_k^Q)^\perp, \forall \mathbf{u} \in W_{k-1}^Q \cap (W_{k-2}^Q)^\perp, \quad 3 \leq k \leq m \quad (44)$$

to avoid duplications of the equations.

To summarize, the equations to be assembled for the Q -system are

$$\mathbf{q}_{k-1} \cdot \mathbf{v} = 0, \quad \forall \mathbf{v} \in (\tilde{W}_k^Q)^\perp, \quad (Q_k \text{ equation}), \quad 1 \leq k \leq m, \quad (45)$$

$$(\mathbf{A}\mathbf{u}) \cdot \mathbf{v} = 0, \quad \forall \mathbf{v} \in (\tilde{W}_2^Q)^\perp, \forall \mathbf{u} \in W_1^Q, \quad (Q_2 \text{ equation}), \quad k = 2 \quad (46)$$

$$(\mathbf{A}\mathbf{u}) \cdot \mathbf{v} = 0, \quad \forall \mathbf{v} \in (\tilde{W}_k^Q)^\perp, \forall \mathbf{u} \in W_{k-1}^Q \cap (W_{k-2}^Q)^\perp, \quad (Q_k \text{ equation}), \quad 3 \leq k \leq m. \quad (47)$$

Since the system is purely linear, it can be formed using basis vectors of the test space $\tilde{W}_{k-1}^Q \cap (\tilde{W}_{k-2}^Q)^\perp = \text{span}\{\mathbf{e}_j : j \in \mathbb{Z}_+, \frac{(k-2)(k-3)}{2} + 2 \leq j \leq \frac{(k-1)(k-2)}{2} + 1\}$ and the former space $W_k^Q = \text{span}\{\mathbf{e}_j : j \in \mathbb{Z}_+, 2 \leq j \leq \frac{k(k-1)}{2} + 1\}$. The total number of equations in (42) and (44) on the k^{th} level is $(k-1)(s - \frac{k(k-1)}{2} - 1)$ for $k \geq 2$.

Example 4.3. Consider the construction of ERK methods of order $p = 10$. According to the theoretical framework established in this section, achieving order p requires constructing the Q -type spaces up to level $Q_{p/2-1}$. For $p = 10$, this corresponds to Q_m with $m = 4$. We now illustrate the complete formulation of the Q -system for this case, demonstrating how the abstract theory translates into concrete computational procedures.

For a 10th-order method, we have $n = p/2 = 5$ and employ the Lobatto quadrature with $N = n + 1 = 6$ nodes. Q -space construction will occupy $l = \dim W_4^Q = \frac{m(m-1)}{2} = 6$ stages. The total number of stages is $s = 1 + l + s_2 = 22$, and the parameter $s_2 = 15$ is the number of stages occupied by the D -space construction, which was discussed earlier in the previous subsection. These values determine the structure of the Butcher tableau $\mathbf{A} \in \mathbb{R}^{22 \times 22}$ and the index sets for the Q -system variables.

Applying the general formulation from (40) and (44), the variable index sets for $p = 10$ are:

$$\begin{aligned} I_1^Q &= \{(i, 1) : 2 \leq i \leq 22\}, \\ I_2^Q &= \{(i, 2) : 3 \leq i \leq 22\}, \\ I_3^Q &= \{(i, j) : 5 \leq i \leq 22, 3 \leq j \leq 4\}, \\ I_4^Q &= \{(i, j) : 8 \leq i \leq 22, 5 \leq j \leq 7\}. \end{aligned}$$

The total number of variables in the Q -system is $\sum_{k=1}^4 |I_k^Q| = 21 + 20 + 2 \times 18 + 3 \times 15 = 122$.

For each level $k = 1, \dots, 4$, the test space $(\tilde{W}_k^Q)^\perp$ has dimension $(s - \frac{k(k-1)}{2} - 1) = 21 - \frac{k(k-1)}{2}$. Consequently, the number of equations at level k is:

$$M_k^{\text{eq}} = \begin{cases} 21, & \text{for } k = 1, \\ (k-1) \left(21 - \frac{k(k-1)}{2} \right), & \text{for } k \geq 2, \end{cases}$$

yielding $M_1^{\text{eq}} = 21$, $M_2^{\text{eq}} = 20$, $M_3^{\text{eq}} = 36$, and $M_4^{\text{eq}} = 45$. The total number of equations is $\sum_{k=1}^4 M_k^{\text{eq}} = 122$, which is exactly the same as the number of variables.

Table 4: Subspaces involved in the recursive Q -type construction for tenth-order ERK methods: filtration levels W_k^Q , increment spaces $W_k^Q \cap (W_{k-1}^Q)^\perp$, and test spaces $(\tilde{W}_k^Q)^\perp$.

k	filtration level W_k^Q	increment space	test space $(\tilde{W}_k^Q)^\perp$
1	$W_1^Q = \text{span}\{\mathbf{0}\}$	$W_1^Q = \text{span}\{\mathbf{0}\}$	$(\tilde{W}_1^Q)^\perp = \text{span}\{e_2, \dots, e_s\}$
2	$W_2^Q = \text{span}\{e_2\}$	$W_2^Q \cap (W_1^Q)^\perp = \text{span}\{e_2\}$	$(\tilde{W}_2^Q)^\perp = \text{span}\{e_3, \dots, e_s\}$
3	$W_3^Q = \text{span}\{e_2, e_3, e_4\}$	$W_3^Q \cap (W_2^Q)^\perp = \text{span}\{e_3, e_4\}$	$(\tilde{W}_3^Q)^\perp = \text{span}\{e_5, \dots, e_s\}$
4	$W_4^Q = \text{span}\{e_2, \dots, e_7\}$	$W_4^Q \cap (W_3^Q)^\perp = \text{span}\{e_5, e_6, e_7\}$	$(\tilde{W}_4^Q)^\perp = \text{span}\{e_8, \dots, e_s\}$

Figure 10 visualizes the spatial distribution of equations on the Butcher tableau \mathbf{A} for $p = 10$. The figure illustrates how different types of constraints (\mathbf{q}_k residuals and $\mathbf{A}\mathbf{e}_j$ products) occupy distinct regions of the matrix when the linear system is assembled. The Q -region is enclosed by the dashed line. Blank regions within the Q -region are entries initialized to zero, shaded regions indicate entries that are zero as a result of solving the Q -system equations, and labeled rectangles show the blocks affected by each type of equation. This design allows the equations to be assembled into a block diagonal linear system. The dashed lines clearly separate the Q -region

Table 5: The complete set of linear constraints imposed by the construction of Q_4 for tenth-order ERK methods.

k	equations
1	$\mathbf{q}_0 \cdot \mathbf{v} = 0, \quad \forall \mathbf{v} \in (\tilde{W}_1^Q)^\perp$
2	$\mathbf{q}_1 \cdot \mathbf{v} = 0, \quad \forall \mathbf{v} \in (\tilde{W}_2^Q)^\perp$ $(\mathbf{A}\mathbf{u}) \cdot \mathbf{v} = 0, \quad \forall \mathbf{v} \in (\tilde{W}_2^Q)^\perp, \forall \mathbf{u} \in W_1^Q$
3	$\mathbf{q}_2 \cdot \mathbf{v} = 0, \quad \forall \mathbf{v} \in (\tilde{W}_3^Q)^\perp$ $(\mathbf{A}\mathbf{u}) \cdot \mathbf{v} = 0, \quad \forall \mathbf{v} \in (\tilde{W}_3^Q)^\perp, \forall \mathbf{u} \in W_2^Q \cap (W_1^Q)^\perp$
4	$\mathbf{q}_3 \cdot \mathbf{v} = 0, \quad \forall \mathbf{v} \in (\tilde{W}_4^Q)^\perp$ $(\mathbf{A}\mathbf{u}) \cdot \mathbf{v} = 0, \quad \forall \mathbf{v} \in (\tilde{W}_4^Q)^\perp, \forall \mathbf{u} \in W_3^Q \cap (W_2^Q)^\perp$

from the D -region, highlighting the modular structure of the overall construction.

This concrete example for $p = 10$ demonstrates the scalability and generality of the recursive construction framework. The same principles apply to arbitrary even orders p , with the number of levels $p/2 - 1$ and the dimensions of the index sets scaling accordingly. The efficient parallel solution procedure enabled by the block diagonal structure is crucial for practical implementation at high orders, where the number of variables and equations only grows quadratically with p . The modular separation of Q -system and D -system constructions also facilitates independent verification and optimization of each component.

4.6 Verification of the sufficient conditions

In this subsection, we verify that the constructed Butcher tableau satisfies all conditions in the sufficiency theorem, Theorem 3.2, and hence indeed defines a method of order p . At the same time, we check that the construction also fulfills the three design principles introduced in Section 4.2. These principles play an essential role in ensuring that all conditions of Theorem 3.2 are satisfied.

Most requirements imposed by the three design principles have already been built directly into the choice of nodes, the definition of basis vectors, and the recursive construction of the spaces. More precisely, in the subspace-placement requirement (19) from Principle 1, the condition $\mathbf{b} \in V_l$ is ensured by setting the weights corresponding to the Q -type group nodes to zero, while the inclusion $Q_m \subseteq V_l^*$ is guaranteed by the choice of the basis vectors used in the construction of the Q -spaces. The cluster condition from Principle 2 is enforced directly through the definition of the generators of the D -spaces. Finally, the closure requirements from Principle 3 are already built into the recursive definitions of the D - and Q -spaces.

Summarizing these observations, we obtain the following lemma.

Lemma 4.1. *Let $p \geq 4$ be even, set $m = \frac{p}{2} - 1$ and $n = \frac{p}{2}$, and write $l = \dim Q_m$. Then*

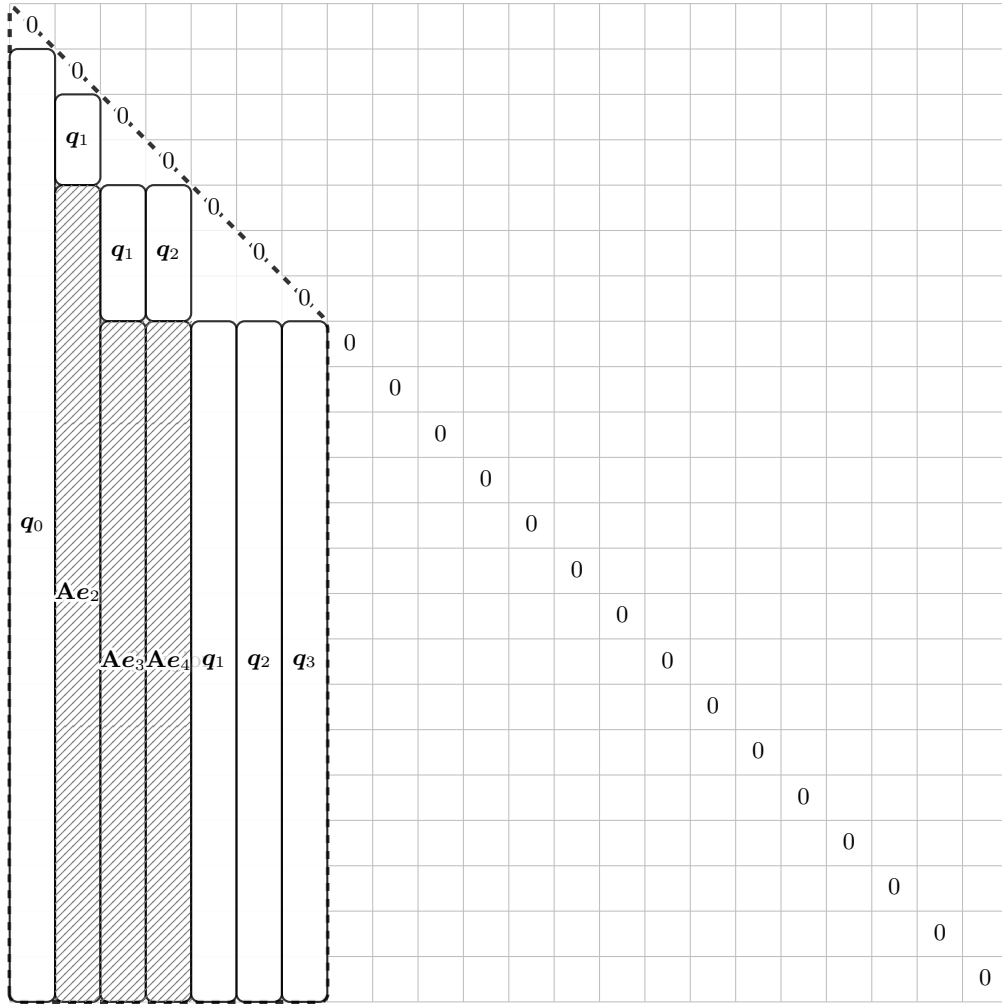


Figure 10: Spatial configuration of the Q -system equations on the Butcher tableau \mathbf{A} for $p = 10$. The matrix shows the distribution of different equation types: \mathbf{q}_k regions and \mathbf{Ae}_j regions. Blank areas in the Q -region represent the entries that are initialized to zero, and shaded areas indicate entries that become zero as a direct consequence of solving the constructed Q -system equations. Dashed lines represent the boundary of the Q -region.

the construction in Section 4 yields a stage vector \mathbf{c} , a weight vector \mathbf{b} , and recursive spaces Q_m and D_n satisfying the following properties, which are guaranteed directly by the three design principles:

1. $\mathbf{b} \in V_l$ and $Q_m \subseteq V_l^*$;
2. the generators of D_n satisfy the cluster condition (20);
3. the closure requirements (21) and (22) from Principle 3 hold for the recursively constructed D - and Q -spaces.

Therefore, within the space-placement requirement (19), the only remaining point that still

needs to be verified is the inclusion $D_n \subseteq V_l^0$. This will be established in Propositions 4.3 and 4.4.

We next turn to the conditions appearing in the sufficiency theorem itself. The quadrature condition $B(p)$ follows from the Lobatto quadrature rule used for the nodes and weights. The condition $QO(m)$ follows from the subspace design $\mathbf{b} \in V_l$ and $Q_m \subseteq V_l^*$, since these two subspaces have disjoint supports. The closure condition $QR(m)$ is already built into the nested support structure used in the recursive construction of Q_m . Hence we obtain the following lemma.

Lemma 4.2. *Let $p \geq 4$ be even. Then the stage vector \mathbf{c} , the weight vector \mathbf{b} , and the recursively constructed spaces Q_m and D_n obtained in this chapter satisfy the conditions $B(p)$, $QO(m)$, and $QR(m)$ in Theorem 3.2.*

To prove the remaining conditions, we establish the following two lemmas.

Lemma 4.3. *Let $(\mathbf{A}, \mathbf{b}, \mathbf{c})$ be the Butcher tableau produced by the construction in this chapter, let Q_m and D_n be the corresponding recursive spaces, and write $l = \dim Q_m$. For any $0 \leq k \leq n-1$, if the residual vector \mathbf{d}_k satisfies the cluster condition in Definition 4.2, namely, for every node cluster $S(x_r)$,*

$$\sum_{i \in S(x_r)} (\mathbf{d}_k)_i = 0$$

then $\mathbf{d}_k \in V_l^0$.

Proof. Note that, by the subspace design, $\mathbf{b} \in V_l$ and

$$\mathbf{A}\mathbf{e}_2, \dots, \mathbf{A}\mathbf{e}_{(m-1)(m-2)/2+1} \in Q_m \subseteq V_l^*.$$

Since the supports of V_l and V_l^* are disjoint, this implies

$$\mathbf{b} \odot (\mathbf{A}\mathbf{e}_j) = \mathbf{0}, \quad j = 2, \dots, \frac{(m-1)(m-2)}{2} + 1.$$

By the definition of the D -residual, $\mathbf{d}_k = (\mathbf{b} \odot \mathbf{c}^{\odot k}) \times^1 \mathbf{A} - \frac{1}{k+1} \mathbf{b} \odot (\mathbf{1} - \mathbf{c}^{\odot(k+1)})$, and by direct componentwise computation, we obtain

$$\mathbf{d}_k \cdot \mathbf{e}_j = 0, \quad j = 2, \dots, \frac{(m-1)(m-2)}{2} + 1. \quad (48)$$

Furthermore, for $0 \leq j \leq m-1$, we compute

$$\begin{aligned} \mathbf{d}_k \cdot \mathbf{c}^{\odot j} &= ((\mathbf{b} \odot \mathbf{c}^{\odot k}) \times^1 \mathbf{A}) \cdot \mathbf{c}^{\odot j} - \frac{1}{k+1} (\mathbf{b} \odot (\mathbf{1} - \mathbf{c}^{\odot(k+1)})) \cdot \mathbf{c}^{\odot j} \\ &= (\mathbf{b} \odot \mathbf{c}^{\odot k}) \cdot (\mathbf{A}\mathbf{c}^{\odot j}) - \frac{1}{k+1} \mathbf{b} \cdot (\mathbf{c}^{\odot j} - \mathbf{c}^{\odot(k+j+1)}) \\ &= (\mathbf{b} \odot \mathbf{c}^{\odot k}) \cdot \left(\frac{1}{j+1} \mathbf{c}^{\odot(j+1)} + \mathbf{q}_j \right) - \frac{1}{k+1} \mathbf{b} \cdot (\mathbf{c}^{\odot j} - \mathbf{c}^{\odot(k+j+1)}) \end{aligned}$$

$$\begin{aligned}
&= \frac{1}{j+1} \mathbf{b} \cdot \mathbf{c}^{\odot(k+j+1)} + (\mathbf{b} \odot \mathbf{c}^{\odot k}) \cdot \mathbf{q}_j - \frac{1}{k+1} \left(\frac{1}{j+1} - \frac{1}{k+j+2} \right) \\
&= \frac{1}{(j+1)(k+j+2)} + 0 - \frac{1}{k+1} \left(\frac{k+1}{(j+1)(k+j+2)} \right) = 0.
\end{aligned}$$

Here we used the Q -orthogonality condition together with the quadrature condition.

Using the cluster condition to eliminate the components of \mathbf{d}_k on the support of V_l^0 , the above identities can be rewritten as

$$\mathbf{d}_k|_{(V_l^0)^\perp} \cdot \mathbf{e}_j|_{(V_l^0)^\perp} = 0, \quad j = 2, \dots, \frac{(m-1)(m-2)}{2} + 1, \quad (49)$$

$$\mathbf{d}_k|_{(V_l^0)^\perp} \cdot \mathbf{c}^{\odot j}|_{(V_l^0)^\perp} = 0, \quad j = 0, \dots, m-1. \quad (50)$$

This gives a homogeneous linear system for $\mathbf{d}_k|_{(V_l^0)^\perp}$ with

$$\frac{(m-1)(m-2)}{2} + m = \frac{m(m-1)}{2} + 1 = l + 1.$$

equations. Since the nodes are distinct, the coefficient matrix of this system is of Vandermonde type and is therefore nonsingular. Hence the only solution is

$$\mathbf{d}_k|_{(V_l^0)^\perp} = \mathbf{0}.$$

Therefore $\mathbf{d}_k \in V_l^0$. □

Lemma 4.4 (D_n -embedding by construction). *Let $(\mathbf{A}, \mathbf{b}, \mathbf{c})$ be the Butcher tableau produced by the construction in this chapter, let Q_m and D_n be the corresponding recursive spaces, and write $l = \dim Q_m$. If the space D_k ($k \leq n$) satisfies the cluster condition in Definition 4.2, namely, for every $\mathbf{d} \in D_k$ and every node cluster $S(x_r)$,*

$$\sum_{i \in S(x_r)} (\mathbf{d})_i = 0,$$

then $D_k \subseteq V_l^0$. In particular, when $k = n$, we have $D_n \subseteq V_l^0$.

Proof. Assume that the statement holds for D_k , that is, if D_k satisfies the cluster condition, then $D_k \subseteq V_l^0$. We show that if D_{k+1} satisfies the cluster condition, then $D_{k+1} \subseteq V_l^0$.

Take any $\mathbf{d} \in D_{k+1}$. By the recursive definition of the D -spaces, \mathbf{d} is a linear combination of vectors of the following forms:

- $\tilde{\mathbf{d}} \in D_k$;
- \mathbf{d}_{k+1} ;
- $\tilde{\mathbf{d}} \odot \mathbf{c}$, where $\tilde{\mathbf{d}} \in D_k$;
- $\tilde{\mathbf{d}} \times^1 \mathbf{A}$, where $\tilde{\mathbf{d}} \in D_k$.

Note that

$$(\tilde{\mathbf{d}} \times^1 \mathbf{A}) \cdot \mathbf{e}_j = \tilde{\mathbf{d}} \cdot (\mathbf{A}\mathbf{e}_j) = 0, \quad j = 2, \dots, \frac{(m-1)(m-2)}{2} + 1, \quad (51)$$

because $\mathbf{A}\mathbf{e}_2, \dots, \mathbf{A}\mathbf{e}_{(m-1)(m-2)/2+1} \in Q_m \subseteq V_l^*$.

Moreover, for $0 \leq j \leq m-1$, we have

$$(\tilde{\mathbf{d}} \times^1 \mathbf{A}) \cdot \mathbf{c}^{\odot j} = \tilde{\mathbf{d}} \cdot (\mathbf{A}\mathbf{c}^{\odot j}) = \tilde{\mathbf{d}} \cdot \left(\frac{1}{j+1} \mathbf{c}^{\odot(j+1)} + \mathbf{q}_j \right) = 0. \quad (52)$$

Here the first term is zero because $\tilde{\mathbf{d}} \in V_l^0$ and satisfies the cluster condition, and the second term is zero because $\tilde{\mathbf{d}} \in V_l^0$ and $\mathbf{q}_j \in Q_m \subseteq V_l^*$ are orthogonal.

By the induction hypothesis, $\tilde{\mathbf{d}} \in V_l^0$. Hence $\tilde{\mathbf{d}} \odot \mathbf{c} \in V_l^0$. By Lemma 4.3, $\mathbf{d}_{k+1} \in V_l^0$. Also, since $\mathbf{e}_j \in Q_{m-1} \subseteq V_l^*$ for $j = 2, \dots, \frac{(m-1)(m-2)}{2} + 1$, the orthogonality of V_l^0 and V_l^* gives

$$\tilde{\mathbf{d}} \cdot \mathbf{e}_j = 0, \quad (\tilde{\mathbf{d}} \odot \mathbf{c}) \cdot \mathbf{e}_j = 0, \quad \mathbf{d}_{k+1} \cdot \mathbf{e}_j = 0, \quad (53)$$

for all $j = 2, \dots, \frac{(m-1)(m-2)}{2} + 1$.

On the other hand, since $\tilde{\mathbf{d}}, \tilde{\mathbf{d}} \odot \mathbf{c}, \mathbf{d}_{k+1} \in V_l^0$ and all satisfy the cluster condition, we have

$$\tilde{\mathbf{d}} \cdot \mathbf{c}^{\odot j} = 0, \quad (\tilde{\mathbf{d}} \odot \mathbf{c}) \cdot \mathbf{c}^{\odot j} = 0, \quad \mathbf{d}_{k+1} \cdot \mathbf{c}^{\odot j} = 0, \quad (54)$$

for all $j = 0, \dots, m-1$.

By linearity, combining (51), (52), (53), and (54), we obtain

$$\mathbf{d} \cdot \mathbf{e}_j = 0, \quad j = 2, \dots, \frac{(m-1)(m-2)}{2} + 1, \quad (55)$$

$$\mathbf{d} \cdot \mathbf{c}^{\odot j} = 0, \quad j = 0, \dots, m-1. \quad (56)$$

As in Lemma 4.3, using that \mathbf{d} satisfies the cluster condition, we obtain a homogeneous linear system for $\mathbf{d}|_{(V_l^0)^\perp}$ with $l+1$ equations:

$$\mathbf{d}|_{(V_l^0)^\perp} \cdot \mathbf{e}_j|_{(V_l^0)^\perp} = 0, \quad j = 2, \dots, \frac{(m-1)(m-2)}{2} + 1, \quad (57)$$

$$\mathbf{d}|_{(V_l^0)^\perp} \cdot \mathbf{c}^{\odot j}|_{(V_l^0)^\perp} = 0, \quad j = 0, \dots, m-1. \quad (58)$$

Since the coefficient matrix is nonsingular, this system has only the zero solution $\mathbf{d}|_{(V_l^0)^\perp} = 0$. Therefore $\mathbf{d} \in V_l^0$. Since \mathbf{d} was arbitrary, $D_{k+1} \subseteq V_l^0$.

The induction proceeds up to $k = n-1$, and hence $D_n \subseteq V_l^0$. \square

The above lemmas show that every vector in the space D_n satisfies the condition of belonging to V_l^0 . In other words, the requirement $D_n \subseteq V_l^0$ in the subspace-placement condition (19) from Principle 1 is now completely verified.

At this point, all requirements imposed by the three design principles have been verified. On the one hand, the subspace-placement relations $\mathbf{b} \in V_l$, $Q_m \subseteq V_l^*$, and $D_n \subseteq V_l^0$ all hold. On the other hand, the cluster condition and the Hadamard closure conditions with respect to \mathbf{c} are also guaranteed by the construction itself. Therefore, it remains only to match these structural conclusions with the sufficiency theorem (Theorem 3.2), from which it follows that the method constructed in this chapter satisfies all Q/D conditions and hence has the claimed algebraic order. We summarize the result in the following theorem.

Theorem 4.5. *Let $p \geq 4$ be even, set $m = \frac{p}{2} - 1$, $n = \frac{p}{2}$, and write $l = \dim Q_m$. Then the stage vector \mathbf{c} , the weight vector \mathbf{b} , and the recursive spaces Q_m and D_n produced by the construction in this chapter satisfy all conditions in Theorem 3.2. Therefore, the constructed Butcher tableau \mathbf{A} defines an ERK method of order p .*

Proof. By the preceding lemmas, the conditions $B(p)$, $QO(m)$, and $QR(m)$ are already satisfied. The condition $DO(n)$ follows from the inclusion $D_n \subseteq V_l^0$ together with the fact that every vector in D_n satisfies the cluster condition. Finally, the mixed orthogonality condition $QD(m, n)$ follows immediately from $Q_m \subseteq V_l^*$ and $D_n \subseteq V_l^0$, since these two subspaces have disjoint supports. Hence all conditions in Theorem 3.2 are satisfied, and the constructed Butcher tableau $(\mathbf{A}, \mathbf{b}^\top, \mathbf{c})$ defines an ERK method of order p . \square

4.7 Solvability and condition number of the systems

The recursive construction is well-posed if the linear systems for the D - and Q -type coefficients are non-singular at each step. We now formalize this property.

Proposition 4.6 (Solvability of the systems). *Given the stage vector $\mathbf{c} = \{c_i\}$ and weight vector $\mathbf{b} = \{b_i\}$, if the c_i 's are distinct within each Q -group, and all b_i 's are nonzero for $i \in \text{supp } V_l = \{1, l+2, l+3, \dots, s\}$, then the linear systems arising in the construction of the D -type and Q -type spaces are square and non-singular. Consequently, the RK coefficients a_{ij} are uniquely determined by the recursion.*

Proof. The D -system and the Q -system equations are given in Section 4.4 and Section 4.5, respectively. By arranging the equations and variables according to the specific sequences—right to left and bottom to top for the D -systems, and top to bottom and left to right for the Q -systems.

For the D -systems, the coefficient matrix is block lower-triangular.

$$\mathbf{M}_D = \begin{bmatrix} \mathbf{L}_{1,1}^D & 0 & 0 & \cdots & 0 \\ * & \mathbf{L}_{2,2}^D & 0 & \cdots & 0 \\ * & * & \mathbf{L}_{3,3}^D & \cdots & 0 \\ \vdots & \vdots & \vdots & \ddots & \vdots \\ * & * & * & \cdots & \mathbf{L}_{s_2, s_2}^D \end{bmatrix}, \quad (59)$$

where $s_2 = \frac{n(n+1)}{2}$ is the number of stages occupied by the D -space construction. The size of the blocks corresponds to the number of variables in each column of \mathbf{A} . Each diagonal block exhibits the following structure (upon reordering the variables and equations within the block):

$$\mathbf{L}_{i,i} = \begin{bmatrix} \mathbf{V}_{i,i}^D & \mathbf{W}_{i,i}^D \\ \mathbf{0} & \mathbf{I} \end{bmatrix}, \quad (60)$$

where $\mathbf{V}_{i,i}^D$ is a Vandermonde matrix and $\mathbf{W}_{i,i}^D$ is a non-square Vandermonde matrix, and \mathbf{I} is an identity matrix. The non-singularity of each block $\mathbf{L}_{i,i}^D$ is guaranteed by the distinctness of the nodes c_k in the same D -group and the non-vanishing of the weights b_k , which ensures that the Vandermonde matrices are invertible. Since \mathbf{M}_D is block lower-triangular with non-singular diagonal blocks, it follows that \mathbf{M}_D itself is non-singular. Furthermore, according to Figure 9 and the definition of I^D , we observe that the size of the matrix $\mathbf{L}_{i,i}^D$ increases with i , and the dimension of $\mathbf{L}_{i,i}^D$ is at most $i + 1$.

For the Q -systems, the coefficient matrix is block diagonal:

$$\mathbf{M}_Q = \begin{bmatrix} \mathbf{L}_1^Q & 0 & 0 & \cdots & 0 \\ 0 & \mathbf{L}_2^Q & 0 & \cdots & 0 \\ 0 & 0 & \mathbf{L}_3^Q & \cdots & 0 \\ \vdots & \vdots & \vdots & \ddots & \vdots \\ 0 & 0 & 0 & \cdots & \mathbf{L}_{s-1}^Q \end{bmatrix}. \quad (61)$$

The size of the blocks corresponds to the number of variables in each row of the Q -region of \mathbf{A} . It is obvious that the size of \mathbf{L}_i^Q is at most $l + 1$ (if the shadowing part of Figure 10 is evaluated in prior, then the size should be at most m). Each diagonal block has the following structure (upon reordering the variables and equations within the block):

$$\mathbf{L}_i^Q = \begin{bmatrix} \mathbf{V}_i^Q & \mathbf{W}_i^Q \\ \mathbf{0} & \mathbf{I} \end{bmatrix}, \quad (62)$$

where \mathbf{V}_i^Q is a Vandermonde matrix and \mathbf{W}_i^Q is a non-square Vandermonde matrix, and I is an identity matrix. The non-singularity of each block \mathbf{L}_i^Q is guaranteed by the distinctness of the nodes c_i in the same Q -group, which ensures that the Vandermonde matrices are invertible. Since \mathbf{M}_Q is block diagonal with non-singular diagonal blocks, it follows that \mathbf{M}_Q itself is non-singular.

Consequently, each block in both the D - and Q -systems is square and non-singular, ensuring that the RK coefficients a_{ij} are uniquely determined by the recursive procedure. \square

Numerical stability. Both the D - and Q -systems are well conditioned: their block-triangular or block-diagonal structures imply that we only need to invert the blocks on the diagonal. For the D -systems blocks, they can be abstractly written as (59). After simple row pivotings this matrix is just a Vandermonde matrix and an identity matrix on the diagonal. Since c_k are Gauss-

Lobatto nodes, the corresponding Vandemonde matrix is well-conditioned. For the Q -system blocks, the blocks (62) are just Vandemonde matrices with respect to the corresponding stages c_i , $2 \leq i \leq l + 1$. In our construction method, these c_i 's are free parameters, as long as they are distinct, so that the corresponding Vandemonde matrix is invertible. When constructing methods with extremely high orders ($p > 30$), we recommended choosing these stage values as Gauss-nodes or Chebyshev nodes for better numerical stability, since the condition number of Vandemonde matrices corresponding to equi-spaced nodes grow exponentially with size [13], while those corresponding to Gauss or Chebyshev nodes has lower growth rate. Moreover, if we use the generalized Vandermonde matrices corresponding to Gauss or Chebyshev nodes, the condition number only grows polynomially with size [12, 18]. Consequently, coefficient computation can be performed accurately in double precision without resorting to rational arithmetic or symbolic simplification.

4.8 Algorithmic Formulation

Algorithm 1 summarizes the complete construction. For clarity, the algorithm is stated in a high-level pseudocode form.

Algorithm 1 Construction of a high-order ERK tableau

Input: Desired even order p of the RK method

Output: RK coefficients $\mathbf{A}, \mathbf{b}, \mathbf{c}$

- 1: Compute auxiliary parameters:
 $m = p/2 - 1$, $n = p/2$, $N = n + 1$, $q = \dim Q_m = \frac{m(m-1)}{2}$, $d = \dim D_n = \frac{n(n+1)}{2}$
 - 2: Determine sub-block sizes $s_1 = q$, $s_2 = n(n + 1)/2$ and number of stages $s = 1 + s_1 + s_2$
 - 3: Construct stage nodes \mathbf{c} and weights \mathbf{b} (N -point Lobatto nodes and free nodes)
 - 4: Initialize coefficient matrix $\mathbf{A} \leftarrow \mathbf{0}_{s \times s}$
// Solve D-type linear systems (block lower-triangular)
 - 5: Form D-system: $\mathbf{M}_D \mathbf{x}_D = \mathbf{r}_D$ using stage clusters
 - 6: **for** $k = 1, \dots, n$ **do**
 - 7: Assemble equations (36), (37) and (38) for each element in I_k^D to get corresponding row of \mathbf{M}_D and corresponding entry in \mathbf{r}_D .
 - 8: **end for**
 - 9: Solve \mathbf{x}_D block-by-block using a custom block-triangular solver
 - 10: Fill \mathbf{A} with \mathbf{x}_D
// Solve Q-type linear systems (block diagonal)
 - 11: Form Q-system: $\mathbf{M}_Q \mathbf{x}_Q = \mathbf{r}_Q$ using solved \mathbf{A} and Q_m space
 - 12: **for** $k = 1, \dots, m$ **do**
 - 13: Assemble equations (45), (46) and (47) for each element in I_k^Q to get corresponding row of \mathbf{M}_Q and corresponding entry in \mathbf{r}_Q .
 - 14: **end for**
 - 15: Solve \mathbf{x}_Q block-by-block using a custom block-diagonal solver
 - 16: Fill \mathbf{A} with \mathbf{x}_Q
// Return final RK tableau
 - 17: **return** $\mathbf{A}, \mathbf{b}, \mathbf{c}$
-

Several implementation issues deserve comment:

- **Choice of c_i :** We did not specify the nodes c_i which lie in the space V_l^* . These nodes may be chosen heuristically (e.g., equally spaced, quadrature nodes) or optimized to minimize local error constants.
- **Rational vs. floating arithmetic:** For small orders (≤ 6) it is convenient to work with rational coefficients; for higher orders ($6 \sim 9$) numerical linear algebra in double precision suffices; for extremely high orders (≥ 10) it is recommended to use arbitrary-precision decimal number representations, for example, the `N[num,length]` operation in Mathematica, the `decimal` library in Python, and the `BigFloat` type in Julia.
- **Stability of recursion:** Each diagonal block matrix of the linear system is typically well-conditioned, the algorithm is numerically stable up to large p .
- **Automatic code generation:** The procedure can be implemented either symbolically or numerically. We have implemented it as a lightweight tool in Julia to generate coefficients automatically.

4.9 Efficiency of Construction

The recursive formulation of Section 4 leads not only to ERK schemes satisfying order conditions but also to a highly efficient algorithm for generating ERK coefficients (Algorithm 1). This subsection present a mathematical analysis of its computational complexity.

Algorithmic structure. After the recursion for constructing Q and D -type spaces is specified, all unknown coefficients of the RK tableau are determined by two linear systems:

- (i) a **D -system**, derived from the construction of D -type spaces, which is a block lower-triangular linear system;
- (ii) a **Q -system**, derived from the construction of Q -type spaces, which is a block diagonal linear system.

The two systems are solved sequentially: the D -system is solved first, yielding all bottom-right coefficients in \mathbf{A} , and its result is then substituted into the Q -system to determine left part of \mathbf{A} . No nonlinear coupling between the two systems remains.

Complexity model. Let p denote the order of an RK scheme and $s = s(p)$ the resulting number of stages ($s(p) \sim p^2/4$ asymptotically). Let the D -system have diagonal blocks of sizes d_1, \dots, d_{s_2-1} , where $s_2 = n(n+1)/2$, which is consistent with the definition in Algorithm 1; the Q -system have diagonal blocks of sizes q_1, \dots, q_{s-1} . The total number of unknowns is

$$\mathcal{N} = \mathcal{N}_D + \mathcal{N}_Q = \sum_{i=1}^{s_2-1} d_i + \sum_{j=1}^{s-1} q_j \leq \sum_{i=1}^{s_2-1} i + \sum_{j=1}^{s-1} (l+1) = \mathcal{O}(s^2),$$

where \mathcal{N}_D and \mathcal{N}_Q are the number of unknowns in the D - and Q -system, respectively. In the following complexity analysis, we assume that solving a dense $r \times r$ block requires $\Theta(r^3)$ arithmetic operations.

Proposition 4.7 (Cost of solving the D -system). *If the D -system matrix is block lower-triangular with diagonal blocks of sizes d_i , then the total arithmetic cost of solving the D -system is*

$$\mathcal{C}_D = \Theta\left(\sum_{i=1}^{s_2-1} d_i^3 + \sum_{i=1}^{s_2-1} \sum_{j<i} d_i d_j\right) \leq \mathcal{O}(s^4).$$

Proof. Backward substitution proceeds blockwise: each diagonal block solve costs $\Theta(d_i^3)$, and each coupling to preceding blocks adds $\Theta(d_i d_j)$ work bounded by the same order. Summing over all blocks yields

$$\begin{aligned} \mathcal{C}_D &= \Theta\left(\sum_{i=1}^{s_2-1} d_i^3 + \sum_{i=1}^{s_2-1} \sum_{j<i} d_i d_j\right) = \Theta\left(\sum_{i=1}^{s_2-1} d_i^3 + \frac{1}{2}\left(\left(\sum_{i=1}^{s_2-1} d_i\right)^2 - \sum_{i=1}^{s_2-1} d_i^2\right)\right) \\ &= \Theta\left(\sum_{i=1}^{s_2-1} d_i^3 + \frac{1}{2}\left(\mathcal{N}_D^2 - \sum_{i=1}^{s_2-1} d_i^2\right)\right). \end{aligned}$$

By our construction, $d_i \leq i$, so

$$\mathcal{C}_D \leq \mathcal{O}\left(\sum_{i=1}^{s_2-1} i^3 + \frac{1}{2}\mathcal{N}_D^2\right) = \mathcal{O}(s^4).$$

□

Proposition 4.8 (Cost of solving the Q -system). *If the Q -system is block diagonal with blocks of size q_j , then the total cost of solving it is*

$$\mathcal{C}_Q = \Theta\left(\sum_{j=1}^{s-1} q_j^3\right) \leq \mathcal{O}(s^4).$$

Proof. Each block is independent and can be solved separately. For block of size q_j , the block solve cost is $\Theta(q_j^3)$, and summing over $s-1$ blocks yields total cost of

$$\mathcal{C}_Q = \Theta\left(\sum_{j=1}^{s-1} q_j^3\right)$$

using the inequality $q_j \leq l+1$, we have

$$\mathcal{C}_Q \leq \mathcal{O}\left(\sum_{j=1}^{s-1} (l+1)^3\right) = \mathcal{O}(s^4).$$

□

Theorem 4.9 (Overall computational complexity). *Under the structural assumptions above, the total arithmetic cost of constructing all coefficients is*

$$\mathcal{C}_{\text{total}} = \mathcal{C}_D + \mathcal{C}_Q + \mathcal{O}(\mathcal{N}) \leq \mathcal{O}(s^4) \quad (63)$$

Proof. The proof is direct from Propositions 4.7 and 4.8. The $\mathcal{O}(\mathcal{N})$ term accounts for assembly and simple vector operations. □

Remark 4.3. In the actual implementation of the algorithm, we further reduce the size of the linear systems by assigning the variables corresponding to the shaded regions in Figures 9 and 10 in advance. This further reduces the complexity of the algorithm. In practice, the computational cost of solving both the Q -system and the D -system can be controlled within $\mathcal{O}(s^3p)$, so the overall complexity can also be reduced to $\mathcal{O}(s^3p)$.

4.10 A $p(p-2)$ Embedded Pair

The preceding construction yields an ERK method $(\mathbf{A}, \mathbf{b}, \mathbf{c})$ of the target order p . Without altering the stage matrix \mathbf{A} or the node vector \mathbf{c} , one may further employ the vector \mathbf{d}_1 introduced in Section 3 to construct an associated weight vector $\tilde{\mathbf{b}}$, thereby deriving an embedded method that shares the same stage values as the principal scheme.

4.10.1 Construction of the Embedded Weights

Definition 4.3 (Embedded RK pair [21, Section II.4, pp. 164–166]). Following the terminology of Hairer, Nørsett, and Wanner, an embedded RK pair consists of two RK formulas that share the same set of stage values. More precisely, let the stage values be given by

$$k_i = f \left(t_n + c_i h, y_n + h \sum_{j=1}^s a_{ij} k_j \right), \quad i = 1, \dots, s,$$

and define two numerical update formulas by

$$y_{n+1} = y_n + h \sum_{i=1}^s b_i k_i,$$

$$\tilde{y}_{n+1} = y_n + h \sum_{i=1}^s \tilde{b}_i k_i.$$

If these two formulas use the same stage matrix $\mathbf{A} = (a_{ij})$ and node vector $\mathbf{c} = (c_i)$, differing only in the weight vectors \mathbf{b} and $\tilde{\mathbf{b}}$, then

$$(\mathbf{A}, \mathbf{b}, \tilde{\mathbf{b}}, \mathbf{c})$$

is called an embedded RK pair. If the principal formula $(\mathbf{A}, \mathbf{b}, \mathbf{c})$ has algebraic order p , whereas the associated formula $(\mathbf{A}, \tilde{\mathbf{b}}, \mathbf{c})$ has algebraic order $p - 2$, then it is called a $p(p - 2)$ embedded RK pair.

Construction In this paper, we adopt the following simple choice:

$$\tilde{\mathbf{b}} = \mathbf{b} + \mathbf{d}_1. \quad (64)$$

Here \mathbf{d}_1 is the residual vector appearing in the definition of D_2 ; see (15). Thus, the difference between the embedded weight vector and the principal weight vector is entirely determined by \mathbf{d}_1 , while the stage structure itself remains unchanged.

To avoid notational ambiguity, for the embedded weight vector $\tilde{\mathbf{b}}$ we denote the corresponding D -residual vectors and simplified D -spaces by

$$\begin{aligned} \tilde{\mathbf{d}}_r &:= (\tilde{\mathbf{b}} \odot \mathbf{c}^{\odot r}) \times^1 \mathbf{A} - \frac{1}{r+1} \tilde{\mathbf{b}} \odot (\mathbf{1} - \mathbf{c}^{\odot(r+1)}), \\ \tilde{D}_r &:= \text{span}\{\tilde{\mathbf{d}}_{r-1}, \tilde{D}_{r-1} \times^1 \mathbf{A}, \tilde{D}_{r-1} \odot \Phi_1\}, \end{aligned}$$

with $\tilde{D}_0 = \text{span}\{\mathbf{0}\}$. Since the definition of the Q -spaces depends only on \mathbf{A} and \mathbf{c} , the Q -spaces associated with the embedded method coincide exactly with those of the original method.

Lemma 4.10 (Two-order shift of the D -spaces for the embedded method). *Let $\tilde{\mathbf{b}} = \mathbf{b} + \mathbf{d}_1$, and define $\tilde{\mathbf{d}}_r$ and \tilde{D}_r accordingly. Then, for any $r \geq 0$,*

$$\tilde{D}_r \subseteq D_{r+2}. \quad (65)$$

Proof. For $r = 0$, we have $\tilde{D}_0 = \text{span}\{\mathbf{0}\} \subseteq D_2$, so the conclusion is immediate. We now proceed by induction for $r \geq 1$.

First consider the case $r = 1$. Since $\tilde{D}_1 = \text{span}\{\tilde{\mathbf{d}}_0\}$, it suffices to verify that $\tilde{\mathbf{d}}_0 \in D_3$. Substituting $\tilde{\mathbf{b}} = \mathbf{b} + \mathbf{d}_1$ into the definition of $\tilde{\mathbf{d}}_0$ yields

$$\tilde{\mathbf{d}}_0 = \mathbf{d}_0 + [\mathbf{d}_1 \times^1 \mathbf{A} - \mathbf{d}_1 \odot (\mathbf{1} - \mathbf{c})].$$

Here $\mathbf{d}_0 \in D_1 \subseteq D_3$. The correction terms $\mathbf{d}_1 \times^1 \mathbf{A}$ and $\mathbf{d}_1 \odot (\mathbf{1} - \mathbf{c})$ in the brackets belongs to D_3 by the recursive definition (15) of D -spaces. Hence $\tilde{D}_1 \subseteq D_3$.

Now let $r \geq 2$, and assume inductively that

$$\tilde{D}_{r-1} \subseteq D_{r+1}.$$

By the recursive definition of \tilde{D}_r , it remains to show that each of its generators belongs to D_{r+2} .

We first examine $\tilde{\mathbf{d}}_{r-1}$. From $\tilde{\mathbf{b}} = \mathbf{b} + \mathbf{d}_1$ and the definition of $\tilde{\mathbf{d}}_{r-1}$,

$$\tilde{\mathbf{d}}_{r-1} = \mathbf{d}_{r-1} + \left[(\mathbf{d}_1 \odot \mathbf{c}^{\odot(r-1)}) \times^1 \mathbf{A} - \frac{1}{r} \mathbf{d}_1 \odot (\mathbf{1} - \mathbf{c}^{\odot r}) \right].$$

Here $\mathbf{d}_{r-1} \in D_r \subseteq D_{r+2}$. Moreover, the correction terms in brackets is generated from \mathbf{d}_1 ; by the recursive definition (15) of the D -spaces, we obtain $(\mathbf{d}_1 \odot \mathbf{c}^{\odot(r-1)}) \times^1 \mathbf{A} \in D_{r+2}$ and $\mathbf{d}_1 \odot (\mathbf{1} - \mathbf{c}^{\odot r}) \in D_{r+2}$. Thus, the correction terms belong to D_{r+2} . Therefore,

$$\tilde{\mathbf{d}}_{r-1} \in D_{r+2}.$$

Next, by the induction hypothesis and the recursive definition (15),

$$\tilde{D}_{r-1} \times^1 \mathbf{A} \subseteq D_{r+1} \times^1 \mathbf{A} \subseteq D_{r+2}.$$

Similarly,

$$\tilde{D}_{r-1} \odot \Phi_1 \subseteq D_{r+1} \odot \Phi_1 \subseteq D_{r+2}.$$

Hence all generators of \tilde{D}_r belong to D_{r+2} , and therefore

$$\tilde{D}_r \subseteq D_{r+2}.$$

This completes the induction. □

4.10.2 Order of the Embedded Method

Theorem 4.11 ($p(p-2)$ embedded property). *Let $(\mathbf{A}, \mathbf{b}, \mathbf{c})$ be the order- p ERK method constructed by Algorithm 1, where $p \geq 4$ is even. Assume further that $n \geq 2$ and that this method satisfies the conditions in Theorem 3.2,*

$$B(p), \quad QO(m), \quad DO(n), \quad QD(m, n), \quad QR(m),$$

where $m \geq n-1$ and $m+n+1 \geq p$. Let $\tilde{\mathbf{b}}$ be given by (64), and denote the corresponding D -residual spaces by \tilde{D}_r . Then the associated method $(\mathbf{A}, \tilde{\mathbf{b}}, \mathbf{c})$ satisfies

$$B(p), \quad QO(m), \quad DO(n-2), \quad QD(m, n-2), \quad QR(m),$$

and therefore has algebraic order at least $p-2$ by Theorem 3.2. Consequently, $(\mathbf{A}, \mathbf{b}, \tilde{\mathbf{b}}, \mathbf{c})$ forms a $p(p-2)$ embedded Runge–Kutta pair.

Proof. We first show that $B(p)$ remains valid after replacing \mathbf{b} by $\tilde{\mathbf{b}}$. For any $k = 1, \dots, p$, by (64),

$$\tilde{\mathbf{b}}^\top \mathbf{c}^{\odot(k-1)} = \mathbf{b}^\top \mathbf{c}^{\odot(k-1)} + \mathbf{d}_1^\top \mathbf{c}^{\odot(k-1)}.$$

Since the original method satisfies $B(p)$, the first term equals $1/k$. The second term vanishes by the cluster property of \mathbf{d}_1 and its orthogonality to the nodal power basis. Hence

$$\tilde{\mathbf{b}}^\top \mathbf{c}^{\odot(k-1)} = \frac{1}{k}, \quad k = 1, \dots, p.$$

Therefore the associated method also satisfies $B(p)$.

Moreover, since the definition of Q_k depends only on \mathbf{A} and \mathbf{c} , replacing \mathbf{b} by $\tilde{\mathbf{b}}$ does not alter the sequence of Q -spaces. Thus $QR(m)$ also remains valid for the embedded method. It remains to verify the other three conditions.

We first prove $QO(m)$. Let $\mathbf{q} \in Q_m$ be arbitrary. By (64),

$$\tilde{\mathbf{b}} \odot \mathbf{q} = \mathbf{b} \odot \mathbf{q} + \mathbf{d}_1 \odot \mathbf{q}.$$

The first term $\mathbf{b} \odot \mathbf{q} = \mathbf{0}$ because the original method satisfies $QO(m)$. By the definition of the D -spaces (Definition 3.10), we have $\mathbf{d}_1 \in D_2$. Combined with $n \geq 2$ and the recursive definition (15), this gives $D_2 \subseteq D_n$. Hence, by $QD(m, n)$, we obtain $\mathbf{d}_1 \odot \mathbf{q} = \mathbf{0}$. Therefore $\tilde{\mathbf{b}}$ satisfies $QO(m)$.

Next we prove $DO(n-2)$ and $QD(m, n-2)$. By Lemma 4.10,

$$\tilde{D}_{n-2} \subseteq D_n.$$

Therefore, for any $\tilde{\mathbf{d}} \in \tilde{D}_{n-2}$ and any $k = 1, \dots, p-n$, the condition $DO(n)$ for the original method yields

$$\tilde{\mathbf{d}}^\top \mathbf{c}^{\odot(k-1)} = 0.$$

Since $p-n = (p-2) - (n-2)$, this index range is exactly the one required for $DO(n-2)$, and hence the embedded method satisfies $DO(n-2)$.

On the other hand, for any $\mathbf{q} \in Q_m$ and any $\tilde{\mathbf{d}} \in \tilde{D}_{n-2}$, the inclusion $\tilde{D}_{n-2} \subseteq D_n$ together with $QD(m, n)$ gives

$$\mathbf{q} \odot \tilde{\mathbf{d}} = \mathbf{0}.$$

So the embedded method satisfies $QD(m, n-2)$.

Finally, we apply Theorem 3.2. From the above, the embedded method satisfies

$$B(p), \quad QO(m), \quad DO(n-2), \quad QD(m, n-2), \quad QR(m).$$

At the same time, the original assumptions $m \geq n-1$ and $m+n+1 \geq p$ immediately imply

$$m \geq (n-2) - 1, \quad m + (n-2) + 1 \geq p - 2,$$

so Theorem 3.2 applies to the associated method $(\mathbf{A}, \tilde{\mathbf{b}}, \mathbf{c})$, yielding algebraic order at least $p-2$. Thus $(\mathbf{A}, \mathbf{b}, \tilde{\mathbf{b}}, \mathbf{c})$ is a $p(p-2)$ embedded RK pair. \square

4.10.3 Error Estimation and Adaptive Implementation

The essential role of an embedded RK method is to produce, from the same set of stage values, two numerical approximations of different orders, and thereby to construct an estimator for the one-step error. This idea can be traced back to Fehlberg and later developments such as the Dormand–Prince formulas, while a systematic treatment of error estimation and variable-stepsize control can be found in the classical exposition of Hairer, Nørsett, and Wanner [16, 11, 32, 21]. For the $p(p-2)$ embedded pair constructed here, the difference takes the form

$$\Delta_{n+1} := h \sum_{i=1}^s (b_i - \tilde{b}_i) k_i = -h \sum_{i=1}^s (d_1)_i k_i, \quad (66)$$

where the k_i are the stage values shared by the principal and embedded methods. Since $\tilde{\mathbf{b}} = \mathbf{b} + \mathbf{d}_1$, this error estimator is determined entirely by \mathbf{d}_1 and requires no additional stage evaluations. Thus, once one step of the principal method has been completed, Δ_{n+1} is obtained by a single terminal linear combination. This is one of the principal reasons why embedded RK methods are so widely used in practical solvers; representative examples include the Fehlberg, Dormand–Prince, and later Bogacki–Shampine pairs [16, 11, 32, 3, 34].

In a standard variable-stepsize implementation, (66) must be combined with absolute and relative tolerances. Hairer et al. provide a fairly standard unified formulation [21]. For a system of dimension d , one may define the componentwise scale

$$sc_i := \text{Atol}_i + \max\{|(y_n)_i|, |(y_{n+1})_i|\} \text{Rtol}_i, \quad i = 1, \dots, d,$$

and the normalized error measure

$$\text{err} := \left(\frac{1}{d} \sum_{i=1}^d \left(\frac{(\Delta_{n+1})_i}{sc_i} \right)^2 \right)^{1/2}. \quad (67)$$

For the $p(p-2)$ embedded pair considered here, the difference between the principal and associated methods satisfies

$$\Delta_{n+1} = O(h^{p-1}),$$

and hence one may use the same stepsize selection strategy as in classical embedded RK methods:

$$h_{\text{new}} = h \cdot \min \left\{ \alpha_+, \max \left[\alpha_-, \eta \left(\frac{1}{\text{err}} \right)^{1/(p-1)} \right] \right\}, \quad (68)$$

where $\eta \in (0, 1)$ is a safety factor, and α_- and α_+ control the decrease and increase of the stepsize, respectively. If $\text{err} \leq 1$, the current step is accepted and the integration proceeds with h_{new} ; if $\text{err} > 1$, the current step is rejected and recomputed with the new stepsize. Such stepsize control strategies have become standard components of modern adaptive embedded RK algorithms [21,

34].

When an embedded pair is used, one must also make the classical and important implementation choice of whether the higher-order approximation should be used to continue the integration. On this point, Hairer et al. note that when the two formulas have different orders, their difference is typically used only for stepsize control, whereas the actual numerical update should be performed with the higher-order approximation; this practice is commonly referred to as local extrapolation [21]. This principle is particularly evident in the design philosophies of the Fehlberg and Dormand–Prince families. Fehlberg’s construction focuses primarily on producing a lower-order associated approximation for use in stepsize control [16, 15]; Dormand and Prince, by contrast, further optimize the error constant of the higher-order approximation itself, leading to embedded formulas that are especially suitable for local extrapolation [11, 32]. Although the $p(p-2)$ embedded pair constructed here differs from the classical 5(4) or 8(7) structures, its mode of use is entirely consistent with this modern embedded-RK framework: the order- p principal method is used for propagation, the order- $(p-2)$ embedded method provides the error indicator, and the stepsize is adjusted through (68).

In summary, the embedded pair obtained here is not an isolated auxiliary structure, but rather a natural bridge between the preceding recursive construction framework and the standard implementation of adaptive RK methods: the principal method retains order p , the embedded method supplies an error indicator, and the entire error-estimation and stepsize-control mechanism is built solely upon the stage values already computed within the same step together with the vector \mathbf{d}_1 . This provides a direct algorithmic foundation for extending the present construction to genuinely adaptive explicit solvers.

4.11 Summary

The recursive construction transforms the abstract Q - and D -conditions into a practical algorithm for generating ERK methods of any prescribed order. The method requires only the repeated solution of small linear systems and produces a sparse, structured RK tableau. In the next section we analyze its stage number, sparsity pattern, and asymptotic properties.

5 Theoretical and numerical properties of the constructed methods

5.1 Stage number estimate

A fundamental question for any family of ERK methods is the minimal number of stages s required to attain a given order p . For explicit methods, it is well believed that s must grow at least quadratically with p , and the leading term in the asymptotic expansion

$$s(p) \sim \kappa p^2$$

is a useful indicator of overall efficiency.

Asymptotic behaviour. The methods obtained by our recursive construction satisfy

$$s(p) = \frac{1}{4}p^2 + \alpha p + \beta, \quad (69)$$

where α and β are moderate constants depending on the particular implementation of the V_l clustering pattern. For the implementation described in section 4, we obtain that for even number $p \geq 4$,

$$\begin{aligned} s(p) &= 1 + l + s_2 = 1 + \dim W_m^Q + (\dim W_n^D + n) \\ &= 1 + \frac{m(m-1)}{2} + \frac{n(n-1)}{2} + n \\ &= 1 + \frac{\binom{p}{2} - 1}{2} + \frac{\binom{p}{2} - 1}{2} + \frac{p}{2} \\ &= (p^2 - 2p + 8)/4 \end{aligned}$$

The leading term $p^2/4$ coincides exactly with Gragg's estimate [19] for extrapolation-based ERK schemes, and therefore represents the asymptotically optimal value currently known for this class of methods. It improves upon Butcher's bound $(3p^2/8)$ [8], which relies on direct satisfaction of order conditions and generalized order conditions. The first-order term $-p/2$ improves upon Gragg's bound whose first-order term is 0.

Low-order behaviour. Our method give better stage estimates than all current methods which can give general upper bounds for s , including Gragg [19], Butcher [8] and Verner's [38] methods. For low orders, it tends to require a few additional stages compared with the minimal-stage families. This is a natural consequence of the stronger Q–D orthogonality constraints enforced at low order. As the order increases, the effect of these initial constraints becomes negligible and (69) dominates. Table 6 gives a representative comparison.

Table 6: Approximate stage numbers s for different families of RK methods. Boldface indicates the smallest value among these families. The last column lists the best stage numbers currently known; these are obtained for specific orders p rather than by a unified construction.

Order p	Gragg	Butcher	Sharp & Verner [35]	Our construction	Best possible known
4	5	4	-	4	4
6	10	9	8	8	7 [6]
8	17	17	14	14	11 [10]
10	26	28	26	22	15 [36]
12	37	42	41	32	25 [30, 14]
14	50	59	60	44	-
16	65	79	83	58	-

Interpretation. Equation (69) shows that the proposed recursive construction achieves the same asymptotic stage/order ratio as Gragg’s extrapolation methods while maintaining a purely explicit and algebraically transparent formulation. Hence, it may be viewed as an alternative pathway to the asymptotic efficiency limit within the ERK framework.

5.2 Structural Properties and Sparsity Pattern

An appealing by-product of the recursive construction under the V_l -constraints is that the resulting RK tableau exhibits a highly structured, and often sparse, coefficient matrix \mathbf{A} .

Sparsity. In the construction of Q -type spaces, we enforced condition of the form $\mathbf{A}e_i \in \text{span}\{e_{i_1}, e_{i_1+1}, \dots, e_{i_2}\}$ with $i \leq i_1 \leq \dots \leq i_2$, which contributes to large zero blocks in the left part of matrix \mathbf{A} ; while in the construction of D -type spaces, we enforced conditions in a similar way: $\varepsilon_{ni}\mathbf{A}$ should lie in the span of some set of ε_{mj} for some $m + j \leq n + i$, this results in large chunks of the bottom right part of \mathbf{A} be zero if we set $a_{ij} = 0$ for $l + 2 \leq i \leq l + n - 1$, $l + 2 \leq j \leq l + n - 1$.

The empirical density of nonzero elements,

$$\rho(\mathbf{A}) = \frac{\#\{a_{ij} \neq 0, i > j\}}{s(s-1)/2},$$

decreases with order: $\rho(\mathbf{A}) \approx 85.7\%$ for $p = 6$, 68.1% for $p = 8$, 56.7% for $p = 10$ and less than 50% for $p \geq 12$. An illustrative sparsity pattern for $p = 10$ is shown in Figure 11. We estimate the number of non-zero elements to grow as $\mathcal{O}(s^{3/2})$, while the total number of elements scales as $\mathcal{O}(s^2)$.

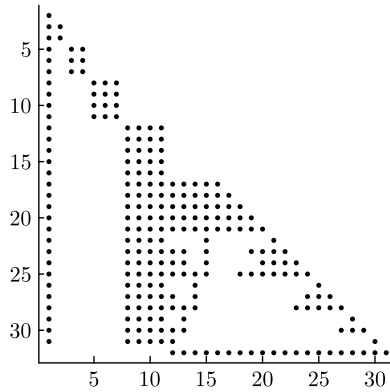


Figure 11: Sparsity pattern for matrix $\mathbf{A} \in \mathbb{R}^{32 \times 32}$ of an order 12 method using our construction. The dotted position indicates nonzero elements.

Computational implications. This structural property has several practical advantages:

- The cost of evaluating all internal stages scales with the number of nonzero coefficients, which is significantly below $s^2/2$ for large p .
- The sparsity pattern can allow for more efficient construction of high order schemes and straightforward implementation of low-storage variants.
- The sparsity pattern is not imposed by hand but arises naturally from the recursive satisfaction of Q -, D - and mutual orthogonality conditions.

Comparison with existing methods. Gragg’s high-order explicit methods are typically dense, with little exploitable structure in \mathbf{A} . Butcher’s and Verner’s methods can give rise to tableaux with some sparsity, however, at the expense of large stage numbers, which means more function evaluations are needed. In contrast, our recursion yields a predictable, hierarchical sparsity pattern that becomes increasingly pronounced with p , while maintaining numerical robustness and algebraic simplicity.

Summary. The observed sparsity and locality of the constructed tableaux translate directly into computational efficiency in both coefficient generation and time-stepping. Together with the asymptotically optimal stage count, these structural properties demonstrate that the present family combines theoretical optimality with practical implementability.

5.3 Stability Regions

Although the present construction was not explicitly optimized for stability, it is instructive to examine the resulting stability regions. For each method, we compute the stability function

$$R(z) = 1 + z\mathbf{b}^\top(I - z\mathbf{A})^{-1}\mathbf{1},$$

and plot the contour $\{z \in \mathbb{C} : |R(z)| = 1\}$. As shown in Figure 12, the stability regions expand regularly with order and remain well-shaped, indicating that the recursive structure does not introduce spurious numerical artifacts.

5.4 Comparison with Existing Methods

For reference, Table 7 compares the constructed schemes with several well-known high-order ERK families. The proposed methods achieve the same or slightly better stage efficiency (asymptotically $s(p) \sim p^2/4$) and exhibit the flexibility to adjust the stability region size.

5.5 Summary

The proposed recursive construction for ERK methods combines theoretical optimality, structural elegance, and practical efficiency. Its key features can be summarized as follows:

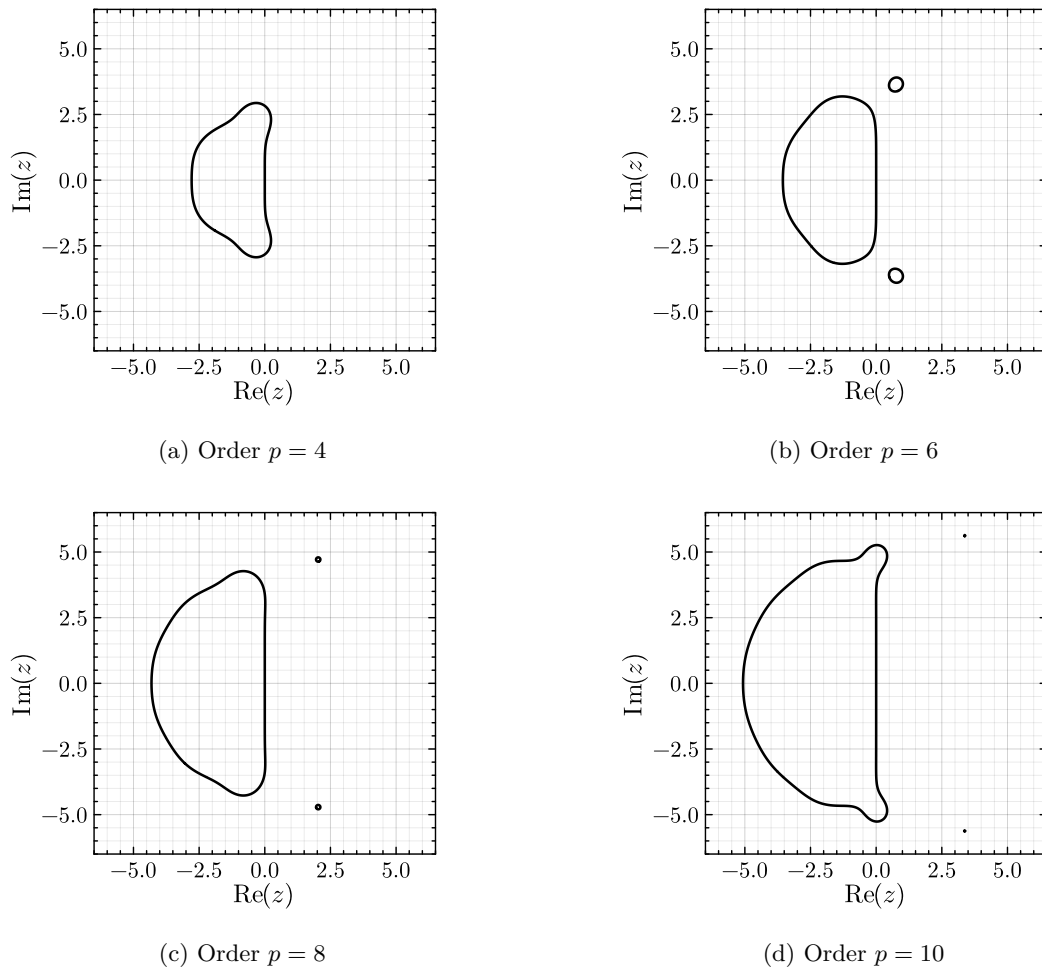


Figure 12: Stability regions of the constructed ERK methods for orders $p = 4, 6, 8, 10$.

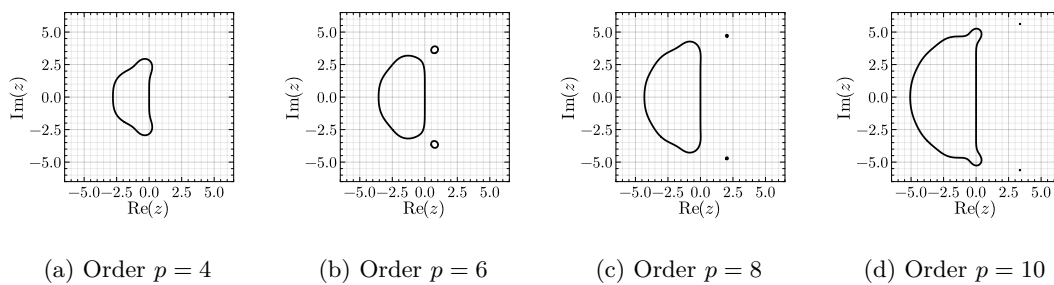


Figure 13: Stability regions of the Butcher's ERK methods for orders $p = 4, 6, 8, 10$.

- **Asymptotically optimal stage growth:** the required number of stages satisfies $s(p) \sim p^2/4$, matching the best known asymptotic bound.

Table 7: Comparison of proposed methods with known explicit RK schemes.

Method	Stage growth	Typical stability	Construction cost
Verner family	$\sim \frac{1}{2}p^2$	good	high (case by case)
Butcher family	$\sim \frac{3}{8}p^2$	moderate	low (constructive)
Gragg family	$\sim \frac{1}{4}p^2$	moderate	very low (recursive)
Proposed family	$\sim \frac{1}{4}p^2$	tunable	low (constructive)

- **Structured sparsity:** the RK matrix \mathbf{A} exhibits an emergent block-banded pattern that becomes sparser with increasing order, enabling efficient storage and evaluation.
- **Low algebraic complexity:** coefficients are obtained recursively from small linear systems, avoiding combinatorial explosion of classical order-condition approaches.
- **Stable and accurate coefficient generation:** each step of the recursion is well-conditioned, allowing reliable computation even in floating-point arithmetic.
- **Implementation flexibility:** the method is simple to automate and naturally compatible with low-storage and partially parallel time-stepping frameworks.

In summary, the present family of ERK schemes achieves a favorable combination of *high order, low cost, and structural transparency*. It offers a new perspective on constructing efficient high-order methods and provides a concrete foundation for further developments, such as adaptive stage selection, embedded error estimation, or hybrid implicit–explicit extensions.

6 Numerical experiments

In this section we provide numerical and symbolic evidence supporting the correctness and efficiency of the proposed recursive construction. Unless otherwise stated, all schemes are ERK methods generated by the algorithm of Section 4.

6.1 Verification of Order Conditions

To confirm that the constructed schemes satisfy the desired order of accuracy, we generate methods of orders $p = 4, 6, 8,$ and 10 . The corresponding RK tableaux are obtained automatically by the recursive procedure and verified in two independent ways:

1. **Symbolic verification.** Each tableau is substituted into the exact Butcher order conditions (up to order p). All computations were carried out in Julia using rational arithmetic and verified numerically in `BigFloat` 256-bit precision. All order conditions are satisfied to machine precision, confirming algebraic correctness.
2. **Numerical convergence test.** The methods are applied to a smooth linear problem,

$$y'(t) = \lambda y, \quad y(0) = 1, \quad \lambda = -1,$$

whose exact solution is $y(t) = e^{-t}$. The numerical solution is computed on the interval $[0, 1]$. The global error at final time is measured as

$$\text{err}(h) = |y_h(1) - y(1)|,$$

where $y_h(t)$ is the numerical solution computed with step size h . A sequence of step sizes $h = 2^{-k}$, $k = 0, 1, \dots, 4$ is used. The observed convergence order is estimated by

$$p_{\text{obs}} = \log_2 \left(\frac{\text{err}(h)}{\text{err}(h/2)} \right).$$

Table 8 reports the errors and the observed convergence orders for the proposed RK methods of orders $p = 4, 6, 8$ and 10. In all cases, the observed orders agree well with the theoretical design order, confirming the correctness of the construction and implementation.

Table 8: Convergence behavior for the test problem $y' = -y$ on $[0, 1]$.

h	Order 4		Order 6		Order 8		Order 10	
	$\text{err}(h)$	p_{obs}	$\text{err}(h)$	p_{obs}	$\text{err}(h)$	p_{obs}	$\text{err}(h)$	p_{obs}
1	7.121e-03	–	1.761e-04	–	2.503e-06	–	2.311e-08	–
2^{-1}	2.914e-04	4.61	1.769e-06	6.64	6.217e-09	8.65	1.424e-11	10.66
2^{-2}	1.476e-05	4.30	2.219e-08	6.32	1.938e-11	8.33	1.105e-14	10.33
2^{-3}	8.308e-07	4.15	3.107e-10	6.16	6.761e-14	8.16	0	–
2^{-4}	4.928e-08	4.08	4.595e-12	6.08	2.220e-16	8.25	0	–

6.2 Numerical stability validation

We next investigate the linear stability properties of the proposed ERK methods by means of a numerical stability validation experiment. The purpose of this test is to verify that the numerically observed stability behavior is consistent with the theoretically derived stability region.

We consider the Dahlquist test equation

$$y'(t) = \lambda y(t), \quad y(0) = 1,$$

with complex-valued parameter $\lambda \in \mathbb{C}$. For a fixed time step $h > 0$, the numerical solution produced by an ERK method satisfies

$$y_{n+1} = R(z)y_n, \quad z = h\lambda,$$

where $R(z)$ denotes the stability function of the method. The associated absolute stability region is defined by

$$\{z \in \mathbb{C} : |R(z)| \leq 1\}.$$

For each method under consideration, the stability boundary $|R(z)| = 1$ is first computed analytically from the Butcher coefficients and plotted in the complex plane. To validate this theoretical stability region numerically, we proceed as follows. A set of test points $z = h\lambda$ is sampled in the complex plane, covering both the interior and exterior of the theoretical stability region. For each such point, the test equation is integrated over a fixed number of time steps n using the corresponding step size h , and the numerical solution is classified as **stable** or **unstable** according to whether its magnitude remains below the magnitude of the initial value, i.e.

$$|y_n| \leq |y_0|.$$

The results are presented in a stability validation plot, where the theoretical stability boundary is shown as a solid curve, and the numerically observed behavior is overlaid using markers: filled markers indicate stable behavior, while hollow markers indicate instability. This representation avoids the misleading interpretation that numerical stability necessarily implies decay to machine precision, and instead directly reflects the definition of absolute stability.

Across all tested methods, the numerical stability classification is in excellent agreement with the theoretically predicted stability regions. In particular, no spurious instabilities are observed inside the stability boundary, and rapid growth is consistently detected outside the region. This confirms the correctness of the derived stability functions and validates the stability region plots used in the theoretical analysis.

6.3 Chaotic dynamics: the Lorenz system

We now assess the behavior of the proposed high-order ERK methods on a strongly chaotic problem, the classical Lorenz-63 system [28]

$$\begin{aligned}\dot{x} &= \sigma(y - x), \\ \dot{y} &= x(\rho - z) - y, \\ \dot{z} &= xy - \beta z,\end{aligned}$$

where $u(t) = (x(t), y(t), z(t))^\top$ with parameters $\sigma = 10$, $\rho = 28$, and $\beta = 8/3$. This system exhibits sensitive dependence on initial conditions and provides a stringent test for the growth of numerical errors.

We consider the initial condition $\mathbf{u}_0 = (1, 1, 1)^\top$ and integrate over the time interval $[0, 40]$. Due to the sensitive dependence on initial conditions, numerical solutions of chaotic systems remain close only for a finite time. Various notions of **predictability** or **shadowing time** have been introduced to quantify this phenomenon, see, e.g. [22, 33, 20]. In this work, we adopt an operational definition based on the divergence of numerical solutions computed with step sizes h and $h/2$.

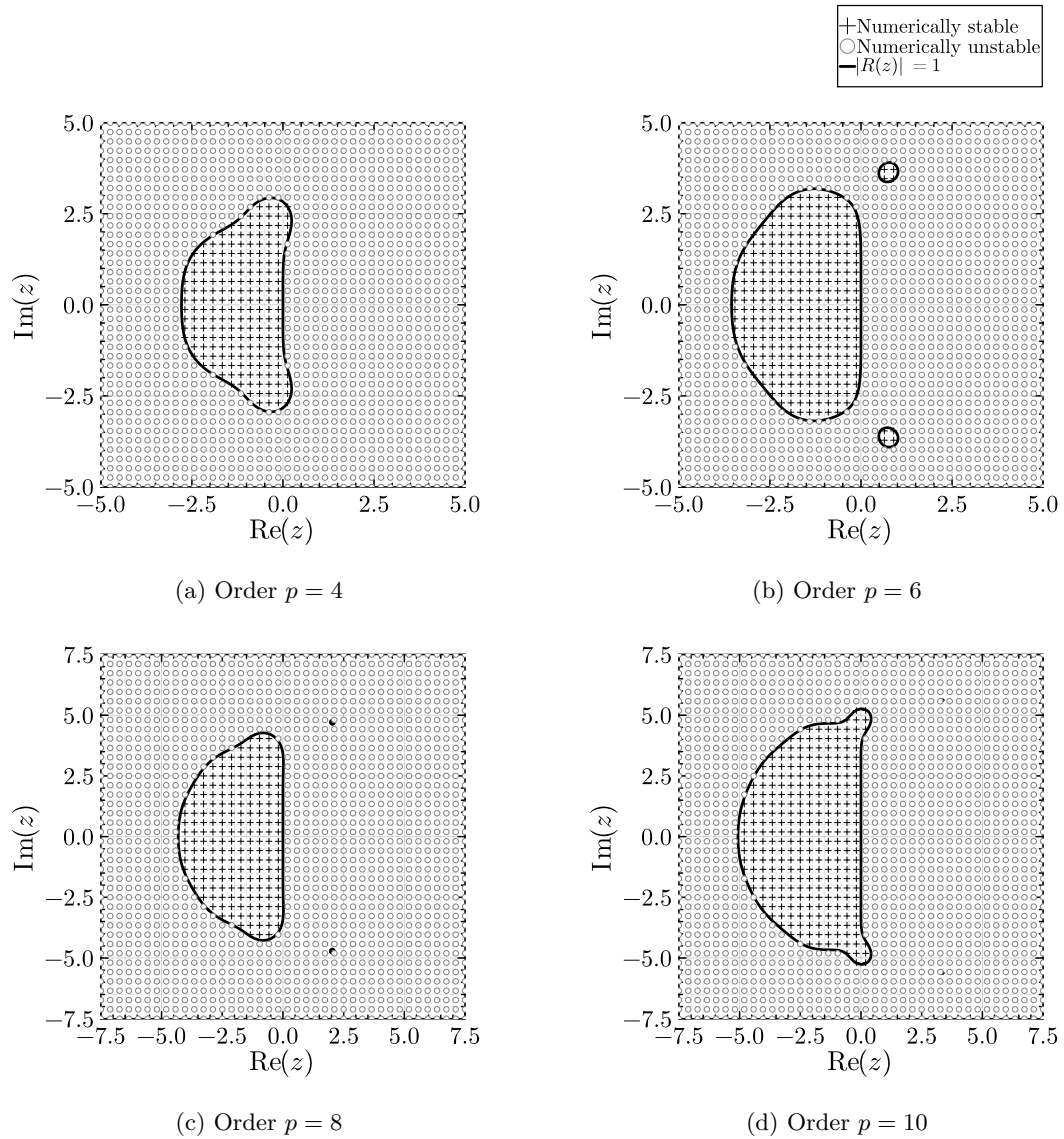


Figure 14: Numerical validation of stability regions of the constructed ERK methods for orders $p = 4, 6, 8, 10$.

Predictability time For a given RK method and step size h , we compute two numerical solutions: one with step size h and another with step size $h/2$. The discrepancy is measured at the coarse time grid points $t_n = nh$ as

$$e_h(t_n) = \|\mathbf{u}_h(t_n) - \mathbf{u}_{h/2}(t_n)\|,$$

where $\|\cdot\|$ denotes the Euclidean norm. We define the *predictability time* T_h as the earliest time at which this discrepancy exceeds a prescribed tolerance ε ,

$$T_h = \inf\{t_n : e_h(t_n) > \varepsilon\}.$$

In the experiments reported below, we use $\varepsilon = 10^{-6}$.

This definition does not imply long-time accuracy of the numerical trajectory. Rather, it provides a practical diagnostic for the rate at which numerical perturbations are amplified by the chaotic dynamics, and it is closely related to shadowing-time concepts commonly used in the numerical study of chaotic systems.

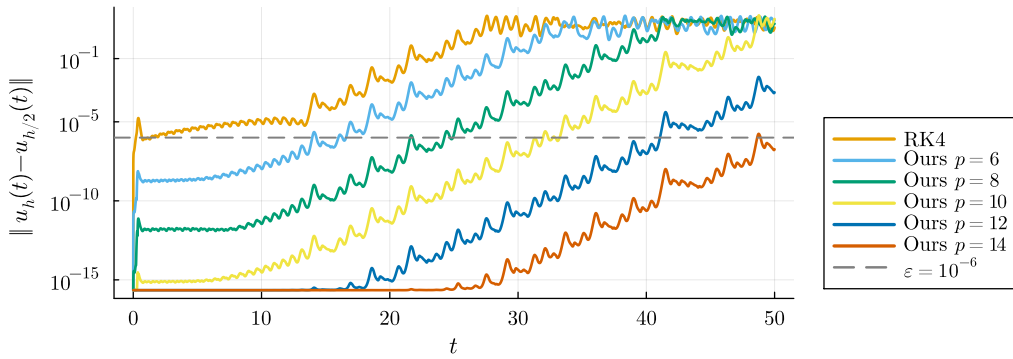


Figure 15: Growth of the numerical discrepancy $\|u_h(t) - u_{h/2}(t)\|$ for the Lorenz-63 system computed with several ERK methods. The discrepancy is measured only at coarse-grid time points. The horizontal dashed line indicates the predictability tolerance $\varepsilon = 10^{-6}$. Higher-order methods exhibit reduced initial transients and longer predictability time.

Numerical results Figure 15 displays the evolution of the discrepancy $e_h(t_h)$ for several ERK methods of increasing order, all computed with the step size $h = 2^{-8}$. After an initial transient, the error grows approximately exponentially in time, consistent with the presence of a positive Lyapunov exponent for the Lorenz system.

A notable qualitative difference is observed in the early-time behavior. Lower-order methods exhibit a pronounced initial jump and short-time oscillations in the error, reflecting the structure of their local truncation errors and their interaction with the nonlinear dynamics. In contrast, higher-order methods display smooth error growth from the initial time, indicating a re-

duced injection of numerical perturbations at early steps. This behavior persists under step-size refinement.

Table 9: Predictability time T_h for the Lorenz–63 system, defined as the earliest time such that $\|u_h(t) - u_{h/2}(t)\| > 10^{-6}$. All methods are run with the same coarse step size $h = 2^{-8}$.

Method	Order	T_h
RK4	4	0.2070
Ours–6	6	13.9531
Ours–8	8	21.5859
Ours–10	10	31.9453
Ours–12	12	41.0664
Ours–14	14	48.6484

Table 9 summarizes the corresponding predictability times T_h . For a fixed step size, higher-order methods consistently yield longer predictability times, demonstrating a delayed emergence of large discrepancies between the two numerical solutions. This indicates that, although all methods eventually diverge due to chaos, high-order accuracy significantly slows the growth of numerical errors.

These results highlight that high-order ERK methods can offer tangible advantages even in strongly chaotic regimes. While they do not extend the validity of individual trajectories indefinitely, they reduce early-time error injection and prolong the interval over which numerical solutions remain close. This property is particularly relevant in applications where reliable short-to-medium time predictions or accurate statistical sampling are required.

7 Optimization within the constructed family

The recursive construction framework presented in the previous sections produces a family of ERK methods parameterized by a set of free variables. While any choice of these parameters (subject to minor solvability constraints) yields a method of the prescribed order p , the numerical properties—such as the size of the stability region and the magnitude of the leading truncation error—depend strongly on these choices. Use of optimization techniques to tune these free parameters can significantly enhance the performance of the resulting schemes.

7.1 Methodology of optimization of methods

7.1.1 The extended family

Let Φ denote the vector of all free parameters available in our construction. For a method of order p constructed with Q -space dimension l and an N -point Lobatto quadrature, the parameter space Φ consists of the following components:

1. **Free stage nodes:** The internal stage values c_2, \dots, c_{l+1} lying in the subspace V_l^* . These nodes are not constrained by the Lobatto quadrature nodes and can be adjusted freely, provided they remain distinct from each other and from the quadrature nodes to ensure the non-singularity of the Vandermonde-type systems.
2. **Free weights:** The weights b_{l+N}, \dots, b_{s-1} corresponding to the non-quadrature stages. While the quadrature weights w_i are fixed, the distribution of these weights among the stages representing the same node is flexible.
3. **Free matrix entries in the Q -region:** For each level k of the Q -space construction ($3 \leq k \leq m$), there are degrees of freedom in the matrix \mathbf{A} . Specifically, the entries a_{ij} with indices in the set:

$$\left\{ (i, j) \in \mathbb{Z}^2 : j < i \leq \frac{k(k-1)}{2} + 1, \frac{(k-1)(k-2)}{2} + 2 \leq j \leq \frac{k(k-1)}{2} + 1 \right\} \quad (70)$$

are free parameters that do not affect the Q -space inclusion properties required for order conditions.

4. **Free matrix entries in the D -region:** Similarly, for each level k of the D -space construction ($3 \leq k \leq n$), the entries a_{ij} with indices in the set:

$$\left\{ (i, j) \in \mathbb{Z}^2 : s - 1 - \frac{k(k-1)}{2} < i \leq s - 1 - \frac{(k-1)(k-2)}{2}, s - \frac{(k-1)(k-2)}{2} \leq j < i \right\} \quad (71)$$

are free.

The total number of free parameters grows quadratically with the order p , providing a rich search space for optimization. We treat the optimization as an unconstrained problem, relying on the optimizer to find valid configurations; practically, constraints such as distinct nodes are rarely violated by random search algorithms. As a case in point, the construction of an eighth-order method ($p = 8$) involves 17 independent degrees of freedom, and a tenth-order method ($p = 10$) involves 36 independent degrees of freedom. This high dimensionality necessitates the use of robust derivative-free global optimization algorithms to effectively explore the landscape for optimal stability and accuracy.

7.1.2 Choice of objective functions

We aim to construct methods that are both accurate and stable. The optimization is driven by a fitness function $J(\Phi)$ that is formulated as a weighted sum of stability and truncation error components:

$$J(\Phi) = w_{\text{err}} J_{\text{err}} + w_{\text{stab}} J_{\text{stab}}, \quad (72)$$

where w_{err} and w_{stab} are positive weights that balance the relative importance of accuracy and stability.

Stability objective. The stability objective J_{stab} is a composite measure designed to promote large and well-shaped stability regions. Let $R(z)$ be the stability function of the RK method. The stability objective is defined as:

$$J_{\text{stab}} = -w_{\text{area}} \cdot L_{\text{Area}} + w_{\text{interval}} \cdot L_{\text{Interval}} + w_{\text{convex}} \cdot P_{\text{ConvexityPenalty}}, \quad (73)$$

where the components are defined as follows:

- **Stability region area:** Maximizing the total area in the complex plane where $|R(z)| \leq 1$. A larger area generally allows for larger time steps across a variety of problems. Since computing the exact area is computationally expensive, we use a proxy objective based on the sum of stability interval lengths along parallel lines in the complex plane:

$$L_{\text{area}} \approx S_{\text{proxy}} := \sum_{k=1}^M \omega_k (L_{+y_k i} + L_{-y_k i}), \quad (74)$$

where $L_{\pm y_k i}$ denotes the length of the stability segment along the line $z = x \pm y_k i$, and ω_k are positive weights. Here, we choose ω_k according to the trapezoidal rule for numerical integration to approximate the area of the stability region.

- **Real stability interval:** Promoting a larger stability interval along the negative real axis. This is particularly important for dissipative problems or parabolic PDEs. We define this length as

$$L_{\text{Interval}} = |\min\{x \in \mathbb{R} : \forall z \in [x, 0], |R(z)| \leq 1\}|. \quad (75)$$

- **Convexity penalty:** To ensure the stability region remains well-shaped and does not exhibit undesirable dents or non-convex sections, we sample the left stability boundary along horizontal lines

$$y_j = j \Delta y, \quad j = 0, 1, \dots, M, \quad x_j = x(y_j), \quad (76)$$

where $x(y_j)$ denotes the leftmost point on the line $z = x + iy_j$ that still belongs to the stability region. We then approximate the second derivative by the centered finite difference

$$x''(y_j) \approx \frac{x_{j+1} - 2x_j + x_{j-1}}{(\Delta y)^2}, \quad j = 1, \dots, M-1. \quad (77)$$

Local inward bending is identified by negative values of this discrete second derivative, and the convexity penalty is defined by

$$P_{\text{ConvexityPenalty}} = \sum_{j=1}^{M-1} \max\left(0, -\frac{x_{j+1} - 2x_j + x_{j-1}}{(\Delta y)^2}\right). \quad (78)$$

Equivalently, this sums the magnitudes of all negative discrete curvatures along the sampled

boundary.

Truncation error objective. To improve accuracy, we minimize the principal truncation error term. For a method of formal order p , the local truncation error is proportional to the elementary weight vector of order $p + 1$. We define the error objective J_{err} as:

$$J_{\text{err}} = -\frac{1}{\|\boldsymbol{\tau}^{(p+1)}\|_2}, \quad (79)$$

where $\|\boldsymbol{\tau}^{(p+1)}\|_2$ is the norm of the principal error coefficient. Minimizing this objective effectively pushes the method towards a smaller leading-order truncation error.

At this stage, every component entering the fitness function $J(\Phi)$ has been specified explicitly, so the optimization problem is now fully defined without ambiguity. The remaining task is therefore purely algorithmic: to search the admissible parameter space for values of Φ that optimize this objective.

7.1.3 Optimization method

The optimization landscape for high-order RK methods is known to be non-convex and high-dimensional, often containing many local optima. Gradient-based methods are typically unsuitable due to the complexity of the objective function and the lack of analytical gradients.

We employ the *Covariance Matrix Adaptation Evolution Strategy (CMA-ES)* [23], a state-of-the-art derivative-free evolutionary algorithm. CMA-ES is particularly effective for continuous domain optimization of non-linear, non-convex functions. It adapts the covariance matrix of the multivariate normal distribution used to sample candidate solutions, allowing it to learn the variable correlations and scale effectively to the dimensionality of our problem.

7.2 Numerical experiments and properties of optimized schemes

The optimization process systematically yields methods that significantly outperform nominal configurations, which are typically chosen with equidistant nodes and zero free parameters. To demonstrate these superior properties, we decouple our analysis into two parts: a direct algebraic visualization of the extended stability regions, and a set of numerical test problems specifically designed to demonstrate the benefits of the optimized local truncation error.

7.2.1 Extended stability regions

The stability properties of the explicit schemes are entirely determined by their stability function $R(z)$. Rather than relying on specific stiff test equations, we demonstrate the improvement in stability by directly computing and plotting the stability domains in the complex plane. Optimized schemes are expected to exhibit a substantially larger real stability interval and a

more expansive overall stability region, which correspondingly increases the maximum allowable time step before instability occurs.

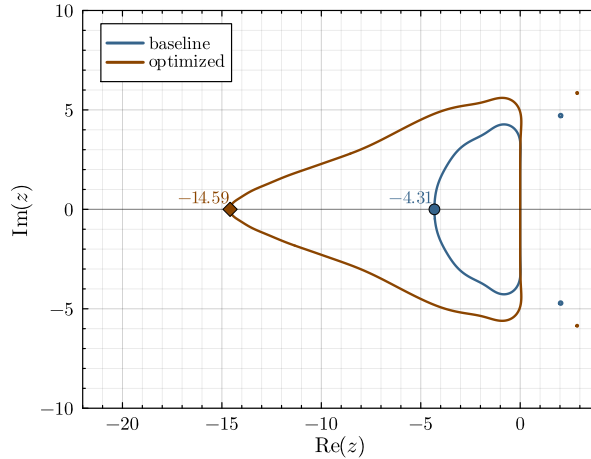


Figure 16: Stability region comparison between optimized and original RK methods. The shaded area represents the stability domain where $|R(z)| < 1$. The optimization directly yields a significantly larger stability region along the real axis.

As shown in Figure 16, a direct comparison of the regions clearly illustrates the enhanced capability of the optimized methods. The extended boundary immediately translates to superior handling of components with eigenvalues near the imaginary or real axes, independent of the specific PDE discretization.

7.2.2 Lorenz attractor benchmark

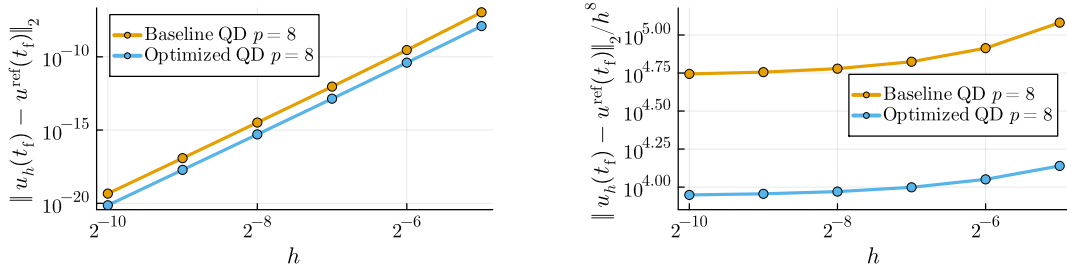
Beyond stability, the optimization framework facilitates a controlled minimization of the leading truncation error coefficient. To empirically validate that this optimization translates to improved computational efficiency via reduced local truncation errors, we integrate a representative test problem from the ordinary differential equation literature, namely the **Lorenz attractor system**, a classical mathematical model of deterministic chaos. Due to its defining characteristic of sensitive dependence on initial conditions, the trajectories of the Lorenz system amplify local truncation errors rapidly. This makes it an exceptionally stringent benchmark for evaluating the enhanced long-term precision yielded by the optimized coefficients.

Experiment description. To complement the short-time global error test, we also consider a Lorenz-63 predictability experiment in the same spirit as previous experiments, but restricted to comparing the baseline and optimized schemes of the same order. The Lorenz system is integrated from the standard initial condition $\mathbf{y}_0 = (1, 1, 1)^\top$ over a fixed time interval, and for each method we compute two numerical solutions using step sizes h and $h/2$. The difference

$\|\mathbf{y}_h(t) - \mathbf{y}_{h/2}(t)\|_2$ is then evaluated at the coarse-grid time nodes and plotted as a function of time.

Since the Lorenz attractor is chaotic, long-time trajectory error is not an appropriate direct indicator of the leading local truncation error constant. However, the coarse-versus-refined comparison still provides a useful practical measure of predictability: a method with smaller effective local error typically delays the onset of rapid trajectory separation. We therefore use the time at which $\|\mathbf{y}_h(t) - \mathbf{y}_{h/2}(t)\|_2$ first exceeds a prescribed threshold as a heuristic predictability indicator.

In addition, to study short-time asymptotic behavior more directly, we perform a final-time global error experiment on the same Lorenz problem, but over a sufficiently short interval $t_f = 2^{-4}$. For a sequence of dyadic step sizes $h = 2^{-5}, \dots, 2^{-10}$, the numerical solution $\mathbf{y}_h(t_f)$ is compared against a high-accuracy reference solution $\mathbf{y}^{\text{ref}}(t_f)$ computed with a 10th-order method and a much finer time step $h = 10^{-16}$. We then plot both the final-time error $\|\mathbf{y}_h(t_f) - \mathbf{y}^{\text{ref}}(t_f)\|_2$ and the normalized quantity $\|\mathbf{y}_h(t_f) - \mathbf{y}^{\text{ref}}(t_f)\|_2/h^p$, where $p = 8$ is the formal order of the method. The latter acts as a practical proxy for the global error constant in the pre-asymptotic-to-asymptotic transition regime.



(a) **Final-time global error plot.** This figure shows $\|\mathbf{y}_h(t_f) - \mathbf{y}^{\text{ref}}(t_f)\|_2$ versus h on logarithmic scales.

(b) **Normalized global error plot.** This figure shows $\|\mathbf{y}_h(t_f) - \mathbf{y}^{\text{ref}}(t_f)\|_2/h^p$ versus h .

Figure 17: Lorenz system global error measurements. (a) shows the absolute error down to machine precision, while (b) demonstrates the scaled asymptotic proxy. Lower curves indicate a correspondingly smaller effective global error constant.

Interpretation. The numerical results show a clear short-time improvement from the optimization. In Figure 17 and table 10, the optimized method consistently attains a smaller final-time error than the baseline at the same step size, and the normalized quantity $\|err\|_2/h^p$ is reduced by approximately a factor of six throughout the asymptotic regime. This indicates that both methods retain order $p = 8$, but the optimized tableau has a substantially smaller effective error constant.

The predictability experiment shows that this gain does carry over to the chaotic setting, but only mildly. In Figure 18, the predictability time increases from 21.58 to 21.62. Such a

Table 10: Data for the short-time Lorenz global error test at $t_f = 0.0625$ ($p = 8$). For very small $h \leq 1.95 \times 10^{-3}$, the error approaches machine precision limits.

h	Steps	Baseline QD $p = 8$		Optimized QD $p = 8$	
		$\ err\ _2$	$\ err\ _2/h^p$	$\ err\ _2$	$\ err\ _2/h^p$
2^{-5}	2	1.10×10^{-7}	1.21×10^5	1.25×10^{-8}	1.38×10^4
2^{-6}	4	2.91×10^{-10}	8.19×10^4	4.00×10^{-11}	1.12×10^4
2^{-7}	8	9.26×10^{-13}	6.67×10^4	1.38×10^{-13}	9.97×10^3
2^{-8}	16	3.26×10^{-15}	6.01×10^4	5.06×10^{-16}	9.34×10^3
2^{-9}	32	1.21×10^{-17}	5.70×10^4	1.91×10^{-18}	9.03×10^3
2^{-10}	64	4.59×10^{-20}	5.55×10^4	7.35×10^{-21}	8.88×10^3

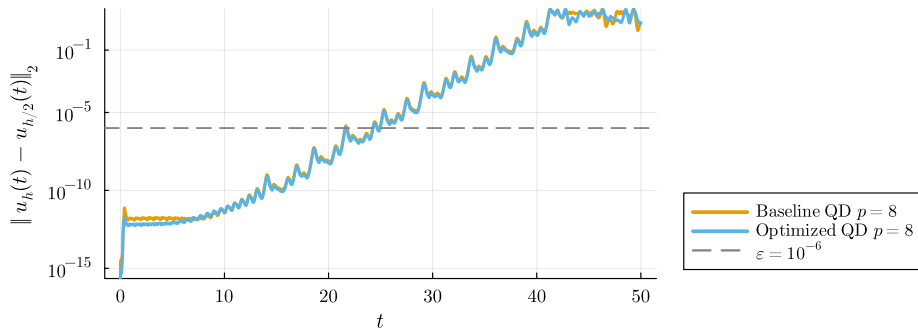


Figure 18: **Predictability plot** showing $\|y_h(t) - y_{h/2}(t)\|_2$ versus time. A horizontal tolerance line captures trajectory separation threshold. The optimized method records a predictability time of 21.62, exhibiting a slight improvement over the original baseline method (21.58).

modest increase is consistent with the Lorenz dynamics: once trajectory separation enters the exponential-growth regime, even a noticeable reduction in local or short-time global error can yield only a limited extension of the agreement interval. Thus, the optimization produces a genuine accuracy improvement, while the chaotic benchmark also shows the practical limit of how much such an improvement can extend long-time predictability.

8 Discussion

The results presented above demonstrate that the proposed reformulation of the RK order theory—through the Q - and D -conditions—provides both a conceptual and algorithmic simplification for constructing high-order explicit methods. In this section we summarize the main implications of this framework, highlight its current limitations, and outline several open directions.

8.1 Interpretation of the Q/D framework

The Q - and D -spaces offer a powerful way to deconstruct the structure of high-order explicit RK methods. The framework follows the idea of simplifying assumptions, but extends it by defining residual vectors \mathbf{q}_n and \mathbf{d}_n and forming spaces given by trees involving these vectors. The Q -conditions are conditions imposed on the Q -type spaces, which aims to capture the *quadrature consistency (stage order)*, ensuring that the method approximates the integral of the function f correctly. On the other hand, the D -conditions imposed on the D -type spaces, capture the *stage-coupling consistency (stage co-order)*, ensuring that the interactions between the stages are properly balanced. This separation of concerns simplifies the order conditions significantly, and is still valid for explicit RK methods.

The idea of considering residual vectors when simplifying assumptions cannot be satisfied has a long history. Almost all construction of high order explicit RK schemes of a specific order follows this idea. However, formulation of it to deal with general order p is difficult, so most general constructions are not based on this. Gragg's construction [19] is based on extrapolation of a symmetric scheme. Butcher's construction [8, Theorem 324C] is based on the stage order yet neglects the stage co-order, so the resulting stage number is relatively large. Verner considered putting the two aspects together, and gave a categorization of trees based on \mathbf{q} and \mathbf{d} 's and formed an equivalent order condition [38], yet it is still fairly difficult to utilize those condition for construction of schemes. Our theory gives a simple, recursive definition of Q and D spaces, as well as sufficient theorems for order, which is suitable for constructive purposes.

Moreover, the recursive interpretation clarifies the algebraic mechanism behind order increase: each new stage is added to account for the expansion Q - and D -spaces when the desired order increases, and the orthogonality pattern controls how Q and D conditions can be satisfied by different parts of matrix \mathbf{A} , as well as how local changes in \mathbf{A} propagate to global order.

8.2 Relation to existing methods

From a structural viewpoint, the new framework subsumes several known families:

- Can the extrapolation-based methods of Gragg be considered as a special case in the Q/D framework? (Not sure yet)
- The Butcher's family of methods can be interpreted as a special case where only Q -spaces are considered. (I guess so but still not considered)

This perspective not only offers a way to reinterpret existing schemes but also facilitates the design of new methods by allowing one to control both quadrature consistency (via Q -spaces) and stage coupling consistency (via D -spaces) independently.

8.3 Limitations and practical constraints

While the recursive construction achieves optimal asymptotic stage growth ($s(p) \sim p^2/4$), it does not necessarily yield minimal stages for small orders.

This inefficiency arises because the structural constraints (orthogonality, cluster co-order) introduce additional degrees of freedom that become beneficial only asymptotically. Moreover, the construction focuses on algebraic order and sparsity; it does not yet incorporate secondary design goals such as stability optimization, strong stability preservation (SSP), or embedded error estimation.

In practice, the resulting methods are therefore best viewed as *reference families*—theoretical baselines that can later be refined or optimized within the Q/D framework.

8.4 Extensions and open questions

Our version of Q/D framework and the present formulation open several promising research directions.

Necessity of the Q/D conditions. The sufficiency theorem of the Q - and D -conditions has been established (Theorem 3.2, Theorem 3.3), but their necessity of the conditions in Theorem 3.3 for ERK schemes remains conjectural. A proof (or counterexample) would clarify whether these spaces fully characterize all explicit methods of a given order.

Relation between our Q/D conditions and Stepanov-type ones. We gave sufficiency theorems for our definition of Q - and D -spaces. Similar theorems can be given for Stepanov’s definition of Q - and D -spaces, which is not directly given but implied in their construction [36]. How to properly formulate the theorems based on Stepanov’s definition and the relation between these two sets of theorems remain open questions.

Optimal stage order estimate. We gave a general upper bound for the least number of stages required to construct RK methods of order p . Though this bound is better than previous bounds, it is certainly not optimal and can be improved.

Optimal sparse forms. Although the construction leads to partially sparse tableaux, the precise trade-off between sparsity, order, and stability radius is not yet understood. A systematic analysis of optimal sparsity patterns could enable high-order methods with minimal memory footprint.

Stability region optimization. We have tested that via simple modifications of free parameters in \mathbf{A} in our construction, the stability region can be vastly enlarged. The question remains that what is the general strategy to choose these parameters to obtain optimal stability region.

Leading order truncation error optimization. The free parameters retained by the construction also provide a systematic framework for optimizing the leading-order truncation error coefficients. However, our current numerical experiments suggest that the Dormand-Prince 8(7) method and the Verner’s 8(7) method has better leading order error coefficients than the methods obtained by our construction, which suggests that the optimization of these coefficients within our construction is not trivial and may require a more careful analysis of the structure of the leading order error terms.

Extensions to other families. The recursive pattern can in principle be adapted to embedded explicit pairs, strong-stability-preserving (SSP) forms, and IMEX (implicit–explicit) couplings. Each requires a modified orthogonality structure on the Q/D -spaces, which may yield novel hybrid schemes.

Implicit and generalized schemes. A longer-term direction is to extend the concept of Q - and D -spaces to implicit Runge–Kutta methods. This may give rise to other implicit families with desirable properties. Such a generalization might unify explicit and implicit order theories and provide new insight into high-order A-stable designs.

9 Conclusion

This work introduces a unified theoretical and constructive framework for explicit Runge–Kutta methods based on the reformulated Q - and D -conditions. These conditions generalize Butcher’s simplifying assumptions and provide a linear-algebraic foundation that makes order verification and method construction straightforward.

Building on this framework, a algorithm was proposed for constructing explicit Runge–Kutta methods of arbitrary order. It only involves solution of two structured linear systems, enabling fast symbolic or numerical generation of high-order schemes. The resulting methods exhibit a stage–order relationship which is better than Gragg’s currently optimal asymptotic estimate, while maintaining structural sparsity and computational simplicity.

Beyond its immediate algorithmic benefits, the Q/D formulation offers a new perspective on the internal algebraic structure of explicit Runge–Kutta schemes. It provides a foundation for future developments in the automated design, optimization, and analysis of high-order time integrators.

A Assembly of the linear systems

A.1 Assembly of the D -system

Before we go into details of the assembly process for general order p , we first give an example for $p = 10$.

Table 11: The assembly of the D -system for $p = 10$.

Variables	Equations	Variables	Equations	Variables	Equations
$a_{22,21}$	$\mathbf{d}_0 \cdot \mathbf{e}_{21} = 0$	$a_{22,13}$	$\mathbf{d}_0 \cdot \mathbf{e}_{13} = 0$	$a_{22,10}$	$\mathbf{d}_0 \cdot \boldsymbol{\mu}_3 = 0$
$a_{22,20}$	$\mathbf{d}_0 \cdot \mathbf{e}_{20} = 0$	$a_{21,13}$	$\boldsymbol{\varepsilon}_{1,1} \mathbf{A} \cdot \mathbf{e}_{13} = 0$	$a_{21,10}$	$\boldsymbol{\varepsilon}_{1,1} \mathbf{A} \cdot \boldsymbol{\mu}_3 = 0$
$a_{21,20}$	$\mathbf{d}_1 \cdot \mathbf{e}_{20} = 0$	$a_{20,13}$	$\boldsymbol{\varepsilon}_{2,1} \mathbf{A} \cdot \mathbf{e}_{13} = 0$	$a_{20,10}$	$\boldsymbol{\varepsilon}_{2,1} \mathbf{A} \cdot \boldsymbol{\mu}_3 = 0$
$a_{22,19}$	$\mathbf{d}_0 \cdot \mathbf{e}_{19} = 0$	$a_{19,13}$	$\boldsymbol{\varepsilon}_{2,2} \mathbf{A} \cdot \mathbf{e}_{13} = 0$	$a_{19,10}$	$\boldsymbol{\varepsilon}_{2,2} \mathbf{A} \cdot \boldsymbol{\mu}_3 = 0$
$a_{21,19}$	$\mathbf{d}_1 \cdot \mathbf{e}_{19} = 0$	$a_{18,13}$	$\mathbf{d}_1 \cdot \mathbf{e}_{13} = 0$	$a_{18,10}$	$\boldsymbol{\varepsilon}_{3,1} \mathbf{A} \cdot \boldsymbol{\mu}_3 = 0$
$a_{22,18}$	$\mathbf{d}_0 \cdot \mathbf{e}_{18} = 0$	$a_{17,13}$	$\mathbf{d}_2 \cdot \mathbf{e}_{13} = 0$	$a_{17,10}$	$\boldsymbol{\varepsilon}_{3,2} \mathbf{A} \cdot \boldsymbol{\mu}_3 = 0$
$a_{21,18}$	$\boldsymbol{\varepsilon}_{1,1} \mathbf{A} \cdot \mathbf{e}_{18} = 0$	$a_{16,13}$	$\mathbf{d}_3 \cdot \mathbf{e}_{13} = 0$	$a_{16,10}$	$\boldsymbol{\varepsilon}_{3,3} \mathbf{A} \cdot \boldsymbol{\mu}_3 = 0$
$a_{20,18}$	$\mathbf{d}_1 \cdot \mathbf{e}_{18} = 0$	$a_{22,12}$	$\mathbf{d}_0 \cdot \mathbf{e}_{12} = 0$	$a_{15,10}$	$\mathbf{d}_1 \cdot \boldsymbol{\mu}_3 = 0$
$a_{19,18}$	$\mathbf{d}_2 \cdot \mathbf{e}_{18} = 0$	$a_{21,12}$	$\boldsymbol{\varepsilon}_{1,1} \mathbf{A} \cdot \mathbf{e}_{12} = 0$	$a_{14,10}$	$\mathbf{d}_2 \cdot \boldsymbol{\mu}_3 = 0$
$a_{22,17}$	$\mathbf{d}_0 \cdot \mathbf{e}_{17} = 0$	$a_{20,12}$	$\boldsymbol{\varepsilon}_{2,1} \mathbf{A} \cdot \mathbf{e}_{12} = 0$	$a_{13,10}$	$\mathbf{d}_3 \cdot \boldsymbol{\mu}_3 = 0$
$a_{21,17}$	$\boldsymbol{\varepsilon}_{1,1} \mathbf{A} \cdot \mathbf{e}_{17} = 0$	$a_{19,12}$	$\boldsymbol{\varepsilon}_{2,2} \mathbf{A} \cdot \mathbf{e}_{12} = 0$	$a_{12,10}$	$\mathbf{d}_4 \cdot \boldsymbol{\mu}_3 = 0$
$a_{20,17}$	$\mathbf{d}_1 \cdot \mathbf{e}_{17} = 0$	$a_{18,12}$	$\mathbf{d}_1 \cdot \mathbf{e}_{12} = 0$	$a_{22,9}$	$\mathbf{d}_0 \cdot \boldsymbol{\mu}_2 = 0$
$a_{19,17}$	$\mathbf{d}_2 \cdot \mathbf{e}_{17} = 0$	$a_{17,12}$	$\mathbf{d}_2 \cdot \mathbf{e}_{12} = 0$	$a_{21,9}$	$\boldsymbol{\varepsilon}_{1,1} \mathbf{A} \cdot \boldsymbol{\mu}_2 = 0$
$a_{22,16}$	$\mathbf{d}_0 \cdot \mathbf{e}_{16} = 0$	$a_{16,12}$	$\mathbf{d}_3 \cdot \mathbf{e}_{12} = 0$	$a_{20,9}$	$\boldsymbol{\varepsilon}_{2,1} \mathbf{A} \cdot \boldsymbol{\mu}_2 = 0$
$a_{21,16}$	$\boldsymbol{\varepsilon}_{1,1} \mathbf{A} \cdot \mathbf{e}_{16} = 0$	$a_{22,11}$	$\mathbf{d}_0 \cdot \boldsymbol{\mu}_4 = 0$	$a_{19,9}$	$\boldsymbol{\varepsilon}_{2,2} \mathbf{A} \cdot \boldsymbol{\mu}_2 = 0$
$a_{20,16}$	$\mathbf{d}_1 \cdot \mathbf{e}_{16} = 0$	$a_{21,11}$	$\boldsymbol{\varepsilon}_{1,1} \mathbf{A} \cdot \boldsymbol{\mu}_4 = 0$	$a_{18,9}$	$\boldsymbol{\varepsilon}_{3,1} \mathbf{A} \cdot \boldsymbol{\mu}_2 = 0$
$a_{19,16}$	$\mathbf{d}_2 \cdot \mathbf{e}_{16} = 0$	$a_{20,11}$	$\boldsymbol{\varepsilon}_{2,1} \mathbf{A} \cdot \boldsymbol{\mu}_4 = 0$	$a_{17,9}$	$\boldsymbol{\varepsilon}_{3,2} \mathbf{A} \cdot \boldsymbol{\mu}_2 = 0$
$a_{22,15}$	$\mathbf{d}_0 \cdot \mathbf{e}_{15} = 0$	$a_{19,11}$	$\boldsymbol{\varepsilon}_{2,2} \mathbf{A} \cdot \boldsymbol{\mu}_4 = 0$	$a_{16,9}$	$\boldsymbol{\varepsilon}_{3,3} \mathbf{A} \cdot \boldsymbol{\mu}_2 = 0$
$a_{21,15}$	$\boldsymbol{\varepsilon}_{1,1} \mathbf{A} \cdot \mathbf{e}_{15} = 0$	$a_{18,11}$	$\boldsymbol{\varepsilon}_{3,1} \mathbf{A} \cdot \boldsymbol{\mu}_4 = 0$	$a_{15,9}$	$\mathbf{d}_1 \cdot \boldsymbol{\mu}_2 = 0$
$a_{20,15}$	$\boldsymbol{\varepsilon}_{2,1} \mathbf{A} \cdot \mathbf{e}_{15} = 0$	$a_{17,11}$	$\boldsymbol{\varepsilon}_{3,2} \mathbf{A} \cdot \boldsymbol{\mu}_4 = 0$	$a_{14,9}$	$\mathbf{d}_2 \cdot \boldsymbol{\mu}_2 = 0$
$a_{19,15}$	$\boldsymbol{\varepsilon}_{2,2} \mathbf{A} \cdot \mathbf{e}_{15} = 0$	$a_{16,11}$	$\boldsymbol{\varepsilon}_{3,3} \mathbf{A} \cdot \boldsymbol{\mu}_4 = 0$	$a_{13,9}$	$\mathbf{d}_3 \cdot \boldsymbol{\mu}_2 = 0$
$a_{18,15}$	$\mathbf{d}_1 \cdot \mathbf{e}_{15} = 0$	$a_{15,11}$	$\mathbf{d}_1 \cdot \boldsymbol{\mu}_4 = 0$	$a_{12,9}$	$\mathbf{d}_4 \cdot \boldsymbol{\mu}_2 = 0$
$a_{17,15}$	$\mathbf{d}_2 \cdot \mathbf{e}_{15} = 0$	$a_{14,11}$	$\mathbf{d}_2 \cdot \boldsymbol{\mu}_4 = 0$	$a_{22,8}$	$\mathbf{d}_0 \cdot \boldsymbol{\mu}_1 = 0$
$a_{16,15}$	$\mathbf{d}_3 \cdot \mathbf{e}_{15} = 0$	$a_{13,11}$	$\mathbf{d}_3 \cdot \boldsymbol{\mu}_4 = 0$	$a_{21,8}$	$\boldsymbol{\varepsilon}_{1,1} \mathbf{A} \cdot \boldsymbol{\mu}_1 = 0$
$a_{22,14}$	$\mathbf{d}_0 \cdot \mathbf{e}_{14} = 0$	$a_{12,11}$	$\mathbf{d}_4 \cdot \boldsymbol{\mu}_4 = 0$	$a_{20,8}$	$\boldsymbol{\varepsilon}_{2,1} \mathbf{A} \cdot \boldsymbol{\mu}_1 = 0$
$a_{21,14}$	$\boldsymbol{\varepsilon}_{1,1} \mathbf{A} \cdot \mathbf{e}_{14} = 0$			$a_{19,8}$	$\boldsymbol{\varepsilon}_{2,2} \mathbf{A} \cdot \boldsymbol{\mu}_1 = 0$
$a_{20,14}$	$\boldsymbol{\varepsilon}_{2,1} \mathbf{A} \cdot \mathbf{e}_{14} = 0$			$a_{18,8}$	$\boldsymbol{\varepsilon}_{3,1} \mathbf{A} \cdot \boldsymbol{\mu}_1 = 0$
$a_{19,14}$	$\boldsymbol{\varepsilon}_{2,2} \mathbf{A} \cdot \mathbf{e}_{14} = 0$			$a_{17,8}$	$\boldsymbol{\varepsilon}_{3,2} \mathbf{A} \cdot \boldsymbol{\mu}_1 = 0$
$a_{18,14}$	$\mathbf{d}_1 \cdot \mathbf{e}_{14} = 0$			$a_{16,8}$	$\boldsymbol{\varepsilon}_{3,3} \mathbf{A} \cdot \boldsymbol{\mu}_1 = 0$
$a_{17,14}$	$\mathbf{d}_2 \cdot \mathbf{e}_{14} = 0$			$a_{15,8}$	$\mathbf{d}_1 \cdot \boldsymbol{\mu}_1 = 0$
$a_{16,14}$	$\mathbf{d}_3 \cdot \mathbf{e}_{14} = 0$			$a_{14,8}$	$\mathbf{d}_2 \cdot \boldsymbol{\mu}_1 = 0$
				$a_{13,8}$	$\mathbf{d}_3 \cdot \boldsymbol{\mu}_1 = 0$
				$a_{12,8}$	$\mathbf{d}_4 \cdot \boldsymbol{\mu}_1 = 0$

Using the definition $\mathbf{d}_n = (\mathbf{b} \cdot \mathbf{c}^{\odot n}) \times^1 \mathbf{A} - \frac{1}{n+1} \mathbf{b} \odot (\mathbf{1} - \mathbf{c}^{\odot(n+1)})$ and the definition of basis vectors \mathbf{e}_i and $\boldsymbol{\varepsilon}_{i,j}$, the system can be assembled as follows:

$$\mathbf{M}_D = \begin{bmatrix} \mathbf{L}_{1,1}^D & 0 & 0 & 0 & 0 & 0 & 0 & 0 & 0 & 0 & 0 & 0 & 0 & 0 \\ 0 & \mathbf{L}_{2,2}^D & 0 & 0 & 0 & 0 & 0 & 0 & 0 & 0 & 0 & 0 & 0 & 0 \\ 0 & 0 & \mathbf{L}_{3,3}^D & 0 & 0 & 0 & 0 & 0 & 0 & 0 & 0 & 0 & 0 & 0 \\ 0 & 0 & 0 & \mathbf{L}_{4,4}^D & 0 & 0 & 0 & 0 & 0 & 0 & 0 & 0 & 0 & 0 \\ 0 & 0 & 0 & 0 & \mathbf{L}_{5,5}^D & 0 & 0 & 0 & 0 & 0 & 0 & 0 & 0 & 0 \\ 0 & 0 & 0 & 0 & 0 & \mathbf{L}_{6,6}^D & 0 & 0 & 0 & 0 & 0 & 0 & 0 & 0 \\ 0 & 0 & 0 & 0 & 0 & 0 & \mathbf{L}_{7,7}^D & 0 & 0 & 0 & 0 & 0 & 0 & 0 \\ 0 & 0 & 0 & 0 & 0 & 0 & 0 & \mathbf{L}_{8,8}^D & 0 & 0 & 0 & 0 & 0 & 0 \\ 0 & 0 & 0 & 0 & 0 & 0 & 0 & 0 & \mathbf{L}_{9,9}^D & 0 & 0 & 0 & 0 & 0 \\ 0 & 0 & 0 & 0 & 0 & 0 & 0 & 0 & 0 & \mathbf{L}_{10,10}^D & 0 & 0 & 0 & 0 \\ 0 & 0 & 0 & 0 & 0 & 0 & \mathbf{L}_{11,7}^D & 0 & 0 & 0 & \mathbf{L}_{11,11}^D & 0 & 0 & 0 \\ 0 & 0 & 0 & \mathbf{L}_{12,4}^D & 0 & 0 & 0 & \mathbf{L}_{12,8}^D & 0 & 0 & 0 & \mathbf{L}_{12,12}^D & 0 & 0 \\ 0 & \mathbf{L}_{13,2}^D & 0 & 0 & \mathbf{L}_{13,5}^D & 0 & 0 & 0 & \mathbf{L}_{13,9}^D & 0 & 0 & 0 & \mathbf{L}_{13,13}^D & 0 \\ \mathbf{L}_{14,1}^D & 0 & \mathbf{L}_{14,3}^D & 0 & 0 & \mathbf{L}_{14,6}^D & 0 & 0 & 0 & \mathbf{L}_{14,10}^D & 0 & 0 & 0 & \mathbf{L}_{14,14}^D \end{bmatrix} \quad (80)$$

where

$$\mathbf{L}_{1,1}^D = \begin{bmatrix} b_{22} \end{bmatrix}, \quad \mathbf{L}_{2,2}^D = \mathbf{L}_{3,3}^D = \begin{bmatrix} b_{22} & b_{21} \\ b_{22}c_{22} & b_{21}c_{21} \end{bmatrix}, \quad (81)$$

$$\mathbf{L}_{4,4}^D = \mathbf{L}_{5,5}^D = \mathbf{L}_{6,6}^D = \begin{bmatrix} b_{22} & b_{21} & b_{20} & b_{19} \\ 0 & 1 & 0 & 0 \\ b_{22}c_{22} & b_{21}c_{21} & b_{20}c_{20} & b_{19}c_{19} \\ b_{22}c_{22}^2 & b_{21}c_{21}^2 & b_{20}c_{20}^2 & b_{19}c_{19}^2 \end{bmatrix}, \quad (82)$$

$$\mathbf{L}_{7,7}^D = \mathbf{L}_{8,8}^D = \mathbf{L}_{9,9}^D = \mathbf{L}_{10,10}^D = \begin{bmatrix} b_{22} & b_{21} & b_{20} & b_{19} & b_{18} & b_{17} & b_{16} \\ 0 & 1 & 0 & 0 & 0 & 0 & 0 \\ 0 & 0 & 1 & 0 & 0 & 0 & 0 \\ 0 & 0 & 0 & 1 & 0 & 0 & 0 \\ b_{22}c_{22} & b_{21}c_{21} & b_{20}c_{20} & b_{19}c_{19} & b_{18}c_{18} & b_{17}c_{17} & b_{16}c_{16} \\ b_{22}c_{22}^2 & b_{21}c_{21}^2 & b_{20}c_{20}^2 & b_{19}c_{19}^2 & b_{18}c_{18}^2 & b_{17}c_{17}^2 & b_{16}c_{16}^2 \\ b_{22}c_{22}^3 & b_{21}c_{21}^3 & b_{20}c_{20}^3 & b_{19}c_{19}^3 & b_{18}c_{18}^3 & b_{17}c_{17}^3 & b_{16}c_{16}^3 \end{bmatrix}, \quad (83)$$

$$\begin{aligned}
\mathbf{L}_{11,11}^D &= \mathbf{L}_{12,12}^D = \mathbf{L}_{13,13}^D = \mathbf{L}_{14,14}^D \\
&= \begin{bmatrix}
b_{22} & b_{21} & b_{20} & b_{19} & b_{18} & b_{17} & b_{16} & b_{15} & b_{14} & b_{13} & b_{12} \\
0 & 1 & 0 & 0 & 0 & 0 & 0 & 0 & 0 & 0 & 0 \\
0 & 0 & 1 & 0 & 0 & 0 & 0 & 0 & 0 & 0 & 0 \\
0 & 0 & 0 & 1 & 0 & 0 & 0 & 0 & 0 & 0 & 0 \\
0 & 0 & 0 & 0 & 1 & 0 & 0 & 0 & 0 & 0 & 0 \\
0 & 0 & 0 & 0 & 0 & 1 & 0 & 0 & 0 & 0 & 0 \\
0 & 0 & 0 & 0 & 0 & 0 & 1 & 0 & 0 & 0 & 0 \\
b_{22}c_{22} & b_{21}c_{21} & b_{20}c_{20} & b_{19}c_{19} & b_{18}c_{18} & b_{17}c_{17} & b_{16}c_{16} & b_{15}c_{15} & b_{14}c_{14} & b_{13}c_{13} & b_{12}c_{12} \\
b_{22}c_{22}^2 & b_{21}c_{21}^2 & b_{20}c_{20}^2 & b_{19}c_{19}^2 & b_{18}c_{18}^2 & b_{17}c_{17}^2 & b_{16}c_{16}^2 & b_{15}c_{15}^2 & b_{14}c_{14}^2 & b_{13}c_{13}^2 & b_{12}c_{12}^2 \\
b_{22}c_{22}^3 & b_{21}c_{21}^3 & b_{20}c_{20}^3 & b_{19}c_{19}^3 & b_{18}c_{18}^3 & b_{17}c_{17}^3 & b_{16}c_{16}^3 & b_{15}c_{15}^3 & b_{14}c_{14}^3 & b_{13}c_{13}^3 & b_{12}c_{12}^3
\end{bmatrix}, \tag{84}
\end{aligned}$$

$$\begin{aligned}
\mathbf{L}_{11,7}^D &= \mathbf{L}_{12,8}^D = \mathbf{L}_{13,9}^D = \mathbf{L}_{14,10}^D = \\
&= \begin{bmatrix}
b_{22} & b_{21} & b_{20} & b_{19} & b_{18} & b_{17} & b_{16} \\
0 & 1 & 0 & 0 & 0 & 0 & 0 \\
0 & 0 & 1 & 0 & 0 & 0 & 0 \\
0 & 0 & 0 & 1 & 0 & 0 & 0 \\
0 & 0 & 0 & 0 & 1 & 0 & 0 \\
0 & 0 & 0 & 0 & 0 & 1 & 0 \\
0 & 0 & 0 & 0 & 0 & 0 & 1 \\
b_{22}c_{22} & b_{21}c_{21} & b_{20}c_{20} & b_{19}c_{19} & b_{18}c_{18} & b_{17}c_{17} & b_{16}c_{16} \\
b_{22}c_{22}^2 & b_{21}c_{21}^2 & b_{20}c_{20}^2 & b_{19}c_{19}^2 & b_{18}c_{18}^2 & b_{17}c_{17}^2 & b_{16}c_{16}^2 \\
b_{22}c_{22}^3 & b_{21}c_{21}^3 & b_{20}c_{20}^3 & b_{19}c_{19}^3 & b_{18}c_{18}^3 & b_{17}c_{17}^3 & b_{16}c_{16}^3 \\
b_{22}c_{22}^4 & b_{21}c_{21}^4 & b_{20}c_{20}^4 & b_{19}c_{19}^4 & b_{18}c_{18}^4 & b_{17}c_{17}^4 & b_{16}c_{16}^4
\end{bmatrix}, \tag{85}
\end{aligned}$$

$$\begin{aligned}
\mathbf{L}_{12,4}^D &= \mathbf{L}_{13,5}^D = \mathbf{L}_{14,6}^D = \\
&= \begin{bmatrix}
b_{22} & b_{21} & b_{20} & b_{19} \\
0 & 1 & 0 & 0 \\
0 & 0 & 1 & 0 \\
0 & 0 & 0 & 1 \\
0 & 0 & 0 & 0 \\
0 & 0 & 0 & 0 \\
0 & 0 & 0 & 0 \\
b_{22}c_{22} & b_{21}c_{21} & b_{20}c_{20} & b_{19}c_{19} \\
b_{22}c_{22}^2 & b_{21}c_{21}^2 & b_{20}c_{20}^2 & b_{19}c_{19}^2 \\
b_{22}c_{22}^3 & b_{21}c_{21}^3 & b_{20}c_{20}^3 & b_{19}c_{19}^3 \\
b_{22}c_{22}^4 & b_{21}c_{21}^4 & b_{20}c_{20}^4 & b_{19}c_{19}^4
\end{bmatrix}, \tag{86}
\end{aligned}$$

$$\mathbf{L}_{13,2}^D = \mathbf{L}_{14,3}^D = \begin{bmatrix} b_{22} & b_{21} \\ 0 & 1 \\ 0 & 0 \\ 0 & 0 \\ 0 & 0 \\ 0 & 0 \\ 0 & 0 \\ b_{22}c_{22} & b_{21}c_{21} \\ b_{22}c_{22}^2 & b_{21}c_{21}^2 \\ b_{22}c_{22}^3 & b_{21}c_{21}^3 \\ b_{22}c_{22}^4 & b_{21}c_{21}^4 \end{bmatrix}, \quad (87)$$

$$\mathbf{L}_{14,1}^D = \begin{bmatrix} b_{22} \\ 0 \\ 0 \\ 0 \\ 0 \\ 0 \\ 0 \\ b_{22}c_{22} \\ b_{22}c_{22}^2 \\ b_{22}c_{22}^3 \\ b_{22}c_{22}^4 \end{bmatrix}. \quad (88)$$

The right-hand side \mathbf{r}_D of the D -system is also assembled from the equations in Table 11. We omit the details of the exact formulas for \mathbf{r}_D since they have little affect on the understanding of the theory and algorithms we present.

Remark. In general, the linear system for the D -system is a block lower-triangular matrix. Upon certain reordering of the variables, any diagonal block can be written as

$$\mathbf{L}_{i,i}^D = \begin{bmatrix} \mathbf{V}_{i,i}^D & \mathbf{W}_{i,i}^D \\ \mathbf{0} & \mathbf{I} \end{bmatrix} \quad (89)$$

where $\mathbf{V}_{i,i}^D$ is a square Vandermonde matrix and $\mathbf{W}_{i,i}^D$ is a non-square Vandermonde matrix.

A.2 Assembly of the Q -system

The variables and equations for the Q -system are introduced in Example 4.3. To assemble them into a structured linear system, we adopt a particular ordering of the variables. For elements (i, j) in the variable index set I^Q , we define a partial ordering ' $<$ ': $(i, j) < (i', j')$ if and only if $i < i'$ or $i = i'$ and $j < j'$. The variables are then ordered as $(2, 1), (3, 1), (3, 2), (4, 1), (4, 2),$

Table 12: The equations for each variable in the Q -system.

Variables	Equations
$a_{2,1}$	$\mathbf{q}_0 \cdot \mathbf{e}_2 = 0$
$a_{3,1}$	$\mathbf{q}_0 \cdot \mathbf{e}_3 = 0$
$a_{3,2}$	$\mathbf{q}_1 \cdot \mathbf{e}_3 = 0$
$a_{4,1}$	$\mathbf{q}_0 \cdot \mathbf{e}_4 = 0$
$a_{4,2}$	$\mathbf{q}_1 \cdot \mathbf{e}_4 = 0$
$a_{5,1}$	$\mathbf{q}_0 \cdot \mathbf{e}_5 = 0$
$a_{5,2}$	$(\mathbf{A}\mathbf{e}_2) \cdot \mathbf{e}_5 = 0$
$a_{5,3}$	$\mathbf{q}_1 \cdot \mathbf{e}_5 = 0$
$a_{5,4}$	$\mathbf{q}_2 \cdot \mathbf{e}_5 = 0$
$a_{6,1}$	$\mathbf{q}_0 \cdot \mathbf{e}_6 = 0$
$a_{6,2}$	$(\mathbf{A}\mathbf{e}_2) \cdot \mathbf{e}_6 = 0$
$a_{6,3}$	$\mathbf{q}_1 \cdot \mathbf{e}_6 = 0$
$a_{6,4}$	$\mathbf{q}_2 \cdot \mathbf{e}_6 = 0$
$a_{7,1}$	$\mathbf{q}_0 \cdot \mathbf{e}_7 = 0$
$a_{7,2}$	$(\mathbf{A}\mathbf{e}_2) \cdot \mathbf{e}_7 = 0$
$a_{7,3}$	$\mathbf{q}_1 \cdot \mathbf{e}_7 = 0$
$a_{7,4}$	$\mathbf{q}_2 \cdot \mathbf{e}_7 = 0$
For $8 \leq i \leq 22$:	
$a_{i,1}$	$\mathbf{q}_0 \cdot \mathbf{e}_i = 0$
$a_{i,2}$	$(\mathbf{A}\mathbf{e}_2) \cdot \mathbf{e}_i = 0$
$a_{i,3}$	$(\mathbf{A}\mathbf{e}_3) \cdot \mathbf{e}_i = 0$
$a_{i,4}$	$(\mathbf{A}\mathbf{e}_4) \cdot \mathbf{e}_i = 0$
$a_{i,5}$	$\mathbf{q}_1 \cdot \mathbf{e}_i = 0$
$a_{i,6}$	$\mathbf{q}_2 \cdot \mathbf{e}_i = 0$
$a_{i,7}$	$\mathbf{q}_3 \cdot \mathbf{e}_i = 0$

$$\mathbf{L}_5^Q = \mathbf{L}_6^Q = \mathbf{L}_7^Q = \begin{bmatrix} 1 & 1 & 1 & 1 \\ 0 & 1 & 0 & 0 \\ c_1 & c_2 & c_3 & c_4 \\ c_1^2 & c_2^2 & c_3^2 & c_4^2 \end{bmatrix}, \quad (92)$$

$$\mathbf{L}_i^Q = \begin{bmatrix} 1 & 1 & 1 & 1 & 1 & 1 & 1 & 1 \\ 0 & 1 & 0 & 0 & 0 & 0 & 0 & 0 \\ 0 & 0 & 1 & 0 & 0 & 0 & 0 & 0 \\ 0 & 0 & 0 & 1 & 0 & 0 & 0 & 0 \\ c_1 & c_2 & c_3 & c_4 & c_5 & c_6 & c_7 & c_8 \\ c_1^2 & c_2^2 & c_3^2 & c_4^2 & c_5^2 & c_6^2 & c_7^2 & c_8^2 \\ c_1^3 & c_2^3 & c_3^3 & c_4^3 & c_5^3 & c_6^3 & c_7^3 & c_8^3 \end{bmatrix}, \quad \text{for } 8 \leq i \leq 22. \quad (93)$$

The right hand side \mathbf{r}_Q of the linear system is also assembled from the equations in Ta-

ble 12. It is not difficult yet tedious to write it out, so we omit the details here. For conceptual understanding of the solvability and condition number of the linear system, focusing on \mathbf{M}_Q is adequate. For implementation, some variables (the shadowed ones in Figure 20) can be decoupled from the system and their values can be determined a priori. Therefore, we only need to solve a smaller block diagonal linear system. Efficient algorithms can be adopted to obtain the solution.

Remark. In general, the linear system for the Q -system is a block diagonal matrix. Upon certain permutations of rows and columns, any diagonal block can be written as

$$\mathbf{L}_i^Q = \begin{bmatrix} \mathbf{V}_i^Q & \mathbf{W}_i^Q \\ \mathbf{0} & \mathbf{I} \end{bmatrix} \quad (94)$$

where \mathbf{V}_i^Q is a square Vandermonde matrix and \mathbf{W}_i^Q is a non-square Vandermonde matrix.

B Tables of coefficients for constructed methods

Coefficients for our method of order 4.

0	0	0	0	0
1/2	1/2	0	0	0
1/2	0	1/2	0	0
1	0	0	1	0
	1/6	1/3	1/3	1/6

Coefficients for our method of order 6.

0	0	0	0	0	0	0	0	0
c_2	a_{21}	0	0	0	0	0	0	0
c_3	a_{31}	a_{32}	0	0	0	0	0	0
c_4	a_{41}	a_{42}	0	0	0	0	0	0
c_5	a_{51}	a_{52}	1/2	a_{54}	0	0	0	0
c_6	a_{61}	a_{62}	a_{63}	1/3	0	0	0	0
c_7	a_{71}	a_{72}	a_{73}	a_{74}	a_{75}	a_{76}	0	0
1	1/6	0	a_{83}	a_{84}	a_{85}	a_{86}	a_{87}	0
	1/12	0	5/36	5/24	5/36	5/24	5/36	1/12

The precise parameters containing extended floating-point representations are defined as follows:

Parameter	Precise Numerical Value
$c_2 = c_4 = c_6$	0.2763932022500210303590826331268723764559
$c_3 = c_5 = c_7$	0.7236067977499789696409173668731276235441
a_{21}	0.2763932022500210303590826331268723764559
a_{31}	-0.2236067977499789696409173668731276235441
a_{32}	0.9472135954999579392818347337462552470881
$a_{41} = a_{42}$	0.1381966011250105151795413165634361882280
a_{51}	0.5854101966249684544613760503096914353161
a_{52}	-1.8944271909999158785636694674925104941762
a_{54}	1.5326237921249263937432107840559466824042
a_{61}	0.1030056647916491413674311390609396862867
a_{62}	-0.1381966011250105151795413165634361882280
a_{63}	-0.0217491947499509291621405227039644549361
a_{71}	-0.2236067977499789696409173668731276235441
a_{72}	0.9472135954999579392818347337462552470881
a_{73}	-0.1381966011250105151795413165634361882280
a_{74}	-1.4208203932499369089227521006193828706322
a_{75}	0.1381966011250105151795413165634361882280
a_{76}	1.4208203932499369089227521006193828706322
a_{83}	-0.0879773408334034345302754437562412548531
a_{84}	0.7893446629166316160681956114552127059068
a_{85}	0.2303276685416841919659021942723936470466
a_{86}	-0.5590169943749474241022934171828190588602
a_{87}	0.4606553370833683839318043885447872940932

Coefficients for our method of order 8. Denote the Butcher tableau as $(\mathbf{A}, \mathbf{b}^\top, \mathbf{c})$. $\mathbf{A} = (a_{ij})$, $\mathbf{b} = (b_i)$, $\mathbf{c} = (c_i)$.

The precise parameters containing extended floating-point representations are defined as follows:

Parameter	Precise Numerical Value
$c_2 = a_{21} = c_3 = c_7 = c_{10}$	0.1726731646460114281008537718765708222154
$a_{31} = a_{32} = a_{13,11}$	0.0863365823230057140504268859382854111077
a_{41}	-0.2239109809347400004117529496080005305615
a_{42}	0.7239109809347400004117529496080005305615
$c_5 = c_8 = c_{11} = c_{13}$	0.8273268353539885718991462281234291777846
$a_{51} = a_{11,1} = a_{13,1}$	0.3472041832132342858711439808030478211663
$a_{53} = a_{11,3} = a_{13,3}$	-0.3121452601573282541773983236104129679043

Parameter	Precise Numerical Value
$a_{54} = a_{11,4} = a_{13,4}$	0.7922679122980825402054005709307943245226
$a_{61} = a_{12,1}$	0.0086963396884199998627490167973331564795
$a_{63} = a_{12,3}$	0.3685974296159088892091411830284448571034
$a_{64} = a_{12,4} = a_{12,9}$	0.1227062306956711109281098001742219864171
a_{71}	0.0763979083933828570644280095984760894169
$a_{73} = a_{11,8}$	0.1015181575196660317721747904513016209880
a_{74}	-0.0052429012670374607357490281732068881895
a_{81}	-0.7558982639254171433277176566948577492132
a_{83}	0.9364357804719847625321949708312389037128
a_{84}	-2.3768037368942476206162017127923829735677
a_{86}	1.6982683863407949218897867670593032042510
a_{87}	0.8808802249164292069766394152756833481572
a_{91}	0.0763573206231600002745019664053336870410
a_{93}	-0.7371948592318177784182823660568897142068
a_{94}	-0.2454124613913422218562196003484439728342
a_{95}	-0.0272608833024616673872343284806675951493
a_{97}	0.9751775499691283340539009951473342618160
$a_{10,1}$	0.0664592344637600000784291332586667677260
$a_{10,3} = a_{11,5}$	-0.1015181575196660317721747904513016209880
$a_{10,4}$	0.0052429012670374607357490281732068881895
$a_{10,5}$	0.0040043319862298409561247368066027703658
$a_{10,6}$	-0.0237373677735720641194965581328262053001
$a_{11,6}$	-0.6419111699433515349492526724849107715542
$a_{11,7}$	0.6242905203146565083547966472208259358085
$a_{11,9}$	0.6419111699433515349492526724849107715542
$a_{11,10}$	-0.6242905203146565083547966472208259358085
$a_{12,5}$	0.0030105722119316669068558872713336428276
$a_{12,6}$	-0.1227062306956711109281098001742219864171
$a_{12,7}$	-0.9098701805298291672671397181783341070689
$a_{12,8}$	-0.0030105722119316669068558872713336428276
$a_{12,10}$	0.9098701805298291672671397181783341070689
$a_{13,5}$	-0.0863365823230057140504268859382854111077
$a_{13,6}$	-1.2606885110156016333701275857118920804337
$a_{13,12}$	1.2606885110156016333701275857118920804337
$a_{14,5}$	-0.0676381975765999989324923528681467726183
$a_{14,6}$	0.7323606311023881494494908036993597015278
$a_{14,7}$	-0.5562780543026933337603363921860746242860
$a_{14,8}$	0.103986041979882221154714575090368994840
$a_{14,9}$	0.0206135459281066663413310027788637783218
$a_{14,10}$	0.9451669431915822226492252810749635131749
$a_{14,11}$	0.1175136814952022219019699280826662540077

Parameter	Precise Numerical Value
$a_{14,10}$	9.4516694319158222264922528107480591e-01
$a_{14,11}$	8.62457805369592634572061465517691453e-02
$a_{14,12}$	-5.30751954808272593568599584255938345e-01
$a_{14,13}$	2.3502736299040444380393985616533733e-01

Coefficients of our methods of order 10, 12 and 14 The coefficient table of our methods of order 10, 12 and 14 are quite large, and we have made them public on GitHub, see [25]. A small piece of Julia script to load, use and test the order of the methods is also provided in the same repository. Try it if you are interested.

References

- [1] Markus Bachmayr, Reinhold Schneider, and André Uschmajew. “Tensor networks and hierarchical tensors for the solution of high-dimensional partial differential equations”. In: *Foundations of Computational Mathematics* 16.6 (2016), pp. 1423–1472.
- [2] Jason P Bell, Stanley N Burris, and Karen A Yeats. “Counting Rooted Trees: The Universal Law $t(n) \sim C\rho^{-n}n^{-3/2}$ ”. In: *the electronic journal of combinatorics* (2006), R63–R63.
- [3] Przemyslaw Bogacki and Lawrence F Shampine. “A 3(2) pair of Runge-Kutta formulas”. In: *Applied Mathematics Letters* 2.4 (1989), pp. 321–325.
- [4] John C Butcher. “Coefficients for the study of Runge-Kutta integration processes”. In: *Journal of the Australian Mathematical Society* 3.2 (1963), pp. 185–201.
- [5] John C Butcher. “Implicit runge-kutta processes”. In: *Mathematics of computation* 18.85 (1964), pp. 50–64.
- [6] John C Butcher. “On Runge-Kutta processes of high order”. In: *Journal of the Australian Mathematical Society* 4.2 (1964), pp. 179–194.
- [7] John Charles Butcher. “A history of Runge-Kutta methods”. In: *Applied numerical mathematics* 20.3 (1996), pp. 247–260.
- [8] John Charles Butcher. *Numerical methods for ordinary differential equations*. John Wiley & Sons, 2016.
- [9] Andrzej Cichocki et al. “Tensor networks for dimensionality reduction and large-scale optimization: Part 1 low-rank tensor decompositions”. In: *Foundations and Trends in Machine Learning* 9.4–5 (2016), pp. 249–429.
- [10] GJ Cooper and JH Verner. “Some Explicit Runge-Kutta Methods of High Order”. In: *SIAM Journal on Numerical Analysis* 9.3 (1972), pp. 389–405.

- [11] John R Dormand and Peter J Prince. “A family of embedded Runge–Kutta formulae”. In: *Journal of Computational and Applied Mathematics* 6.1 (1980), pp. 19–26.
- [12] Alfredo Eisenberg and Giuseppe Fedele. “Vandermonde systems on gauss–lobatto chebyshev nodes”. In: *Applied mathematics and computation* 170.1 (2005), pp. 633–647.
- [13] Alfredo Eisenberg, Giuseppe Fedele, and C Imbrogno. “Vandermonde systems on equidistant nodes in $[0, 1]$: accurate computation”. In: *Applied mathematics and computation* 172.2 (2006), pp. 971–984.
- [14] Terry Feagin. “High-order explicit Runge–Kutta methods using m-symmetry”. In: *Neural, Parallel & Scientific Computations* 20.3-4 (2012), pp. 437–458.
- [15] Erwin Fehlberg. *Classical fifth-, sixth-, seventh-, and eighth-order Runge–Kutta formulas with stepsize control*. Vol. 287. National Aeronautics and Space Administration, 1968.
- [16] Erwin Fehlberg. “Low-order classical Runge–Kutta formulas with stepsize control and their application to some heat transfer problems”. In: *NASA TR R-315* (1969).
- [17] Steven R Finch. *Mathematical constants*. Cambridge university press, 2003, p. 296.
- [18] Walter Gautschi. “The condition of Vandermonde-like matrices involving orthogonal polynomials”. In: *Linear algebra and its applications* 52 (1983), pp. 293–300.
- [19] William B Gragg. “On extrapolation algorithms for ordinary initial value problems”. In: *Journal of the Society for Industrial and Applied Mathematics, Series B: Numerical Analysis* 2.3 (1965), pp. 384–403.
- [20] Ernst Hairer, Gerhard Wanner, and Christian Lubich. *Geometric Numerical Integration: Structure-Preserving Algorithms for Ordinary Differential Equations*. Springer, 2006.
- [21] Ernst Hairer, Gerhard Wanner, and Syvert P Nørsett. *Solving ordinary differential equations I: Nonstiff problems*. Springer, 1993.
- [22] Stephen M Hammel, James A Yorke, and Celso Grebogi. “Do numerical orbits of chaotic dynamical processes represent true orbits?” In: *Journal of Complexity* 3.2 (1987), pp. 136–145.
- [23] Nikolaus Hansen. “The CMA evolution strategy: A tutorial”. In: *arXiv preprint arXiv:1604.00772* (2016).
- [24] Frank Harary, Robert W Robinson, and Allen J Schwenk. “Twenty-step algorithm for determining the asymptotic number of trees of various species”. In: *Journal of the Australian Mathematical Society* 20.4 (1975), pp. 483–503.
- [25] Junyuan He. *qdwithclustersminimalv1-rk-tableaux*. <https://github.com/JunyuanHe/qdwithclustersminimalv1-rk-tableaux>. Accessed: 2026-04-09. 2026.

- [26] Junyuan He, Zhonghao Sun, and Jizu Huang. “Derivatives of tree tensor networks and its applications in Runge–Kutta methods”. In: *arXiv preprint arXiv:2504.15516* (2025).
- [27] Namgil Lee and Andrzej Cichocki. “Fundamental tensor operations for large-scale data analysis using tensor network formats”. In: *Multidimensional Systems and Signal Processing* 29.3 (2018), pp. 921–960.
- [28] Edward N Lorenz. “Deterministic Nonperiodic Flow.” In: *Journal of the Atmospheric Sciences* 20.2 (1963), pp. 130–148.
- [29] Juliette Mattioli. “Minkowski operations and vector spaces”. In: *Set-valued analysis* 3.1 (1995), pp. 33–50.
- [30] Hiroshi Ono. “On the 25 stage 12th order explicit Runge-Kutta method”. In: *Transactions-Japan Society for Industrial and Applied Mathematics* 16.3 (2006), p. 177.
- [31] Richard Otter. “The number of trees”. In: *Annals of Mathematics* 49.3 (1948), pp. 583–599.
- [32] Peter J Prince and John R Dormand. “High order embedded Runge–Kutta formulae”. In: *Journal of Computational and Applied Mathematics* 7.1 (1981), pp. 67–75.
- [33] Tim Sauer, Celso Grebogi, and James A Yorke. “How long do numerical chaotic solutions remain valid?” In: *Physical Review Letters* 79.1 (1997), p. 59.
- [34] Lawrence F Shampine and Mark W Reichelt. “The MATLAB ODE suite”. In: *SIAM Journal on Scientific Computing* 18.1 (1997), pp. 1–22.
- [35] PW Sharp and JH Verner. “Completely imbedded Runge–Kutta pairs”. In: *SIAM journal on numerical analysis* 31.4 (1994), pp. 1169–1190.
- [36] Misha Stepanov. “On Runge-Kutta methods of order 10”. In: *arXiv preprint arXiv:2504.17329* (2025).
- [37] James H Verner. “Explicit Runge–Kutta pairs with lower stage-order”. In: *Numerical Algorithms* 65.3 (2014), pp. 555–577.
- [38] JH Verner. “Strategies for deriving new explicit Runge-Kutta pairs”. In: *Ann. Numer. Math* 1 (1994), pp. 225–244.